INFORMATION TO USERS

This manuscript has been reproduced from the microfilm master. UMI films the text directly from the original or copy submitted. Thus, some thesis and dissertation copies are in typewriter face, while others may be from any type of computer printer.

The quality of this reproduction is dependent upon the quality of the copy submitted. Broken or indistinct print, colored or poor quality illustrations and photographs, print bleedthrough, substandard margins, and improper alignment can adversely affect reproduction.

In the unlikely event that the author did not send UMI a complete manuscript and there are missing pages, these will be noted. Also, if unauthorized copyright material had to be removed, a note will indicate the deletion.

Oversize materials (e.g., maps, drawings, charts) are reproduced by sectioning the original, beginning at the upper left-hand corner and continuing from left to right in equal sections with small overlaps.

Photographs included in the original manuscript have been reproduced xerographically in this copy. Higher quality 6" x 9" black and white photographic prints are available for any photographs or illustrations appearing in this copy for an additional charge. Contact UMI directly to order.

Bell & Howell Information and Learning
300 North Zeeb Road, Ann Arbor, MI 48106-1346 USA

UMI®
800-521-0600

DISSERTATION

IMPLEMENTATION OF A TWO-WAY INTERACTIVE ATMOSPHERIC AND ECOLOGICAL MODEL AND ITS APPLICATION TO THE CENTRAL UNITED STATES

Submitted by

Lixin Lu

Department of Atmospheric Science

In partial fulfillment of the requirements

for the Degree of Doctor of Philosophy

Colorado State University

Fort Collins, Colorado

Summer 1999

COLORADO STATE UNIVERSITY

May 4, 1999

WE HEREBY RECOMMEND THAT THE DISSERTATION PREPARED UNDER OUR SUPERVISION BY LIXIN LU ENTITLED IMPLEMENTATION OF A TWO-WAY INTERACTIVE ATMOSPHERIC AND ECOLOGICAL MODEL AND ITS APPLICATION TO THE CENTRAL UNITED STATES BE ACCEPTED AS FULFILLING IN PART REQUIREMENTS FOR THE DEGREE OF DOCTOR OF PHILOSOPHY.

Committee on Graduate Work

Committee Member

Committee Member

Committee Member

Committee Member

Adviser

Department Head

ABSTRACT

IMPLEMENTATION OF A TWO-WAY INTERACTIVE ATMOSPHERIC AND ECOLOGICAL MODEL AND ITS APPLICATION TO THE CENTRAL UNITED STATES

A coupled RAMS/CENTURY modeling system has been developed to study regional-scale two-way interactions between the atmosphere and biosphere. Both atmospheric forcings and ecological parameters (LAI, etc.) are prognostic variables in the linked system. The atmospheric and ecosystem models exchange information on a weekly time step. CENTURY receives as input: air temperature, precipitation, radiation, wind speed, and relative humidity simulated by RAMS. From CENTURY-produced outputs, variables including leaf area index, vegetation transimissivity, vegetation fractional coverage, displacement height, roughness length, rooting profile, and albedo can be computed and returned to RAMS. In this way, vegetation responses to weekly and seasonal atmospheric changes are simulated and fed back to the atmospheric/land-surface hydrology model.

The coupled model was used to simulate the two-way biosphere and atmosphere feedbacks from 1 January through 31 December, for 1988, 1989 and 1993 which represent dry, average and wet years, respectively, focusing on the central United

States. Validation is performed for the atmospheric portion of the model by comparing with over 3,800 meteorological-station observations over the entire domain, and for the ecological component by comparing to AVHRR remote-sensing NDVI data sets. A series of sensitivity experiments have been conducted to highlight interactions and feedbacks between atmospheric and land surface processes. The coupled control run's atmospheric lateral boundary conditions have been perturbed to create both dry and wet springs. The model's ability to represent the interannual and seasonal variations in both climate and biomass has been examined. The results show that seasonal and interannual vegetation phenological variation strongly influences regional climate patterns through its control over land-surface water and energy exchange. The coupled model captures the key aspects of weekly, seasonal, and annual feedbacks between the atmosphere and ecological systems. In addition, it has demonstrated its usefulness as a research tool for studying complex interactions between the atmosphere, biosphere, and hydrosphere.

Lixin Lu
Department of Atmospheric Science
Colorado State University
Fort Collins, Colorado 80523
Summer 1999

ACKNOWLEDGMENTS

First of all, I would like to express gratitude to my advisor, Dr. Roger Pielke, for bringing me into the fascinating world of land surface and atmosphere interactions, and for his unwavering optimism and continuous guidance during the course of this study. Thanks also go to Drs. Richard Johnson, Graeme Stephens, Bill Parton, and Dennis Ojima for taking the time to serve on my committee. I had my first atmospheric science class in English from Dr. Johnson and I must thank him for his support and encouragement through the years of my graduate study ever since. Drs. Parton and Ojima are thanked for introducing me to ecosystem models and for having me on their "CENTURY ship". Dr. Bill Cotton is greatly appreciated for being a substitute committee member at my oral defense within such a short notice.

Special thanks are due to Dr. Glen Liston, who offered enormous technical and emotional support which have been invaluable to my career advances. Working with him over the past 4 years has benefited me more than I can possibly express. Dr. Bob Walko has always been the ultimate resources for solving my RAMS related problems. Melannie Hartman, a dearest friend of mine, on the other hand, was always there to answer my CENTURY related questions. My office mates Tom Chase, Chris Golaz, and Ethan Greene are thanked for the insightful discussions on many relevant topics. Dr. Scott Denning must be acknowledged for giving me advice on NDVI-to-LAI

conversion algorithm which is crucial to my model validation efforts. The support of Dallas McDonald and her cohort, Tara Pielke, is greatly appreciated.

Finally and most importantly, I would like to thank my husband Zhiming for his support and patience which made the pursuit of this degree possible; and for joining me to experience this exciting episode of my life. I am also grateful to my loving parents, who have always encouraged and supported my education, for standing behind me through all these years.

This research was supported by NASA Grant No. NAG8-1511, EPA Grant No. R824993-01-0, and NPS Contract No. CA 1268-2-9004 CEGR-R92-0193.

TABLE OF CONTENTS

LIST OF TABLES

LIST OF FIGURES

and wet (1993) years for single grid cells with different land cover types. All the LAIs are 7-day running means.

Figure 7.17 Domain-averaged daily maximum and minimum temperatures and precipitation from the perturbed offline ClimRAMS simulation for the time period 1 January through 31 December 1989. The relative humidity of the lateral boundary conditions have been reduced to 50% of its original value from 1 March to 31 May 1989. Also shown are the differences between the perturbed run and the control run, and a 7-day running mean of the difference values.

Figure 7.18 Domain-averaged daily maximum and minimum temperatures and precipitation from the perturbed offline ClimRAMS simulation for the time period 1 January through 31 December 1989. The relative humidity of the lateral boundary conditions have been increased by 50% of its original value from 1 March to 31 May 1989. Also shown are the differences between the perturbed run and the control run, and a 7-day running mean of the difference values.

Figure 7.19 The domain-averaged LAIs simulated by the coupled model for dry, average, and wet springs, respectively. Also shown are the LAIs averaged over grassland, trees, and crops for the same time periods. All the LAIs are 7-day running means.

Figure 7.20 The LAIs simulated by the coupled model for dry, average, and wet springs for single grid cells with different land-cover types. All the LAIs are 7-day running means.

LIST OF ABBREVIATIONS

AVHRR	Advanced Very High Resolution Radiometers
Aglivc	Above-ground live carbon
BATS	Biosphere-Atmosphere Transfer Scheme
BEST	Bare Essentials of Surface Transfer
Bglivc	Below-ground live carbon
ClimRAMS	Climate Version of RAMS
COLA	Center for Ocean-Land-Atmosphere Studies
DayCENT	Daily Time Step CENTURY
FPAR	Fractional Photosynthetic Active Radiation
GCM	General Circulation Model
IPC	Internal Process Control
ISBA	Interaction Soil-Biosphere-Atmosphere
LAI	Leaf Area Index
LAPS	Land-Air Parameterization Scheme
LEAF	Land Ecosystem-Atmosphere Feedback model
LSM	Land Surface Model
NCAR	National Center for Atmospheric Research
NCDC	National Climatic Data Center
NCEP	National Center for Environmental Prediction
NDVI	Normalized Difference Vegetation Index
PILPS	Project for Intercomparison of Land-surface Parameterization Schemes
RAMS	Regional Atmospheric Modeling System
RegCM	Regional Climate Model
SiB	Simple Biosphere Scheme
SSiB	Simple SiB
SOD	Summary-of-the-Day
SOM	Soil Organic Matter
SR	Simple Ratio
STATSGO	State Soil Geographic Database
VEMAP	Vegetation/Ecosystem Modeling and Analysis Project

Chapter 1

INTRODUCTION

1.1 Importance of Land Surface Processes to the Climate System

Land, covering about one third of the Earth surface, is a major component of the climate system. Although the concept that climatic features determine land surface characteristics has long been accepted, only until relatively recent years have scientists begun to vigorously explore how land surface processes interact with atmospheric circulation and feed back to the climate system.

Most land surfaces are covered by vegetation. There is general agreement on the importance of land surface characteristics on microclimate (Rosenberg et al. 1983; Cotton and Pielke 1995) and the planetary boundary layer (Stull 1988). Gash and Nobre (1997) reviewed the climatological measurements from the Anglo-Brazilian Amazonian Climate Observational Study and found that the difference in radiation and energy balance between forest and clearing produces higher air temperatures in the clearings, particularly in the dry season. In areas of substantial deforestation, higher sensible heat fluxes from the cleared forest produce deeper convective boundary layers, with differences in cloud cover being observed and mesoscale circulations being predicted. Based on low-level flight measurements, Segal et al. (1989) have

shown that the atmospheric boundary layer is shallower, cooler, more moist and less turbulent over irrigated cropland than over adjacent bare soil surfaces. An observational study conducted by Rabin et al. (1990) has shown that convective clouds are first formed over a harvested wheat field surrounded by growing vegetation. In addition, he found that clouds are suppressed immediately downstream over lakes and forests. Koster et al. (1986) have also indicated that the observed growing season precipitation peak may be due, in part, to the local recycling of water. While studying the ecosystem variations and their relationship with the monsoon climate, Fu and Wen (1993) found that monsoon-associated rainfall is a major driving force of terrestrial ecosystems in Asia on various time scales. The observational dataset analyses conducted in this dissertation for the central United States also shows that the interannual variations of Normalized Difference Vegetation Index (NDVI) and precipitation are strongly correlated (see Section 5.3 of Chapter 5 and Figure 5.6).

In addition to the above observational studies, climate models have shown significant sensitivities to land surface characteristics. A typical 5% increase in albedo led to a precipitation reduction of 5% to 20% (Charney 1975; Charney et al. 1977), which demonstrated that the model is sensitive to gross, global-scale changes in specified surface albedo. Changes in soil moisture, roughness length, soil and vegetation characteristics have at least comparable effects (Shukla and Mintz 1982; Sud et al. 1985; Wilson et al. 1987a,b; Meehl and Washington 1988). These experiments, among others, have shown that land surface fluxes to the atmosphere have profound influences on climate model simulation results. More recently, Pielke

et al. (1997a) demonstrates the significant role that land-use change has in generating thunderstorms. Chase et al. (1996, 1999) shows that regional landscape changes in the tropics alter climate not only regionally but also globally by modifying the position and intensity of the mid- and high-latitude polar jet through teleconnection. Xue (1997) investigated the impact of land surface degradation over the Sahel area on seasonal variations of atmospheric and hydrological components over tropical north Africa by using a general circulation model (GCM). He found that the desertification increases the surface air temperature and reduces the precipitation, runoff, and soil moisture over the Sahel region during the summer months. The impact is not only limited to the specified desertification area but also propagates to the south of this area and extends into winter months. Copeland (1996) used a regional climate version of the Regional Atmospheric Modeling System (RAMS) to assess the impact of a natural versus current vegetation distribution on the weather and climate of July 1989. The changes in surface meteorological variables in the modeling study are a consequence of land-use change throughout the United States. The simulated changes in the screen-height quantities were closely related to changes in the vegetation parameters of albedo, roughness length, leaf area index, and fractional coverage.

The seasonal cycle and interannual variation of vegetation exert a strong control over surface atmosphere interactions. Dirmeyer (1994), for instance, showed that inclusion of dormant vegetation during the spring and early summer in a GCM greatly reduces surface moisture fluxes by eliminating transpiration from leaves and also prevents further depletion of moisture in the root zone of soil, which led to a soil

moisture rebound in the middle of summer. Xue (1996) found that the erroneous prescription of crop vegetation phenology in the surface model contributed greatly to the temperature biases of United States summer simulation when using Center for Ocean-Land-Atmosphere Studies' (COLA) GCM. Results from Mearns (1996) suggest the potential importance of representing two-way climate-crop interactions when analyzing the effect of climate change on crop yields. Betts et al. (1996) reported on substantial improvements in the accuracy of numerical weather prediction by a more realistic representation of land surface processes in such models. A range of recent work (Claussen 1994, 1998; Foley 1994; Texier et al. 1997; Claussen et al. 1998) has shown that the initial value specification of the land surface exerts a strong control on the subsequent atmospheric circulation in global and regional climate prediction models (Pielke 1998b).

An extensive review of modeling and observational studies of the importance of landscape processes on weather and climate can be found in Pielke et al. (1998a). The conclusion from these, and other related studies, is that land surface process plays a significant role on local, regional, and global climate.

1.2 Including Land Surface Processes in Climate Models

As early as 1969, Manabe included land in a GCM by characterizing the land as a 0.15 m deep reservoir of water. Deardorff (1978) first introduced the "big leaf" or "bulk vegetation layer" approach to parameterize the vegetated surface in a meteorological model. Up to present, the "big leaf" scheme has been the main type

of vegetation parameterization used in meteorological models.

Since 1980s, many mesoscale and global-scale atmospheric models have been used to study the potential effects of land surface processes on climate and weather. These include, the Biosphere-Atmosphere Transfer Scheme (BATS) of Dickinson et al. (1986, 1993), the Simple Biosphere Scheme (SiB) of Sellers et al. (1986), Simple SiB (SSiB) (Xue et al. 1991), the Bare Essentials of Surface Transfer (BEST) (Pitman 1988; Pitman et al. 1991), Interaction Soil-Biosphere-Atmosphere (ISBA) (Noilhan and Planton 1989), Land Ecosystem-Atmosphere Feedback model (LEAF) (Lee 1992; Walko et al. 1999), Land-Air Parameterization Scheme (LAPS) (Mihailovic 1996), and a Land Surface Model (LSM) of Bonan (1996). A review of the Project for Intercomparison of Land-surface Parameterization Schemes (PILPS), which was designed to improve the hydrological, energy, momentum, and carbon exchanges between the surface and atmosphere, can be found in Henderson-Sellers (1993, 1995).

The RAMS land surface module development history is of particular interest in this dissertation. Based on Deardorff's work, McCumber (1980) developed a vegetation model that was later improved by Avissar and Mahrer (1988), which is generally referred to as "old" LEAF. A modified version of this module became a standard option currently used in RAMS Version 3b and ClimRAMS. Lee (1992) formulated a new and improved land surface model (LEAF) that emphasizes the scaling up of evaporation and transpiration to the canopy scale, and the separation of vegetation and soil surface energy budgets. Incorporating the mosaic idea, the newest generation of land surface model, LEAF-2, has been developed (Walko et al. 1999). It

allows the subdivision of each surface grid cell into multiple patches of distinct land-use types. Each patch interacts with the overlying atmospheric column with a weight proportional to its fractional area in the grid cell.

1.3 The Merit of a Two-way Interactive Approach

Evaluating the two-way interactions between the atmosphere and land surface processes is crucial to our understanding of regional and global climate, vegetation dynamics, and watershed hydrology. Weather and climate have deterministic effects on vegetation growth and decay. At the same time, the land surface plays a key role in partitioning radiative energy received at the Earth's surface. Vegetation, through its transpiration and evaporation, modifies the atmospheric and land surface hydrological processes. Any attempt to simulate the climate system without including vegetated land surface effects is significantly deficient.

The current generation of regional and global climate models already have a land surface component in them. Until recently however, these models, including RAMS, assume that vegetation phenology is predefined according to existing climatologies and time of year. This limits the vegetation-related functions from responding to deviations from mean climatology, such as drier or wetter than average seasons or years, or to changes in climate. The underlying hypothesis for this approach is that the atmosphere has no influence on vegetation growth, and that biogeochemical effects on atmospheric processes are not important. Similarly, biogeochemistry models, such as CENTURY (Parton 1987), prescribe the atmospheric

forcing, thus inherently assuming that the vegetation dynamics have no influence on weather and climate. In contrast to these assumptions, in the real world, vegetation responds strongly to atmospheric solar insolation, temperature, precipitation, and soil moisture. Both atmospheric and soil hydrologic processes, including precipitation and runoff, must be adequately accounted for in order to accurately simulate vegetation growth. In turn, the type and quantity of vegetation strongly influences runoff, evaporation, transpiration, surface heat flux, and consequently the air temperature and development of precipitating systems. The intrinsic two-way interactive feature of the climate-vegetation system requires the coupling of all atmospheric, vegetation, and hydrological processes together into a unified modeling system.

Leaf Area Index (LAI) is defined as the one-sided green leaf area per unit ground area in broadleaf canopies, or as the projected needleleaf area per unit ground area in needle canopies. Although in atmospheric models the hydrological processes (e.g., evaporation and transpiration), energy exchanges (e.g., latent heat and sensible heat fluxes), momentum exchanges (e.g., roughness length), and biophysical parameters (e.g., vegetation albedo, transmissivity and stomatal conductance) at the land surface are generally heavily parameterized based on the value of LAI, very few, if any, climate models account for seasonal and interannual LAI variations. The inadequate and unrealistic description of vegetation evolution is one of the major deficiencies of current land surface models. In this dissertation, a coupled RAMS and CENTURY modeling system is developed and implemented, in which both atmospheric variables (air temperatures, precipitation and relative humidity, etc.) and

ecosystem variables (LAI, vegetation transmissivity, etc.) become prognostic variables in the linked system. The vegetation response to weekly, seasonal, and interannual variations of atmospheric forcings will be simulated and fed back to the atmospheric model. The two-way interactive model will form a sophisticated representation of the coupled atmosphere-land system including relevant aspects of the hydrological cycle.

Incorporating interactive vegetation into a land surface model is a fairly new endeavor. Ji (1995) developed a climate-vegetation interaction model (AVIM) to simulate the seasonal variations of biomass, carbon dioxide, energy and water fluxes for temperate forest ecosystems in northeastern China. Foley et al. (1998) directly coupled the GENESIS (version 2) GCM and IBIS (version 1) Dynamic Global Vegetation Model through a common treatment of land surface and ecophysiological processes. He found that the atmospheric portion of the model correctly simulates the basic zonal distribution of temperature and precipitation with several important regional biases, and the biogeographic vegetation model was able to roughly capture the general placement of forests and grasslands. An interactive canopy model (Dickinson 1998) was derived and added to BATS to describe the seasonal growth of leaf area as needed in an atmospheric model, and to provide carbon fluxes and net primary productivity. This scheme differs from other studies by focusing on short time-scale leaf dynamics. Tsvetsinskaya (1999) introduced daily plant growth and development functions into BATS and coupled it to the National Center for Atmospheric Research Regional Climate Model (NCAR RegCM) to simulate the effect of seasonal plant development and growth on the atmosphere-land-surface heat,

moisture, and momentum exchange. She found that the coupled model is in better agreement with observations compared to the non-interactive mode. Eastman (1999) analyzed the effects of CO_2 and landscape change using a coupled plant and meteorological model (GEMTM and RAMS). All of these early attempts, including the one conducted in this dissertation, demonstrate that both atmosphere and ecology communities have begun to realize that the importance of representing the two-way feedbacks between the atmosphere and biosphere.

The primary research goal of this dissertation is to develop and validate a comprehensive hydrologic-biospheric-atmospheric model that integrates known important land and atmospheric processes into a unified interactive system. It differs from other studies by focusing on regional atmosphere and terrestrial ecosystem interactions occurring on weekly, seasonal, and interannual time scales. Vegetation species composition and community structure changes caused by long-term climate changes are beyond the scope of this study.

Chapter 2

MODEL DESCRIPTION

2.1 Climate Version of RAMS (ClimRAMS)

The Regional Atmospheric Modeling System (RAMS) is a three-dimensional, nonhydrostatic, general purpose atmospheric simulation modeling system consisting of equations of motion, heat, moisture, and mass continuity in a terrain-following coordinate system (Pielke et al. 1992). RAMS was developed at Colorado State University primarily to facilitate research into mesoscale and regional, cloud and land-surface atmospheric phenomena and interactions (Pielke 1974; Tripoli and Cotton 1982; Tremback et al. 1985; Pielke et al. 1992; Nicholls 1995; Walko et al. 1995a). The model is three-dimensional; nonhydrostatic (Tripoli and Cotton 1980); includes telescoping, interactive nested grid capabilities (Clark and Farley 1984; Walko et al. 1995b); supports various turbulence closures (Deardorf 1980; McNider and Pielke 1981; Tripoli and Cotton 1986), short and long-wave radiation (Mahrer and Pielke 1977; Chen and Cotton 1983, 1987; Harrington 1997), initialization (Tremback 1990), and boundary condition schemes (Pielke et al. 1992); includes a land-surface energy balance sub-model which accounts for vegetation, open water, and snow-related surface fluxes (Mahrer and Pielke 1977; McCumber and Pielke 1981; Tremback and

Kessler 1985; Avissar and Mahrer 1988; Lee 1992; Liston et al. 1998); and includes explicit cloud microphysical sub-models describing liquid and ice processes related to clouds and precipitation (Meyers et al. 1992; Meyers 1995; Walko et al. 1995a). A modified Kuo (1974) scheme is used for convection-produced precipitation. The RAMS horizontal grid uses a oblique (or rotated) polar-stereographic projection, where the projection pole is near the center of the simulation domain. The vertical grid uses σ_z terrain-following coordinate system (Gal-Chen and Somerville 1975; Clark 1977; Tripoli and Cotton 1982), where the top of the model is flat and the bottom follows the terrain. An Arakawa-C grid configuration is used in the model, where the velocity components u, v, and w are defined at locations staggered one-half a grid length in the x, y, and z directions, respectively, from the thermodynamic, moisture, and pressure variables (Arakawa and Lamb 1977).

The climate version of RAMS (Liston and Pielke 1999) used in this study contains all of the above features, with the addition of several modifications designed to allow single to multi-year integrations. To meet the requirements of a regional model running at both short and long time scales, several modifications to the base modeling system were made. These included: 1) daily updating of sea-surface temperatures and vegetation parameters throughout each year; 2) the addition of a collection of routines which simulates grid-scale snow accumulation, snow melt, and their effects on surface hydrology and surface energy exchanges; 3) the implementation of the "dump-bucket" parameterization scheme (Rhea 1978; Cotton et al. 1995) to account for large-scale precipitation; and 4) the Mahrer and Pielke (1977)

shortwave and longwave radiation model is used in conjunction with the scheme presented by Thompson (1993) to account for the presence of clouds. In addition, sufficient variables to perform complete surface energy and moisture balances over a wide range of time scales (hourly to yearly) are saved, and other data are saved on an hourly, six-hourly, or daily basis, depending on the model-output variable.

The soil sub-model used in this version of RAMS provides prognostic temperature and moisture for both soil and vegetation. For bare soil, RAMS uses a multi-layer soil model described by Tremback and Kessler (1985). The moisture diffusivity, hydrologic conductivity, and moisture potential are given by Clapp and Hornberger (1978). The thermal properties of the soil are a function of the soil moisture. The boundary condition for moisture at the deepest soil level is held constant in time and equal to the initial value. The temperature of the bottom soil layer varies following the deep-soil temperature model of Deardorff (1978). For the vegetated surface, RAMS uses the "big leaf" approach where there is a layer of vegetation overlying a shaded soil (Avissar and Mahrer 1988). The moisture taken from soil by transpiration is accomplished by defining a vertical root profile (Dickinson et al. 1986) and extracting the water masses from the soil depending on the fraction of roots in each soil layer. The surface-layer fluxes of heat, momentum, and water vapor are computed using the method of Louise (1979, 1982), who fitted analytical curves to the flux-profile relationships determined by Businger et al. (1971).

ClimRAMS uses the lateral boundary conditions derived from the output of large-scale atmospheric analysis models (such as ECMWF analyses, NCEP reanalyses)

or a GCM.

2.2 Daily Time Step CENTURY (DayCENT)

Since the mid-1980s, the CENTURY model has been developed, modified, and applied to simulate various ecosystem dynamics over a wide range of spacial and temporal scales.

CENTURY is a biogeochemistry model that was originally designed to simulate long-term dynamics of carbon (C), nitrogen (N), phosphorous (P), and sulfur (S) for different plant-soil systems (Parton et al. 1987, 1988, 1993, 1994a, b, 1995, 1996; Ojima et al. 1993, 1994; Parton and Rasmussen 1994; Parton 1996). The grassland, agriculture crop, forest, and savanna ecosystems have different plant production submodels which are linked to a common soil organic matter submodel (SOM). The SOM simulates the flow of C, N, P and S through plant litter and the different inorganic and organic pools in the soil. The model includes three soil organic matter pools (active, slow and passive) with different potential decomposition rates, above and below-ground litter pools, and a surface microbial pool which is associated with decomposing surface litter. The plant production models assume that plant production is controlled by moisture and temperature, and that plant production rates are decreased if nutrient supplies are insufficient. The fraction of the mineralized pools that are available for plant growth is a function of the root biomass increases.

CENTURY version 4 (Parton 1996) uses a monthly time step and the major input variables for the model include: (1) monthly average maximum and minimum

temperature, (2) monthly precipitation, (3) lignin content of plant material, (4) plant N, P, and S content, (5) soil texture, (6) atmospheric and soil N inputs, and (7) initial soil C, N, P, and S levels. The input variables are available for most natural and agricultural ecosystems and can generally be estimated from existing literature (Parton et al. 1987). The databases required to specify the land-use types, major input variables, and management options are illustrated in Figure 2.1. At the same time, Figure 2.2 further demonstrates how the human management practices modify and interact with the major CENTURY sub-models.

For this study, we use a new version of CENTURY called DayCENT (Parton et al. 1998; Kelly et al. 1998). It is based on CENTURY Version 4 (Parton 1996) described above, and is designed to simulate more temporally-resolved ecological processes. The primary difference between CENTURY and DayCENT lies in the water model and the computation of other processes on a finer time scale. DayCENT uses a daily time step for the water and nutrient cycles, and the above-ground and below-ground biomass are updated weekly.

In DayCENT, a daily water flow submodel and a daily soil temperature submodel are incorporated to compute soil water content and temperature by depth; these submodels replace the monthly water budget and soil surface temperature submodel in CENTURY (Figure 2.3). Decomposition occurrs daily instead of weekly, and organic and inorganic leaching occurs daily instead of monthly. Potential production estimates and growth of trees, crops, and grasses are updated weekly instead of monthly. New equations for the impact of water and temperature on

decomposition have been implemented. When daily solar radiation, relative humidity, and wind speed climate forcings are available, DayCENT uses a Penman potential evapotranspiration calculation (Penman 1948); otherwise it uses the air temperature-based Linacre calculation (Linacre 1977; Parton 1993) from the CENTURY model. Event scheduling is adjusted to accommodate multiple time steps in a given month. When an event or management practice was scheduled for a given month, it either occurs weekly (irrigation), on the first week of the month (organic matter addition, fertilization, and cultivation), or on the last week of the month (grazing, fire, tree removal, harvest).

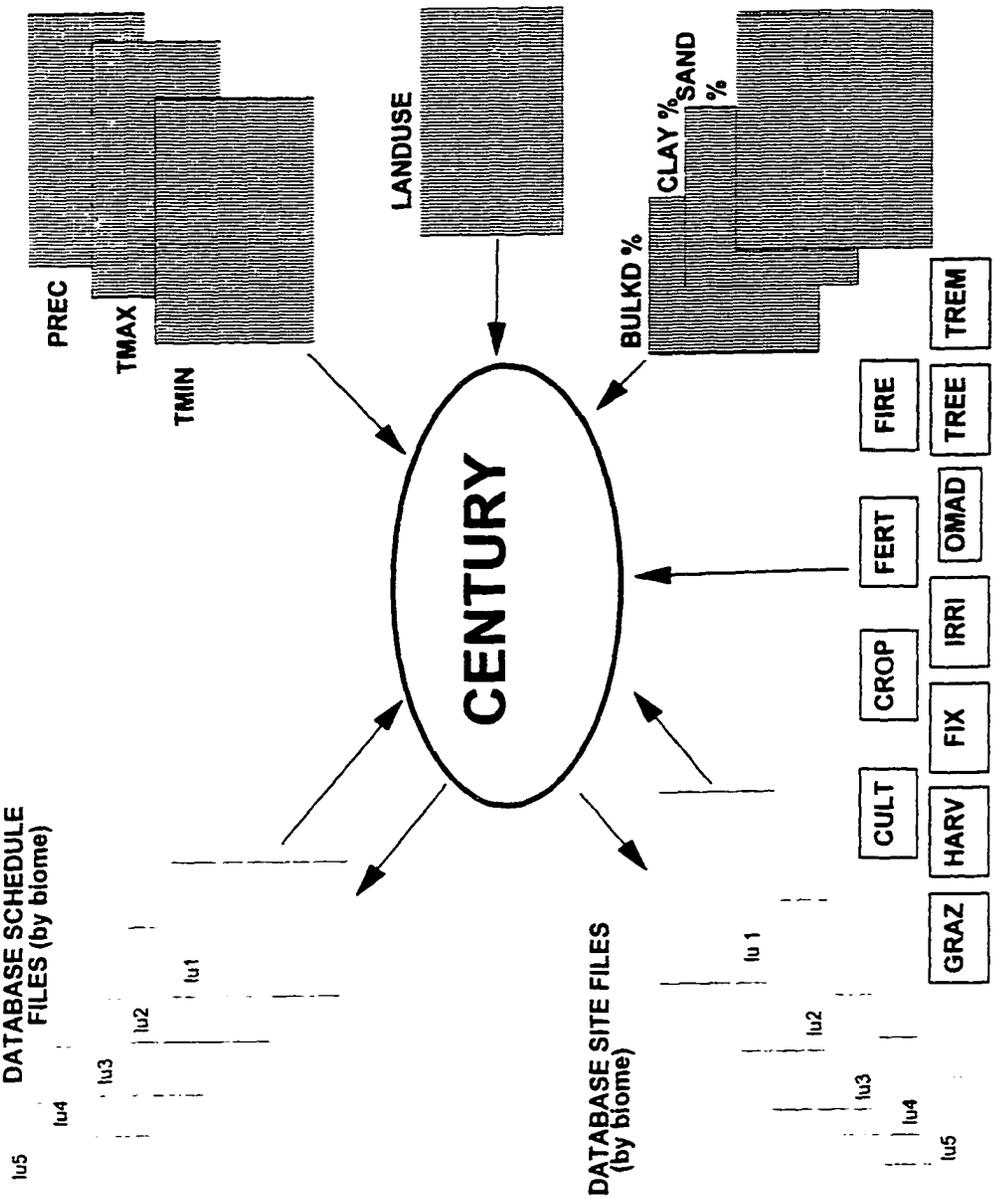

Figure 2.1 Simple conceptual diagram showing the structure of CENTURY Version 4 (Metherell 1993).

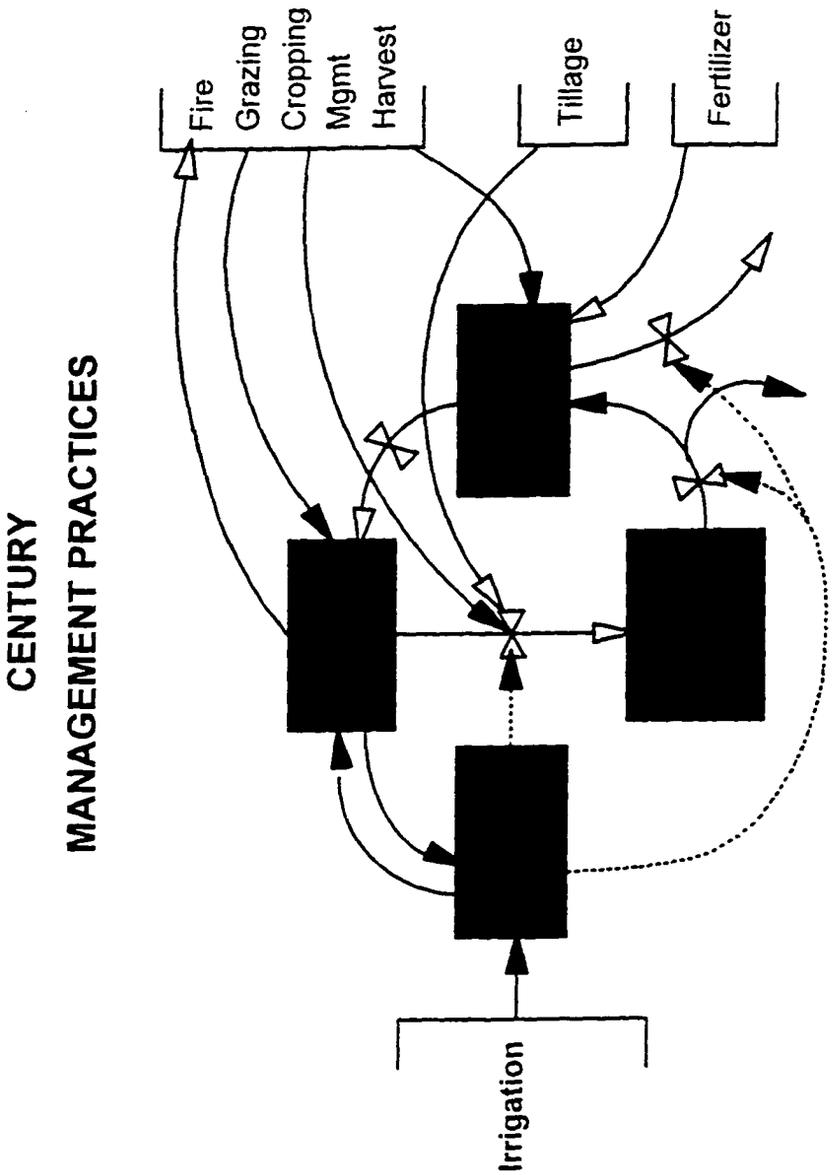

Figure 2.2 Simple conceptual diagram showing the human management practices and their interrelation with the major CENTURY sub-models (Metherell 1993).

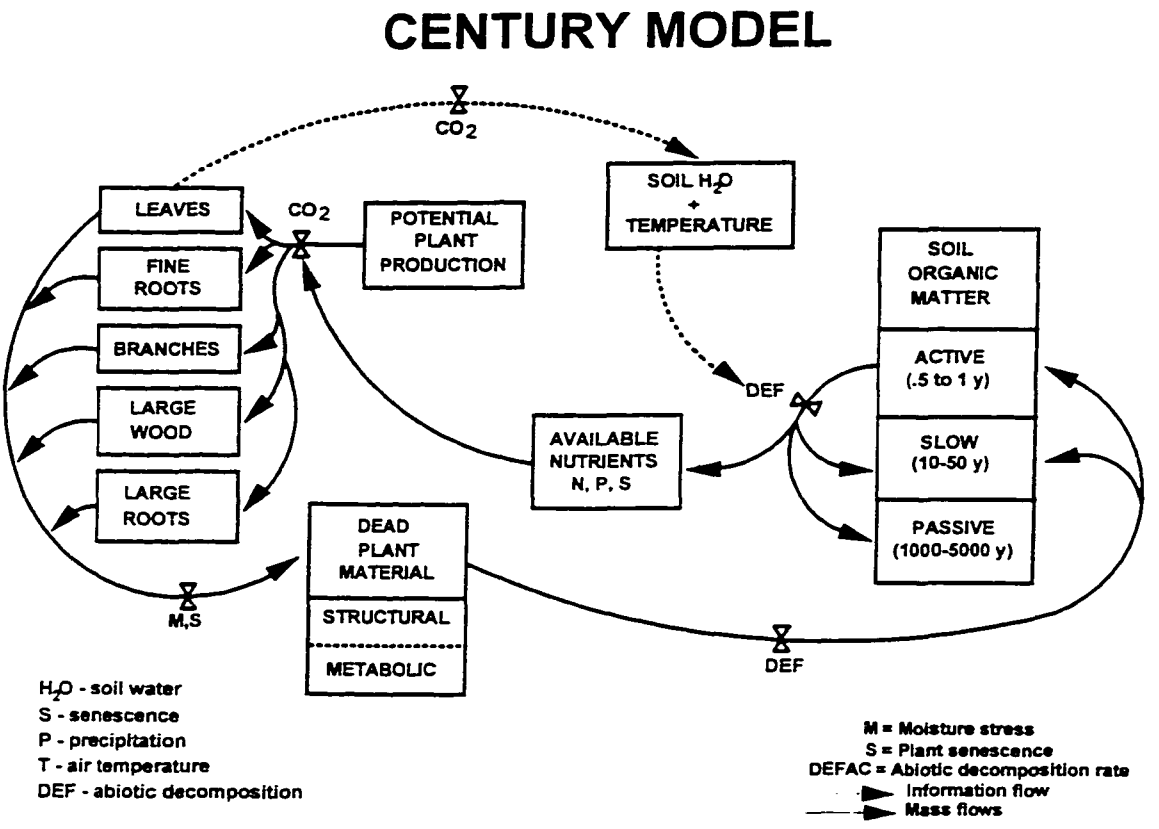

Figure 2.3 Simple conceptual diagram of the DayCENT model (Kelly 1998).

Chapter 3

Offline SENSITIVITY EXPERIMENTS

3.1 "One-at-a-time" Perturbation Approach

The purpose of the offline sensitivity analyses is to investigate the responses of the models to perturbations in the input variables. The most common approach employed for sensitivity analyses has been to conduct a "one-at-a-time" perturbation of each parameter from its standard value to some "large" and "small" values, while all other parameters are kept fixed. By investigating these responses, it helps to better understand the behavior of a complex system and to examine whether the model behavior is consistent with real-world experience.

3.2 Sensitivities of RAMS to Changes in LAI

A series of ClimRAMS simulations were conducted to examine the sensitivities of climate variables, such as maximum temperature, minimum temperature, and precipitation, to the changes of LAI. A control run was first integrated from 1 June 1989 through early 1990 based on a prescribed LAI curve. Then two perturbation experiments were performed with the LAI value reduced by 50% and 25% of its original value. Figure 3.1(a) shows that screen-height maximum air temperature

increases in a nearly uniform manner, while LAI decreases. The vegetation's cooling effects appear to dominate the processes so that the decreased vegetation cover led to the increased surface temperature. Shown in Figure 3.1(b) are the sensitivities of daily precipitation to LAI changes. In summer there are several mm day^{-1} differences in rainfall between the runs which have the higher and lower LAIs. Vegetation directly influences transpiration of water to the atmosphere. At the same time, its existence alters the surface energy budget through modifying the surface albedo and Bowen ratio. Also, the feedback between precipitation and LAI is rather complex and non-linear.

3.3 Sensitivities of CENTURY to Changes in Atmospheric Forcings

CENTURY Version 4 was used to investigate the ecosystem model's sensitivities to changes in atmospheric forcings. CENTURY was driven by observed monthly averaged atmospheric forcings of maximum surface temperature (Tmax), minimum surface temperature (Tmin), and precipitation, and CENTURY outputs the biomass growth. A simple algorithm (discussed in Section 6.1 of Chapter 6) was then applied to convert above-ground live carbon to LAI. All the integrations start in January 1973 and continue through December 1988. The model is running on a monthly time step. Besides the control simulation, six sensitivity runs were conducted with Tmax and Tmin increased and decreased 2 °C, and precipitation increased or decreased 25%, from their original values.

The CENTURY simulated LAI from 1973 to 1988 over Konza, Kansas is

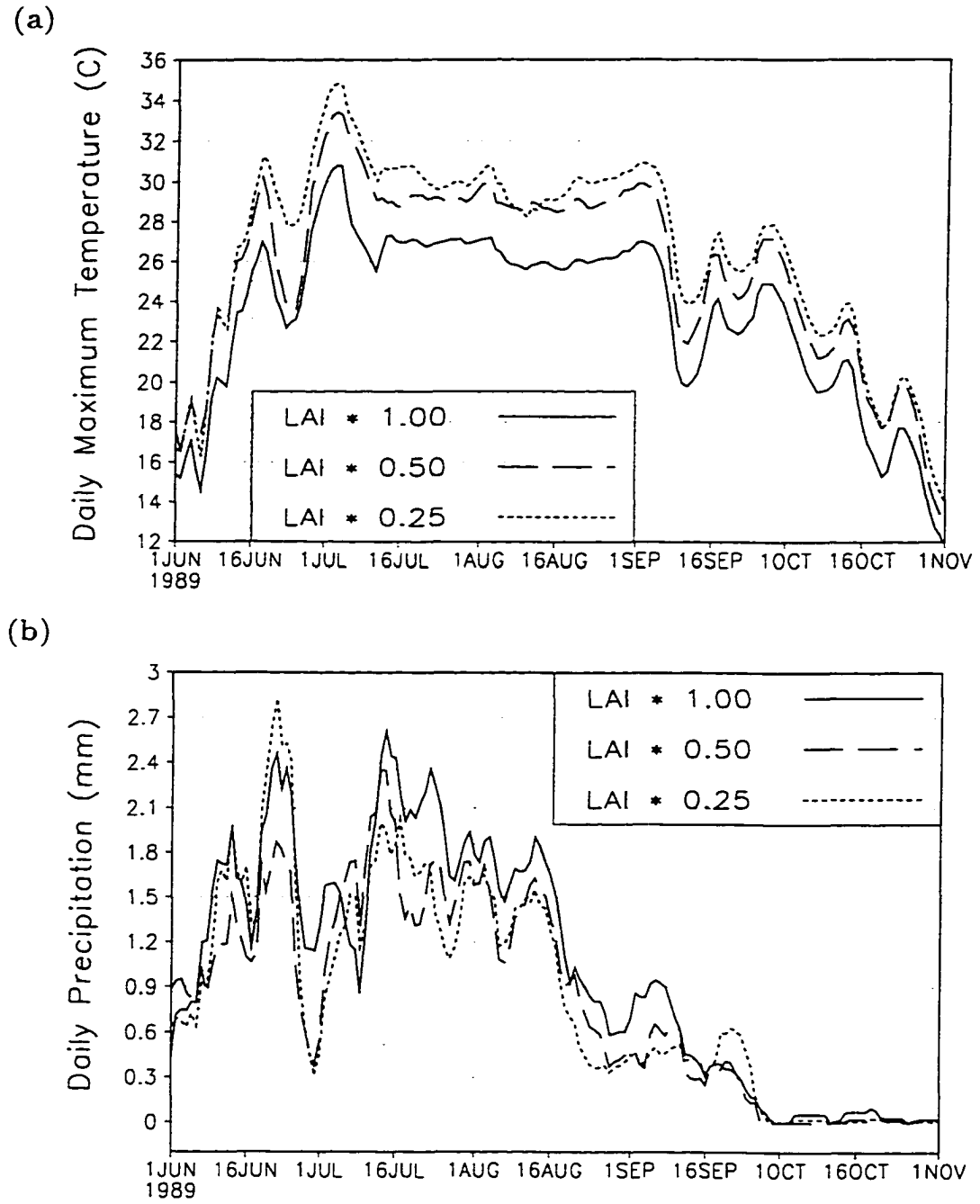

Figure 3.1 (a) The effect of changing leaf area index (LAI) on daily maximum temperature (°C) over Colorado. (b) The effect of changing leaf area index (LAI) on daily precipitation (mm) over Colorado.

shown in Figure 3.2 (a). Large LAI interannual variation clearly occurs in the simulation time span. *This suggests that the prescribed LAI curves used in climate models, which does not vary between different years, are unrealistic and misleading.* Thus, surface fluxes parameterized based on interannually invariant LAI must be incorrect. Errors induced by unrealistic LAI specification in atmospheric models are inevitable. Figure 3.2 (b) shows very significant, up to 50%, LAI changes resulting from a 25% precipitation change. The solid curves indicate the LAI change when precipitation was decreased by 25% and the dashed curves indicate the LAI change when precipitation was increased by 25%. LAI is also sensitive to the Tmax and Tmin changes, but by a smaller magnitude (Figure 3.3 (a) and (b)). The above-ground live carbon (Aglivc) production increases with temperature to a certain threshold, which is vegetation-type dependant. If temperature continues to increase above the threshold, Aglivc begins to decrease. This explains why the temperature increase does not always lead to increased above-ground biomass production.

Figure 3.4 (a) shows the large interannual variations of root biomass production from 1973 to 1988. An interesting feature stands out if you compare the below-ground live carbon (Bglivc) in Figure 3.4 (a) against Aglivc in Figure 3.2 (a). 1977 is a dry year and had the lowest leaf and root production of the whole simulation period. The leaf production recovered immediately in the following year and reached a new LAI maximum compared to the previous years; while root biomass started to recover but the production never exceeded the previous years. The comparison between leaf and root maxima during the simulation time-span demonstrates *that roots react to*

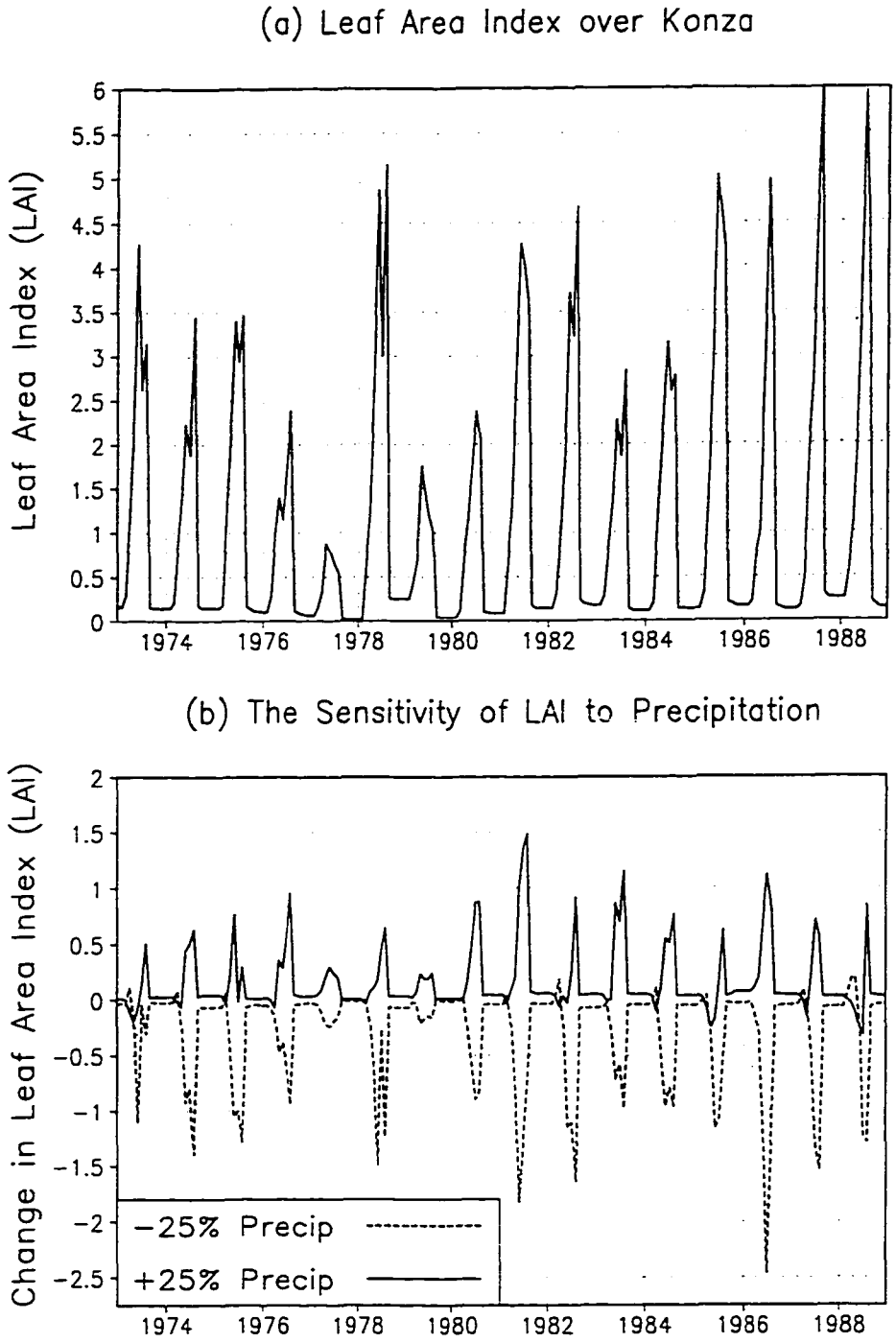

Figure 3.2 (a) CENTURY-simulated leaf area index (LAI) over Konza, Kansas, from 1973 to 1988. (b) The changes of LAI from the control run when precipitation was increased and decreased by 25%.

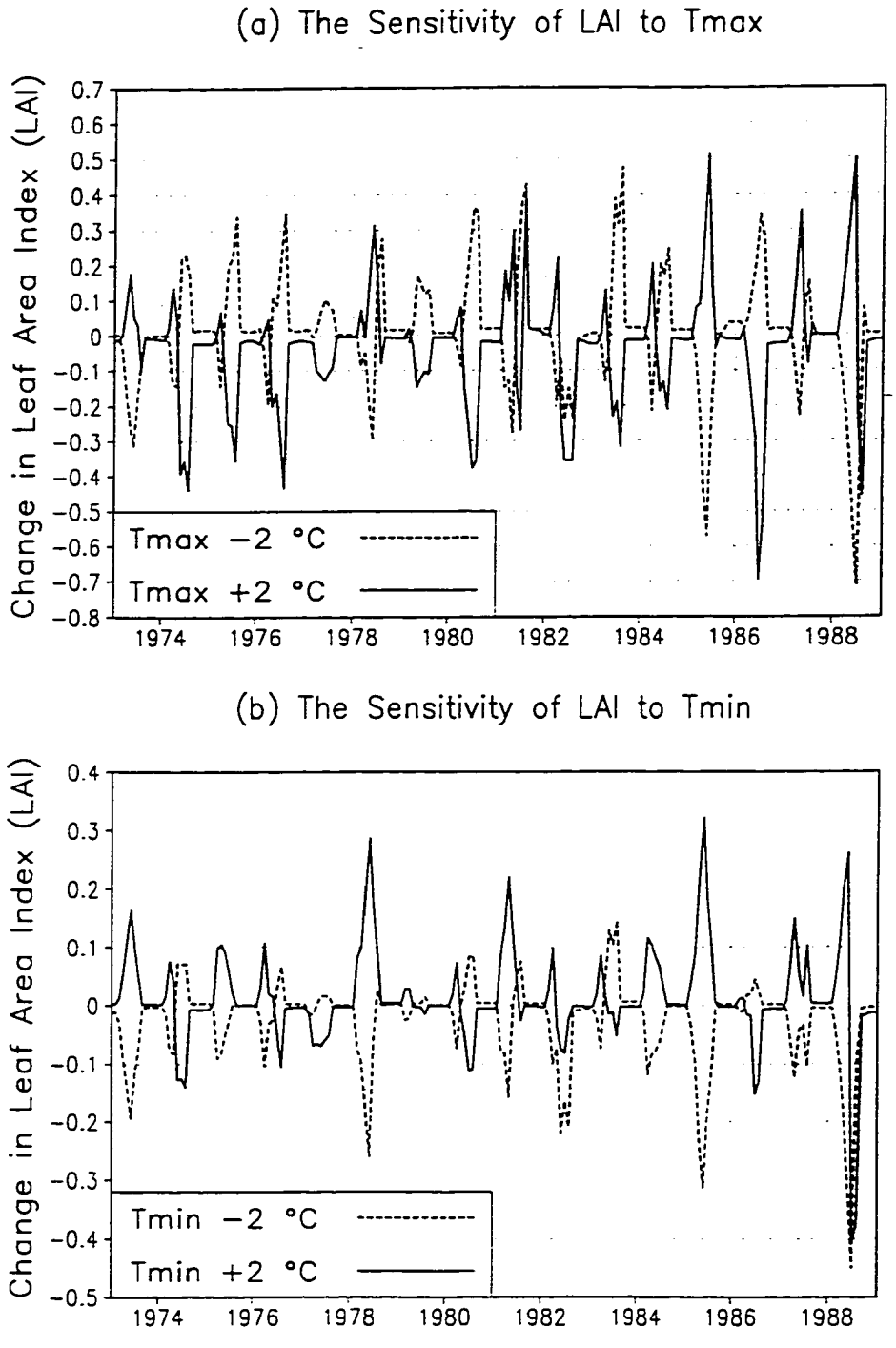

Figure 3.3 (a) Changes in leaf area index (LAI) from the control run when maximum screen-height air temperature was increased and decreased 2 °C. (b) Changes in leaf area index (LAI) from the control run when minimum screen-height air temperature was increased and decreased 2 °C.

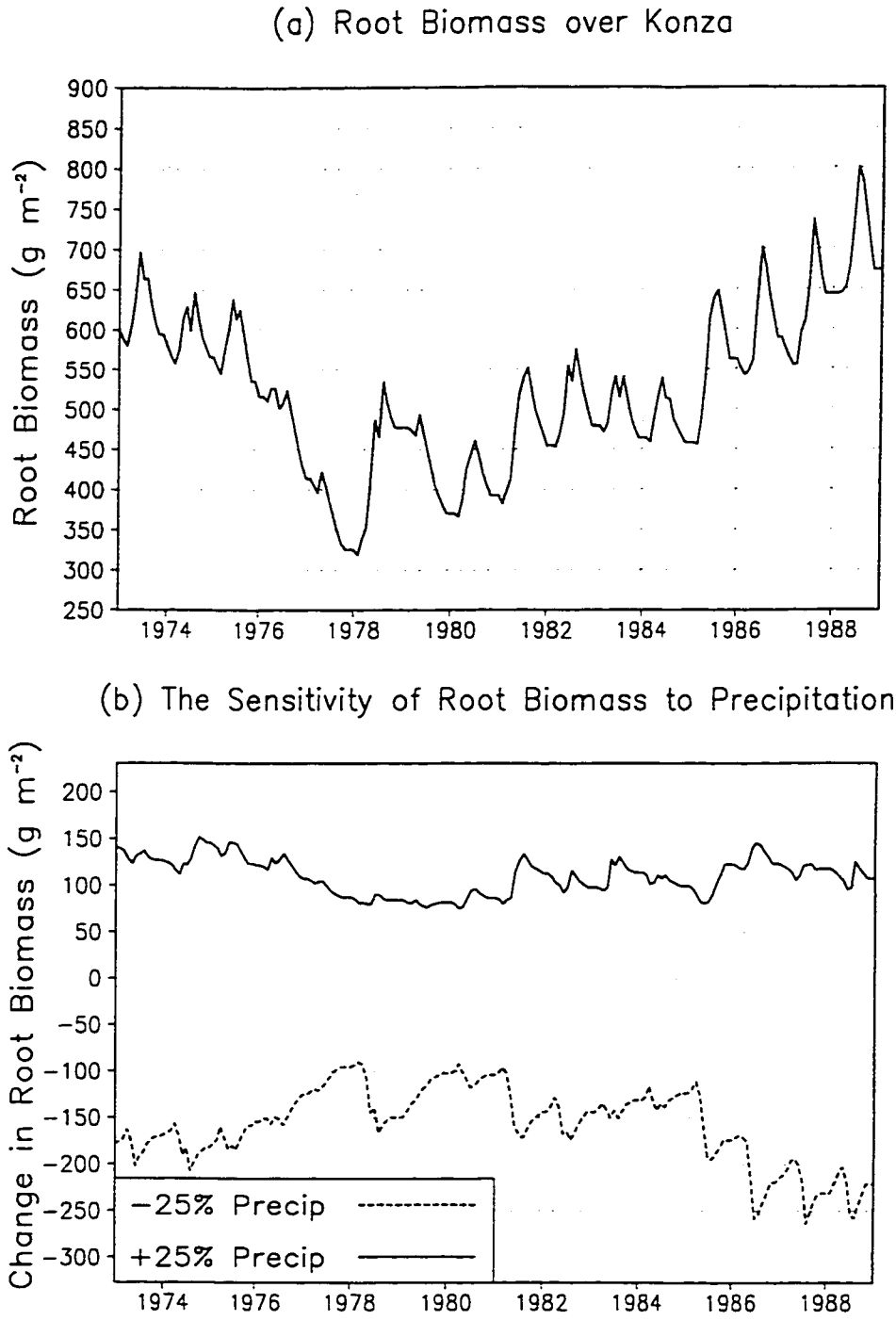

Figure 3.4 (a) CENTURY-simulated below-ground live carbon (roots), g m^{-2}, over Konza, Kansas, from 1973 to 1988. (b) Changes in below-ground live carbon from the control run when precipitation was increased and decreased by 25%.

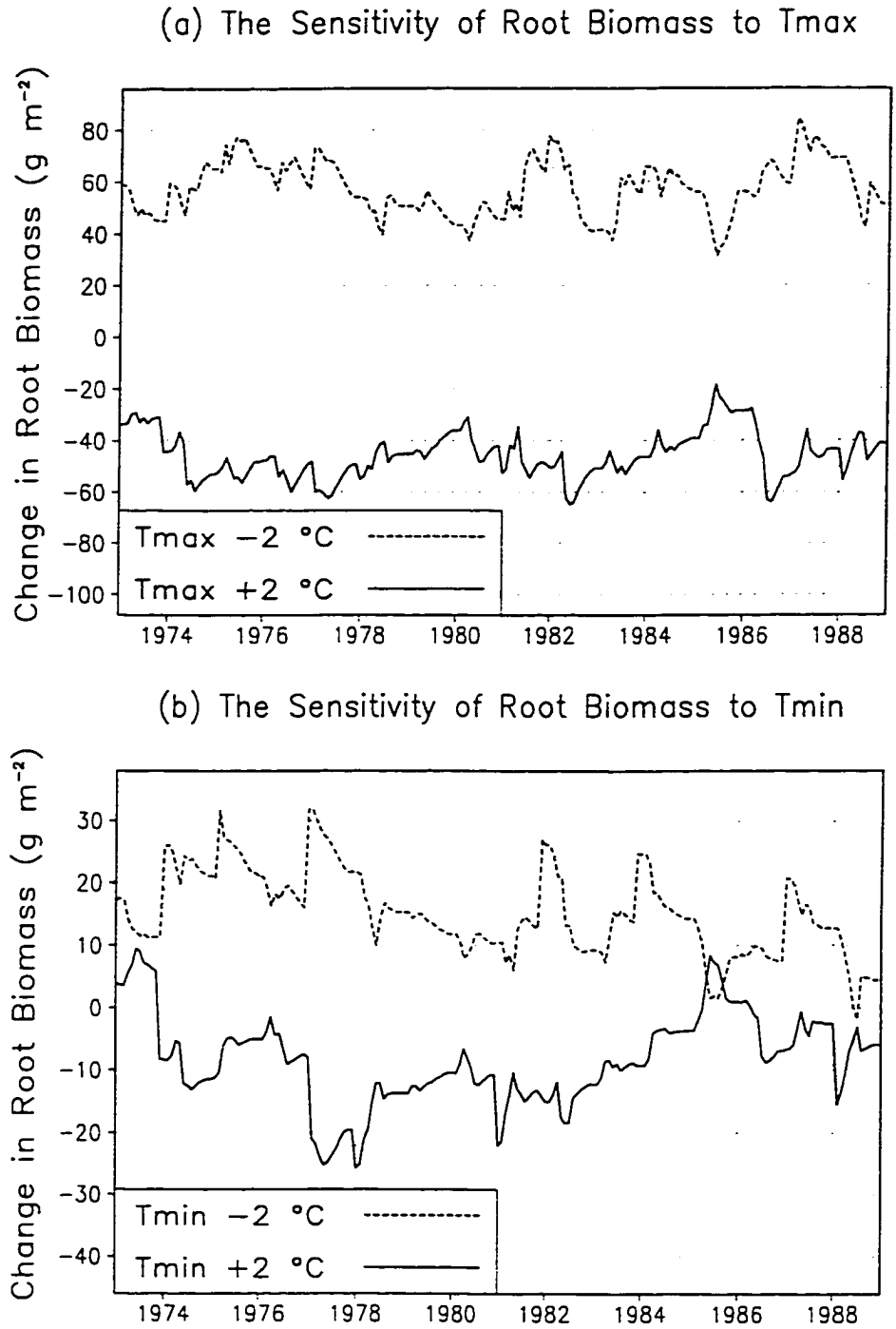

Figure 3.5 (a) Changes in below-ground live carbon (roots), g m^{-2}, from the control run when maximum screen-height air temperature was increased and decreased 2 °C. (b) Changes in below-ground live carbon (roots), g m^{-2}, from the control run when minimum screen-height air temperature was increased and decreased 2 °C.

climate variations at a slower pace and with a smaller magnitude, indicating the "buffering effect" roots might play within a plant system. The other implication is that atmosphere-vegetation interactions exist on different time scales, with short-term feedbacks represented by the leaf and long-term feedbacks represented by the roots. Figure 3.4 (b) and Figure 3.5 (a) and (b) show that root biomass is most sensitive to precipitation, less to Tmax, and least to Tmin. Increased precipitation always grows more roots, while increased temperature reduces root production.

3.4 Conclusion

Offline sensitivity experiments were performed with both atmospheric (ClimRAMS) and ecological (CENTURY) models. The results demonstrate that modifications to the prescribed LAI significantly affects the climate model simulation of temperature and precipitation. Correspondingly, variations in the prescribed climate forcings, such as temperature and precipitation, dramatically influences the biogeochemistry model simulation of above-ground and below-ground biomass. The fact that the two models are sensitive to the output of the other supports the premise that significant feedbacks exist between the atmosphere and terrestrial ecosystem. The conclusion, therefore, is that vegetation dynamics interact with weather and climate through a coupled and nonlinear manner. To account for the two-way feedbacks and provide a better representation of the integrated climate-ecological system, RAMS and CENTURY has been dynamically linked.

Chapter 4

IMPLEMENTATION OF THE COUPLED RAMS/CENTURY MODELING SYSTEM

4.1 Coupling Strategies and Procedures

ClimRAMS and DayCENT are very different models since they represent different physical and biological processes associated with land-atmosphere interactions. ClimRAMS is a three-dimensional model running on approximately minute time scales, while DayCENT is a one-dimensional model running on a daily time step. In terms of plant growth, vegetation needs more time to evolve and react to the atmospheric forcings. From an engineering point of view, it is the slowest process that determines the pace of the feedbacks within an integrated system. Therefore, the coupled model was designed to exchange information on a weekly time step. Table 4.1 summarizes the variables exchanged between the two models; variables marked with stars have not yet been included in the simulations discussed herein.

At the end of every week, ClimRAMS computes a week's worth of daily air temperature, precipitation, radiation, wind speed, and relative humidity and passes them to DayCENT. Then driven by daily atmospheric forcings, DayCENT computes the leaf area index and vegetation transmissivity daily and return the end of the week

values to ClimRAMS. In this way, vegetation responds to weekly and seasonal atmospheric changes, and the atmosphere is able to respond to the associated vegetation changes.

Table 4.1 Information exchanged between ClimRAMS and DayCENT. The variables marked with stars have not been included in the simulations discussed herein.

Climate RAMS	Daily CENTURY
Precipitation	LAI (Leaf Area Index)
Maximum Temperature	Vegetation Transmissivity
Minimum Temperature	*Vegetation Fraction
Incoming Solar Radiation	*Vegetation Albedo
Relative Humidity	*Vegetation Roughness (Z0)
Wind Speed	*Vegetation Displacement Height
*Cloud Coverage	*Root Distribution

Because of the differences in temporal and spatial resolutions of the two models, computational obstacles need to be overcome. The coupling between ClimRAMS and DayCENT has been performed for the finer grid in Figure 4.2. Each grid cell of Grid #2 runs its own DayCENT model according to the land-use type and the atmospheric conditions passed from ClimRAMS. The online coupling between ClimRAMS and DayCENT is achieved through an internet stream socket and client/server mechanism (Stevens 1998). ClimRAMS works as a server to control the timing of the model runs, and DayCENT is a client to be initiated by calls from Internal Process Control (IPC) programs. This innovative idea allows the linked

models to communicate dynamically and efficiently with each other without changing their original platforms.

During the initial testing period, ClimRAMS was run on an IBM RS 6000 workstation at the Foothill Campus at Colorado State University and DayCENT was run on a HP 9000 workstation on Main Campus. It took 16 CPU days for the coupled modeling system to integrate for one year. The simulation relied heavily on the history-restart mechanism since the network connection between the main campus and foothill campus was rarely free of trouble in a period of two weeks. Currently, the two models are run on a two-processor SUN Ultra-2 workstation, where only a local network connection is needed. This reduces the coupled-model annual integration to seven CPU days.

Figure 4.1 is the flow diagram describing the coupling procedures and the information exchanged between the two models. The coupling procedures can be summarized into the following steps: (1) ClimRAMS starts, uses the initial LAI value generated by DayCENT's spin up, integrates for one week; (2) ClimRAMS stops integration; (3) ClimRAMS calls DayCENT, passes one week's weather to DayCENT; (4) DayCENT starts, the ecosystem evolves for a week according to the weather passed from ClimRAMS, DayCENT generates new LAIs and passes them to ClimRAMS; (5) DayCENT stops; (6) ClimRAMS receives new LAIs, starts again, integrates for a week. Steps (2) through (6) are repeated until the simulation finishes.

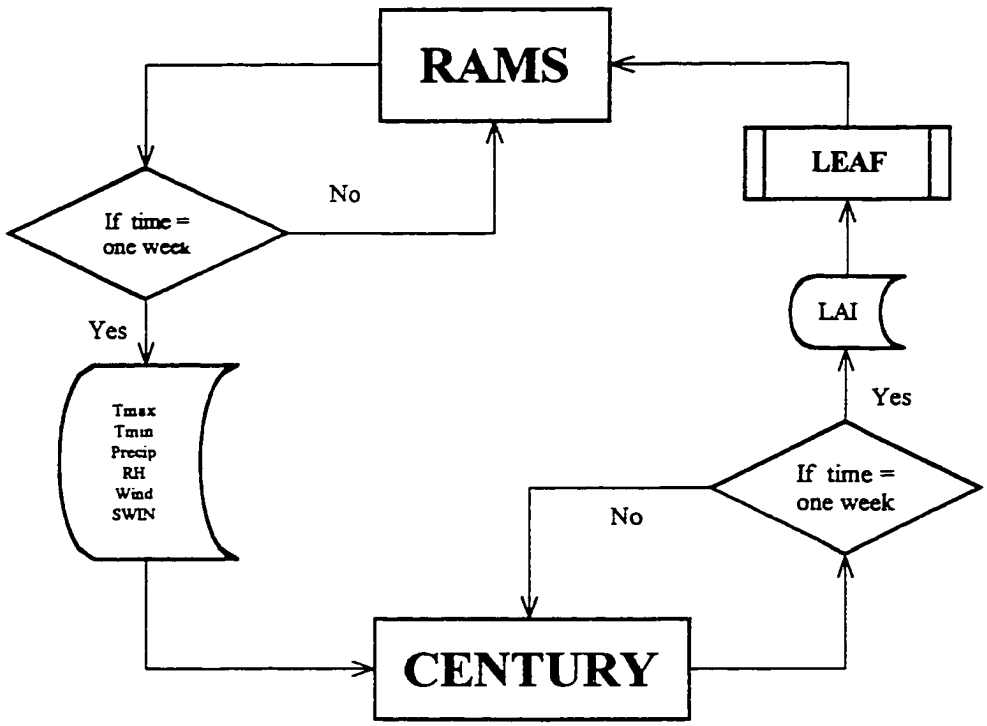

Figure 4.1 The flow diagram of the coupled RAMS and CENTURY modeling system.

4.2 Control Run Design

4.2.1 Simulation Domain and Grid Configuration

The coupled model domain and grid configuration are given in Figure 4.2, which shows a coarse grid covering the entire conterminous United States at 200 km grid spacing, and a finer nested grid covering Kansas, Nebraska, South Dakota, Wyoming, and Colorado at 50 km grid spacing. This region was chosen for several reasons. First, it has rather complex topographic features, covering parts of the Great Plains and the Rocky Mountains. The topographic distribution for the fine grid in Figure 4.2 is given in Figure 4.3. Second, it has rather diversified land-use types including C3 and C4 grassland, various agricultural croplands, evergreen needleleaf trees, shrubland, and tundra; a total of thirty land-use types as defined by Vegetation/Ecosystem Modeling and Analysis Project (VEMAP) database. The vegetation distribution for the fine grid in Figure 4.2 is given in Figure 4.4. The land-use types from DayCENT are derived from VEMAP (Kittel 1996) data set, and then they are converted to the BATS 18 vegetation classes through a look up table (Table 4.2).

A significant deficiency with the BATS classification is its lack of spatial heterogeity within a given vegetation category. For instance, there is no difference between the grassland growing in northern Wyoming and in southern Kansas. Thus, the two regions will, unrealistically, have the same LAI specification. When coupling with the DayCENT ecological model, vegetation growth is controlled by land-use type, site-specific geographic information, and climate forcings. *This implies that LAI*

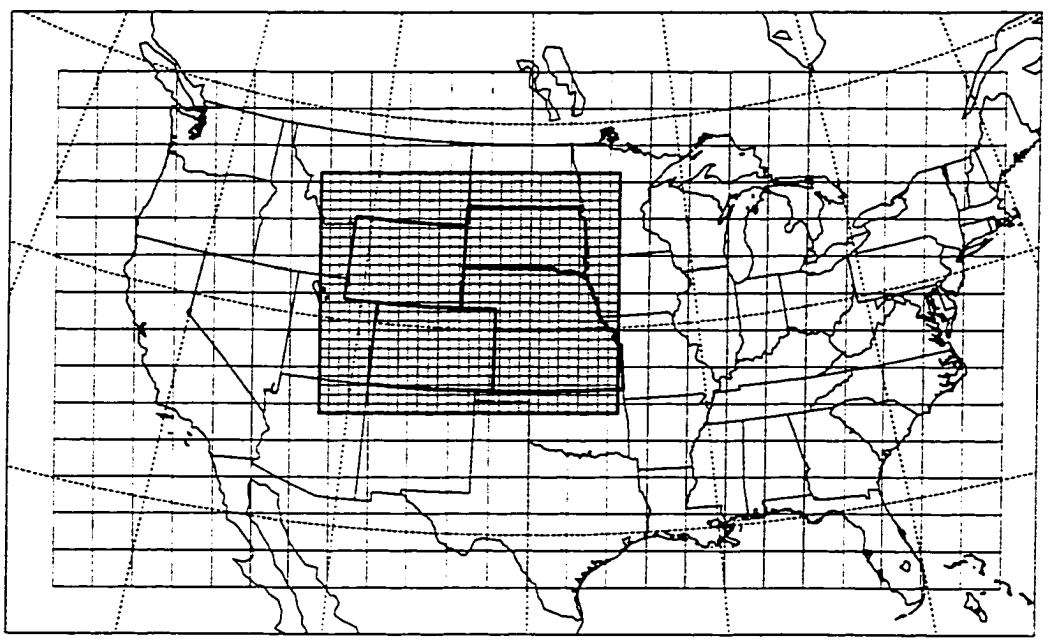

Figure 4.2 Coupled RAMS/CENTURY simulation domain and grid configuration. The coarse and fine grid intervals are 200 km and 50 km, respectively.

TOPOGRAPHY OF RAMS GRID 2

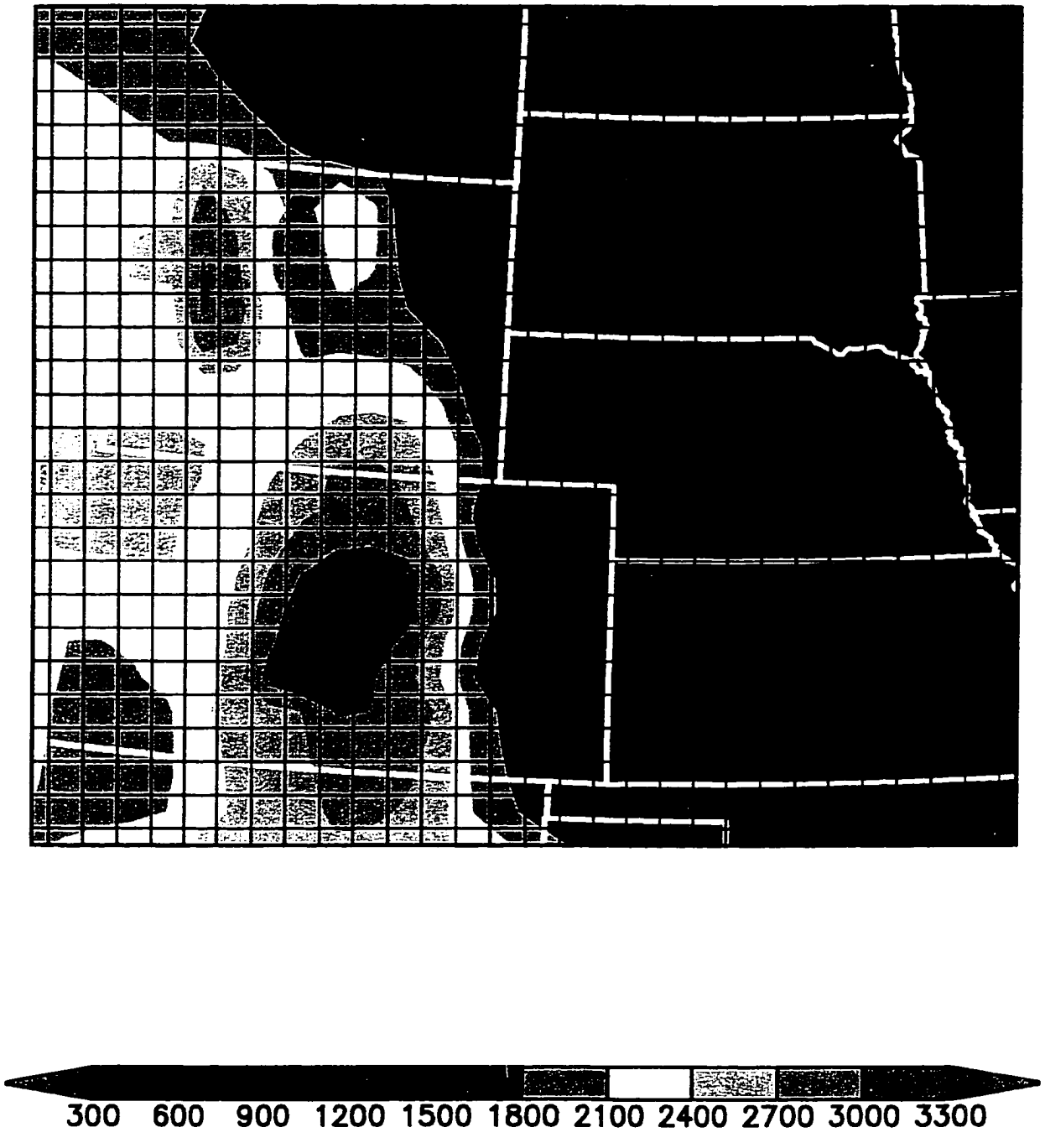

Figure 4.3 The topographic distribution for the fine grid in Figure 4.2.

VEGETATION CLASSIFICATION

(Current Vegmap, Converted from CENTURY to RAMS)

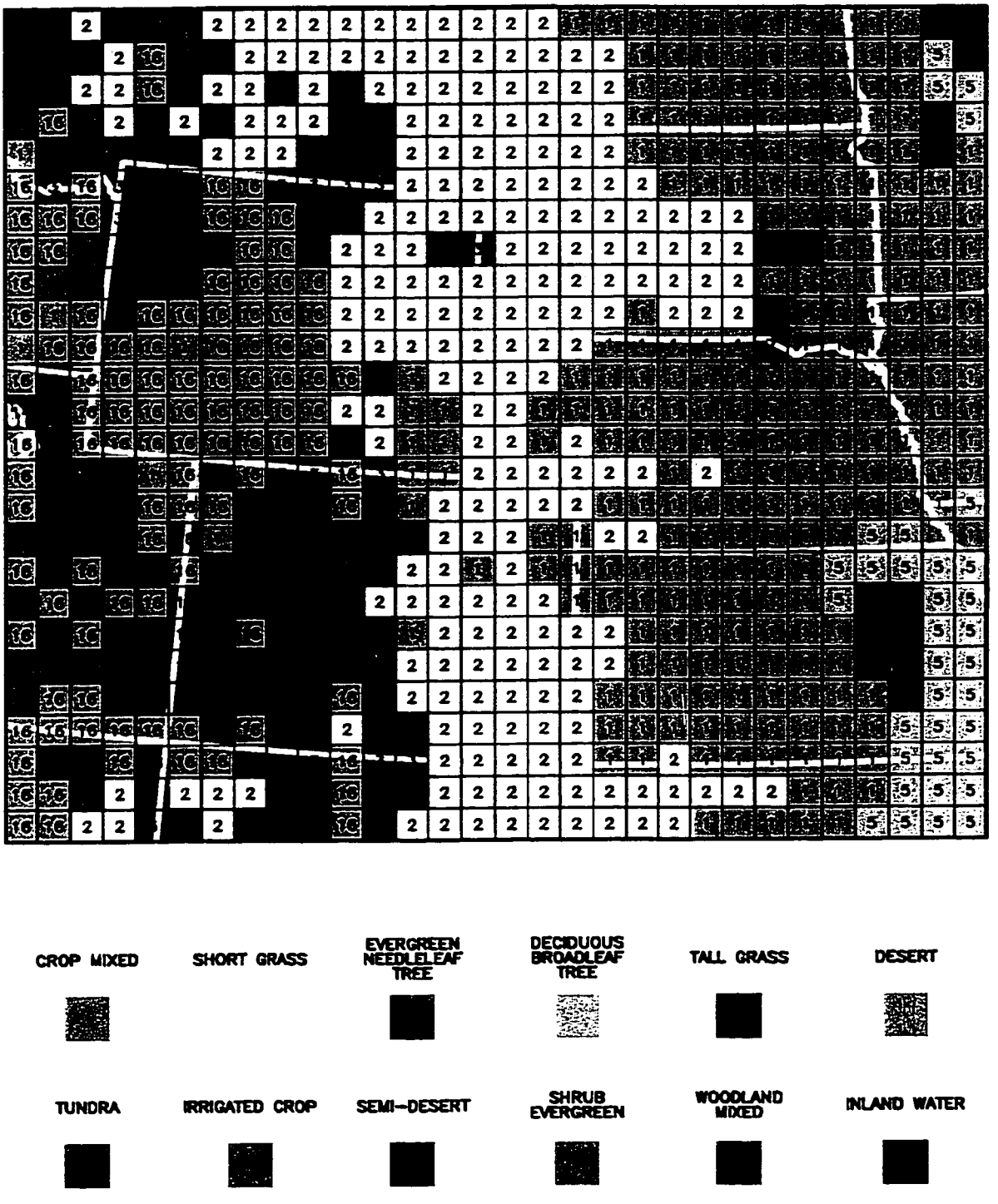

Figure 4.4 The vegetation distribution for the fine grid in figure 4.2.

Table 4.2 RAMS and CENTURY Vegetation Class Conversion Table (xx implies no equivalent classification).

RAMS Classification	DayCENT Classification
1 - Crop/mixed farming	101 - Spring wheat and northern small grains 102 - Small grains 103 - Winter wheat 104 - Corn belt 105 - Southern corn and mixed crops 118 - Grassland and small grain wheat
2 - Short grass	17 - C3 grassland (include short and tall) 18 - C4 grassland (include short and tall)
3 - Evergreen needleleaf tree	4 - Temperate continental coniferous forest 2 - Boreal coniferous forest
4 - Deciduous needleleaf tree	xx
5 - Deciduous broadleaf tree	7 - Temperate deciduous forest 13 - Temperate deciduous savanna 114 - Temperate deciduous forest and corn belt 115 - Temperate deciduous forest and southern corn and mixed crops 116 - Warm temperate/subtropical mixed forest and southern corn and mixed crops
6 - Evergreen broadleaf tree	xx
7 - Tall grass	18 - C4 grassland (include short and tall) 17 - C3 grassland (include short and tall)
8 - Desert	xx
9 - Tundra	1 - Tundra
10 - Irrigated crops	106 - Irrigated crops
11 - Semi-desert	xx
12 - Ice cap/glacier	xx
13 - Bog or marsh	xx
14 - Inland water	91 - Inland water
15 - Ocean	xx
16 - Evergreen shrub	20 - Temperate arid shrubland
17 - Deciduous shrub	20 - Temperate arid shrubland
18 - Mixed woodland	10 - Temperate mixed xeromorphic woodland 11 - Temperate conifer xeromorphic woodland

specification in the coupled system has taken the spatial features of the same vegetation type into account.

The finer grid covers an area of 1,500 km in the east-west direction and 1,300 km in the north-south direction, respectively. The pole point for the oblique polar stereographic projection used to define the grid is 40° N latitude and 100° W longitude. There are 20 vertical levels with a thickness of 119 meters at the surface, stretching to 2,000 meters at the 23-km domain top. The model is driven by six-hourly lateral boundary conditions derived from National Centers for Environmental Prediction (NCEP) atmospheric reanalysis products (Kalnay et al. 1995). Lateral boundary-condition nudging is performed on the two outer-boundary grid cells of the coarse grid. The information provided at the lateral boundary includes, horizontal wind speed, relative humidity, air temperature, and geopotential height on pressure levels. The initial atmospheric fields are also provided by the NCEP reanalyses. The time step for the atmospheric model integrations is 2 minutes.

Heterogeneous soil types were applied to the domain based on United States Department of Agriculture, STATSGO soil database (Miller and White 1998). The soil-texture distribution for the finer grid is given in Figure 4.5. The model has 10 soil layers at 2.0 m, 1.65 m, 1.3 m, 0.95 m, 0.65 m, 0.45 m, 0.3 m, 0.2 m, 0.125 m, and 0.05 m from surface, respectively. Soil moisture initial distributions are generated by first defining a spatially-constant soil moisture content over the domain, and running the model for one year. The soil moisture distribution on the last day of that simulation is then used as the initial condition for the next year's simulation.

DayCENT is configured and initialized for each grid cell on Grid #2 according to the land-use type (VEMAP 1995). DayCENT has been spun up for 2,000 years according to a 30-year mean climatology (averaged over 1961 to 1990), which allows the state variables in the model to reach equilibrium. Then the control run year's climate generated from offline ClimRAMS is used to drive DayCENT cyclically for 3 years before DayCENT enters the coupled mode. Using 3 years to spin up DayCENT to ClimRAMS climate was determined by the numerical experiment shown in Figure 4.6. In that experiment, DayCENT was driven by the offline ClimRAMS-produced 1989 climate cyclically for 10 years after its initial equilibrium state had been reached from the 2,000 year spin-up. The figure shows that after 3 years, the above-ground live carbon, below-ground live carbon, and standing dead material from grass and crops have reached steady states, while carbon in forest leaves and total soil carbon are still in the process of adjusting to the ClimRAMS climate. Since fast dynamics, such as leaf and root carbon, are more relevant to the feedback loops on seasonal to annual time-scale (which is the focus of our current study) than the long-term dynamics such as soil organic matter, and since the computational resources were not available for a longer spin-up, 3-years was chosen to adjust DayCENT to be consistent with the ClimRAMS climate prior to starting the coupled simulations.

4.2.2 Selecting an Average Year for the Control Simulation

In order to select a normal year for the control run, we first obtained National Climatic Data Center (NCDC) Summary-of-the-Day (SOD) meteorological-station

observational data set from 1982 through 1996. Figure 5.1 shows the locations of the approximately 3,800 United States SOD stations. This data set contains daily precipitation, snow fall, snow depth, Tmax, and Tmin. The SOD station data were gridded to the 50-km ClimRAMS grid using an objective analysis scheme (Cressman 1959), and were used to validate ClimRAMS and drive the offline DayCENT simulations.

Figure 4.7 shows the precipitation and screen-height maximum temperature from 1982 through 1996 averaged over the Grid #2 domain. We concluded that 1989 is a near-average year and could be used as the control run. At the same time, 1988 was identified as a dry year and 1993 as a wet year. We will revisit this fact when the coupled model is used to study interannual variability.

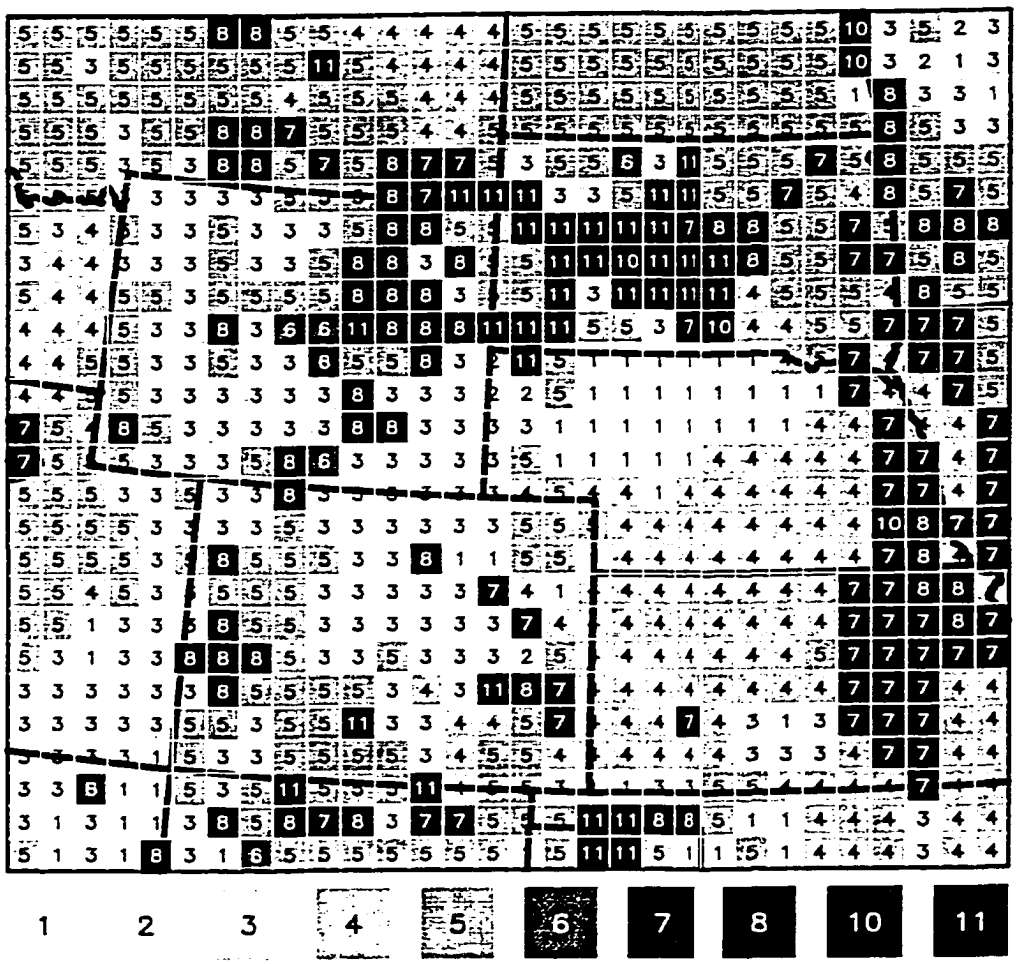

Figure 4.5 The soil-texture-class spatial distribution for the fine grid in Figure 4.2, defined according to the United States Department of Agriculture, STATSGO soils database (Miller and White 1998).

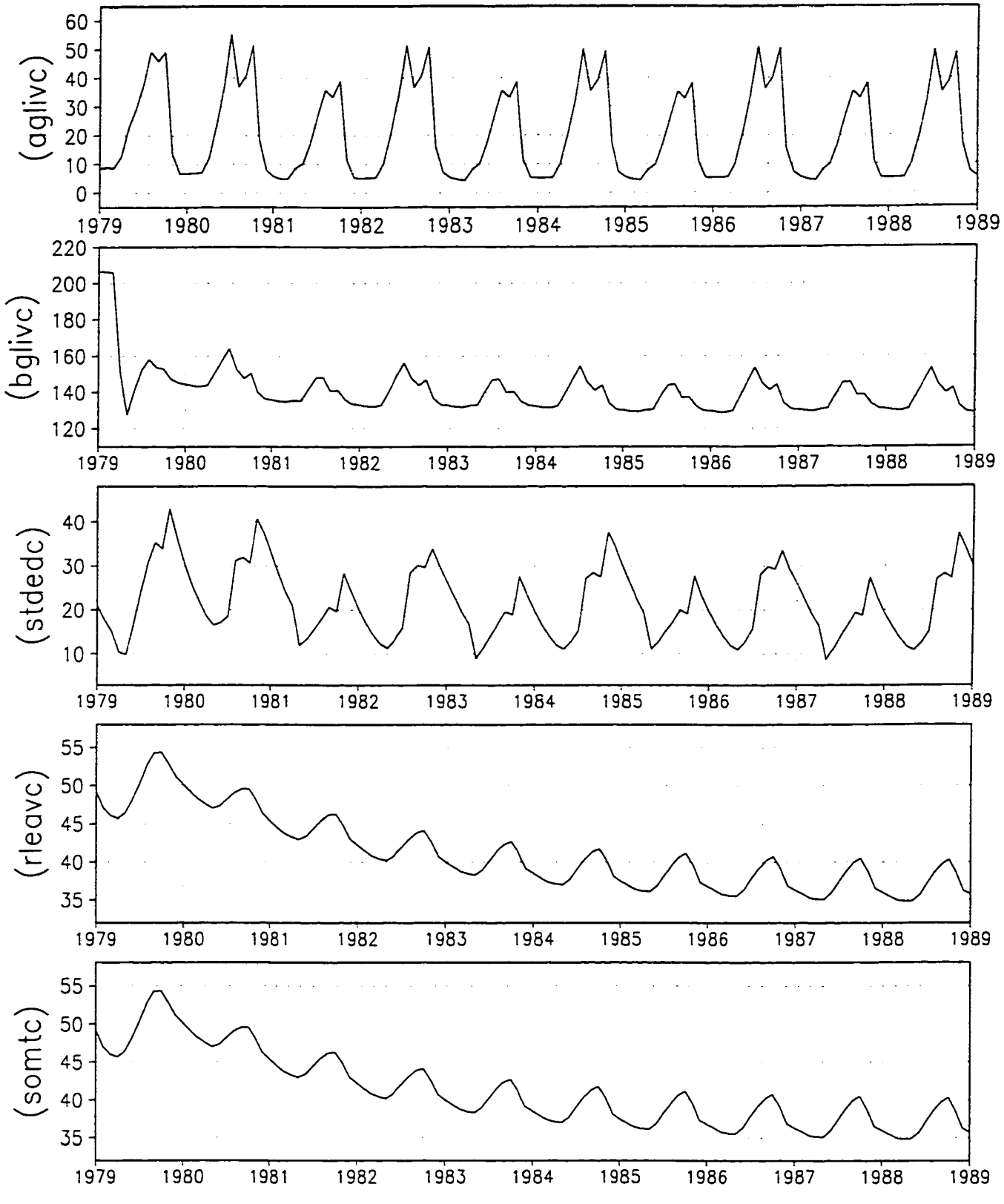

Figure 4.6 DayCENT outputs when driven by the ClimRAMS 1989 climate for ten years.

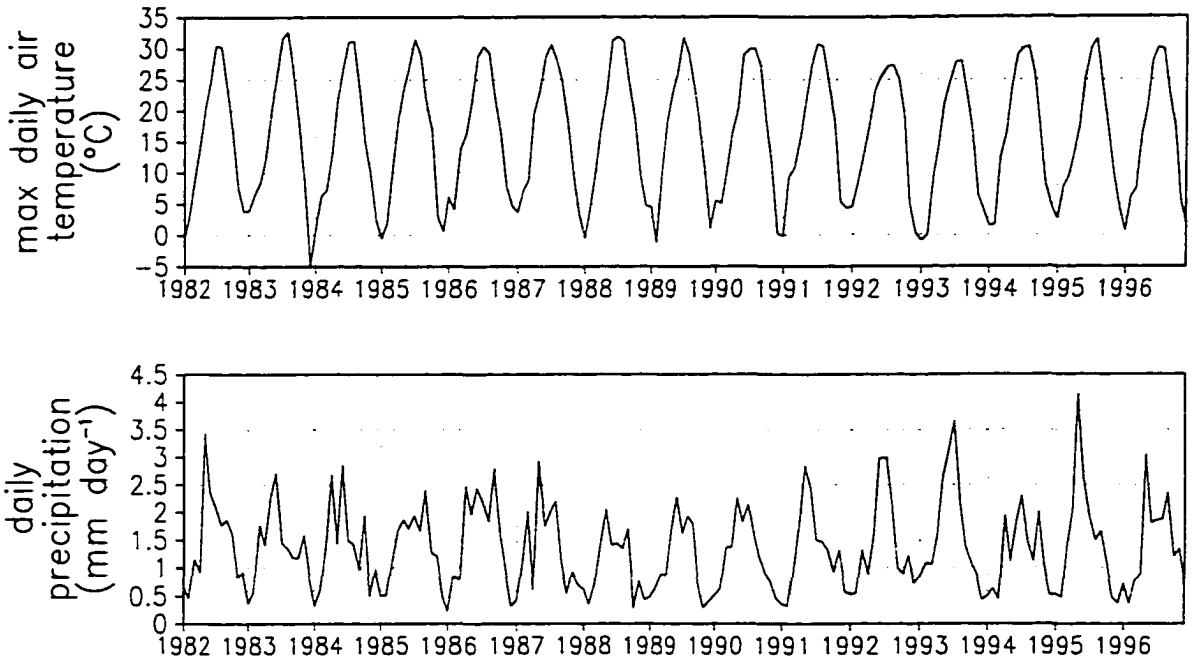

Figure 4.7 Observed domain-averaged monthly-mean screen-height maximum air temperature and precipitation for the period 1982 through 1996 (based on United States SOD station data).

Chapter 5

OBSERVATIONAL DATA SETS

5.1 Surface Climate Observations

Validating ClimRAMS, driving offline CENTURY, and investigating atmosphere-vegetation inter-relationships all require a surface meteorological observational data set that has the spatial and temporal coverage for the domain and time span of interest. First order Summary-of-the-Day (SOD) meteorological-station observational data from National Climatic Data Center (NCDC), which has the daily precipitation, snow fall, snow depth, maximum screen-height air temperature (Tmax), and minimum screen-height air temperature (Tmin), is ideal for this purpose. Figure 5.1 shows the location of 3,800 SOD stations distributed across the United States. Data from 1982 to 1996 has been obtained and gridded to the 50-km ClimRAMS grid using an objective analysis scheme (Cressman 1959). Each grid cell has daily Tmax, Tmin, and precipitation for a 15-year time period.

Displayed in Figure 5.2 are the monthly mean Tmax, Tmin, and precipitation, averaged over the fine-grid domain in Figure 4.2, for 1982 through 1996. All of the three variables demonstrated consistent patterns of seasonal cycles. The winter of the simulated domain is dry and cold, while the summer is warm and receives most of the

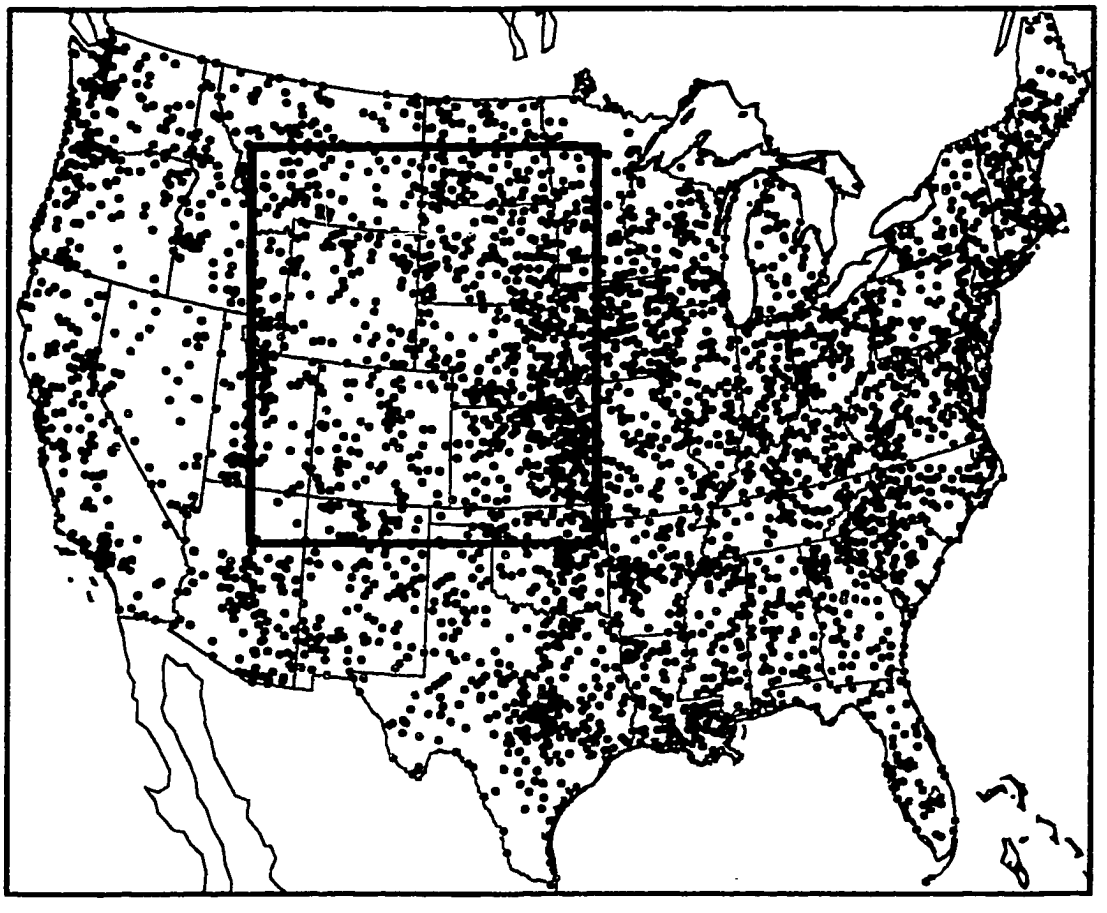

Figure 5.1 Locations of National Climatic Data Center (NCDC) Summary-of-the-Day (SOD) meteorological stations.

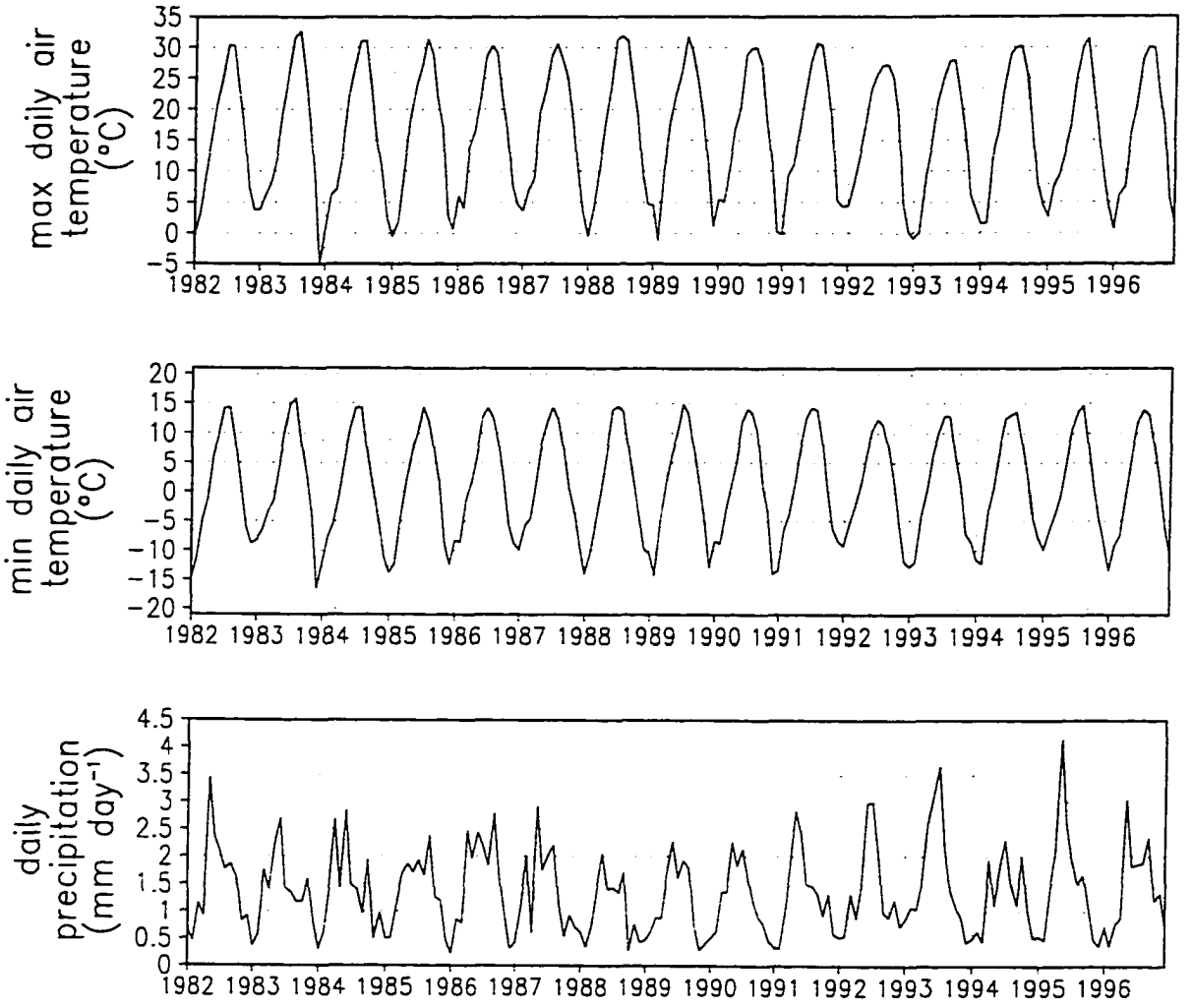

Figure 5.2 Monthly mean precipitation and screen-height maximum and minimum air temperature observations, averaged over the fine grid, for the period of 1982 through 1996.

annual precipitation. The precipitation appears to have larger interannual variability than the temperature time series.

5.2 Vegetation Observations

The Pathfinder Advanced Very High Resolution Radiometers (AVHRR) monthly Normalized Difference Vegetation Index (NDVI) data set for North America at 8-km resolution for the period of January 1982 through December 1993 were utilized for this study. Figure 5.3 is the NDVI spatial distribution for August 1989. The high NDVI spatial variation found within this data set highlights the large vegetation phenological variation across North America. The data were then aggregated from their original 8 km by 8 km pixel information to the 50 km by 50 km fine-grid increment, as shown in Figure 5.4. The NDVI spatial pattern shows a clear gradient from the southeast corner of the domain towards the northwest, which is consistent with the temperature and precipitation spatial distributions.

The purpose of evaluating the spatial average is to study temporal variations. Such a method will highlight NDVI seasonality. Figure 5.5 shows the domain-averaged NDVI for the fine grid of Figure 4.2. The characteristic feature of temporal profiles of NDVI over our simulation domain is its seasonality, where NDVI peaks during the months of June, July and August, and reaches a minimum of around 0.1 during the winter. Averaging the NDVI time series over different vegetation types reveals that the NDVI amplitude, growing season length, and the residue after senescence are vegetation-type dependent features that vary between years. The large

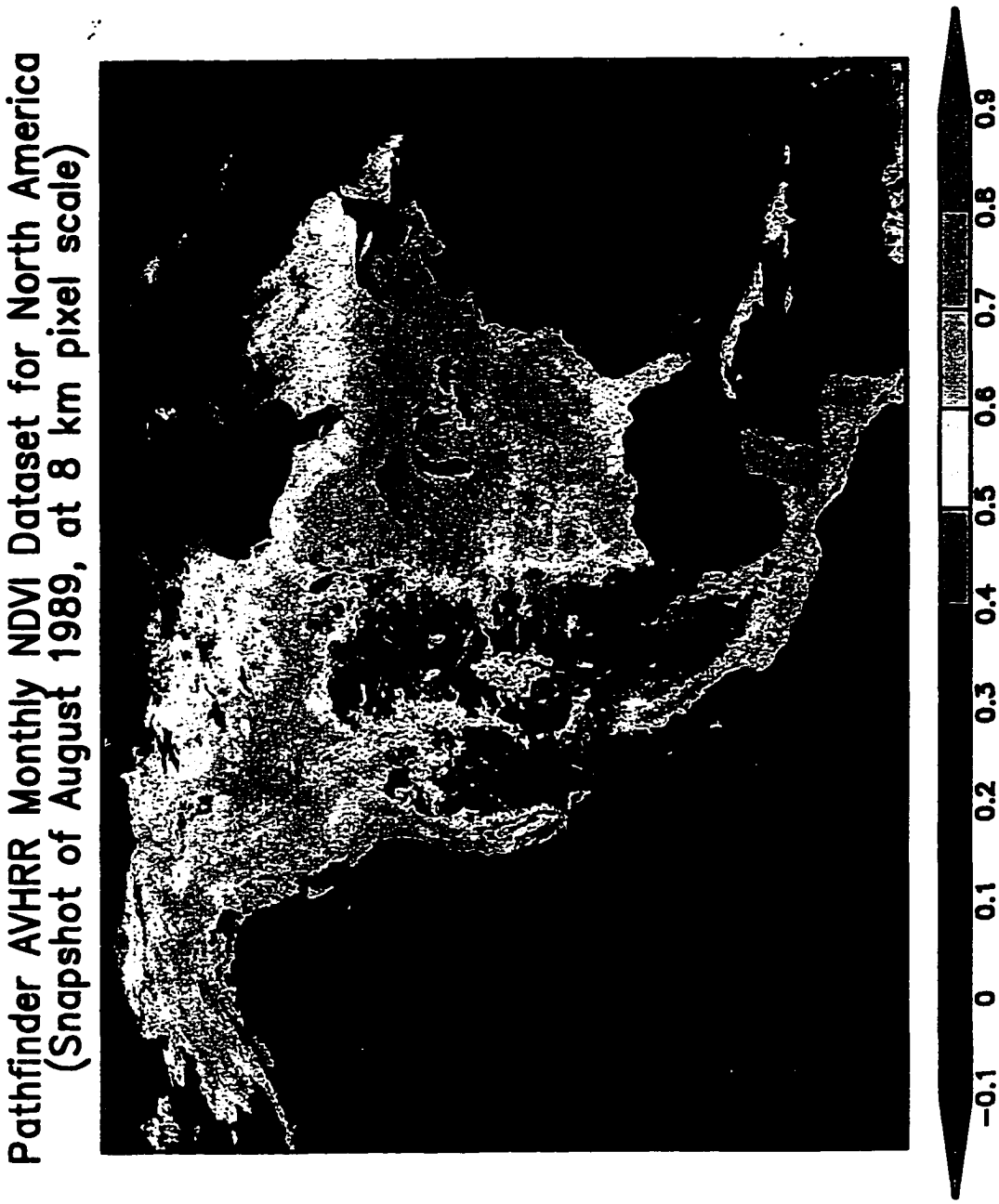

Figure 5.3 NDVI spatial distribution of August 1989 from Pathfinder AVHRR monthly land data set for North America at a 8 km pixel scale.

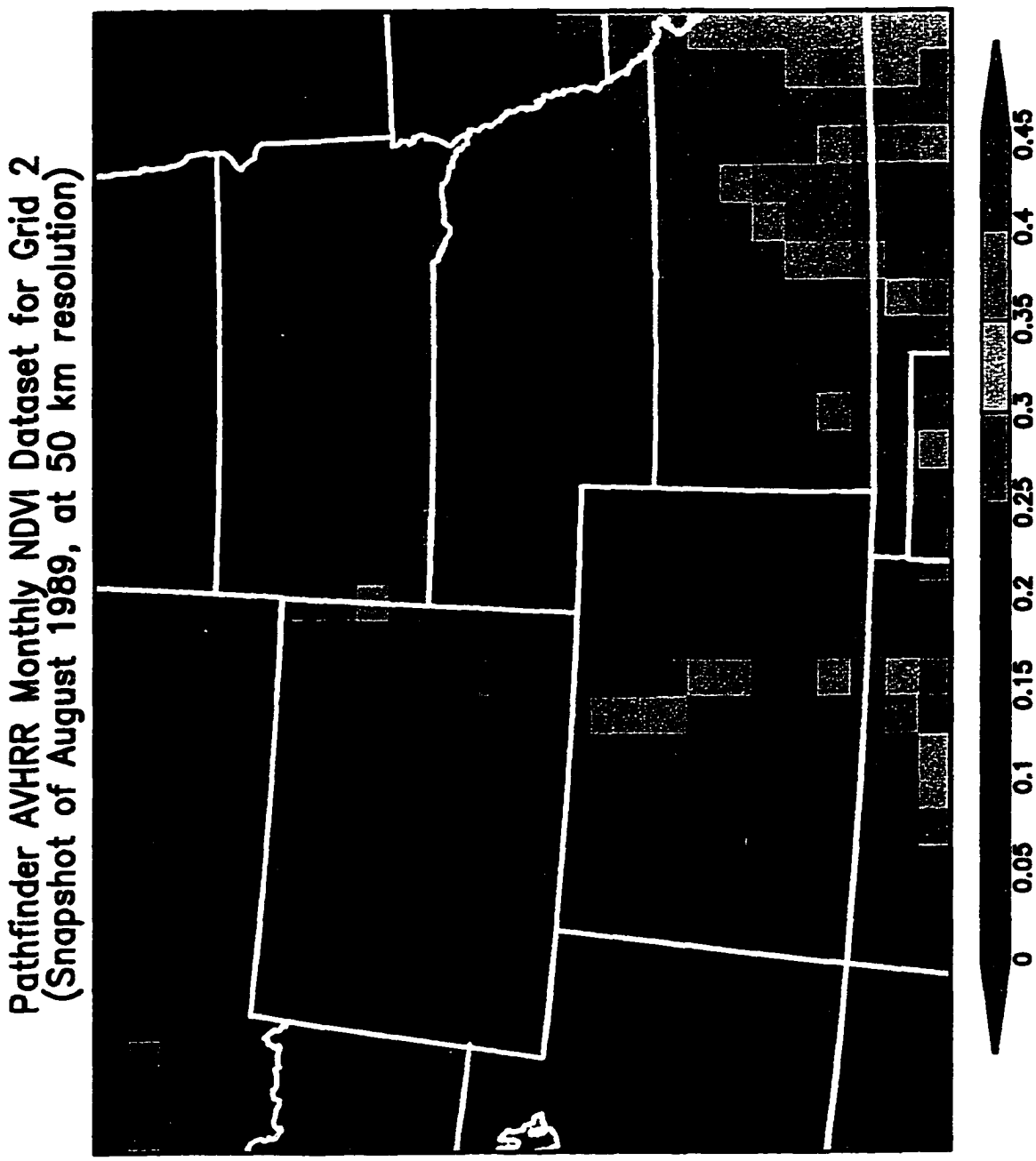

Figure 5.4 NDVI spatial distribution for August 1989 after aggregating from the 8-km pixel scale to the 50-km resolution.

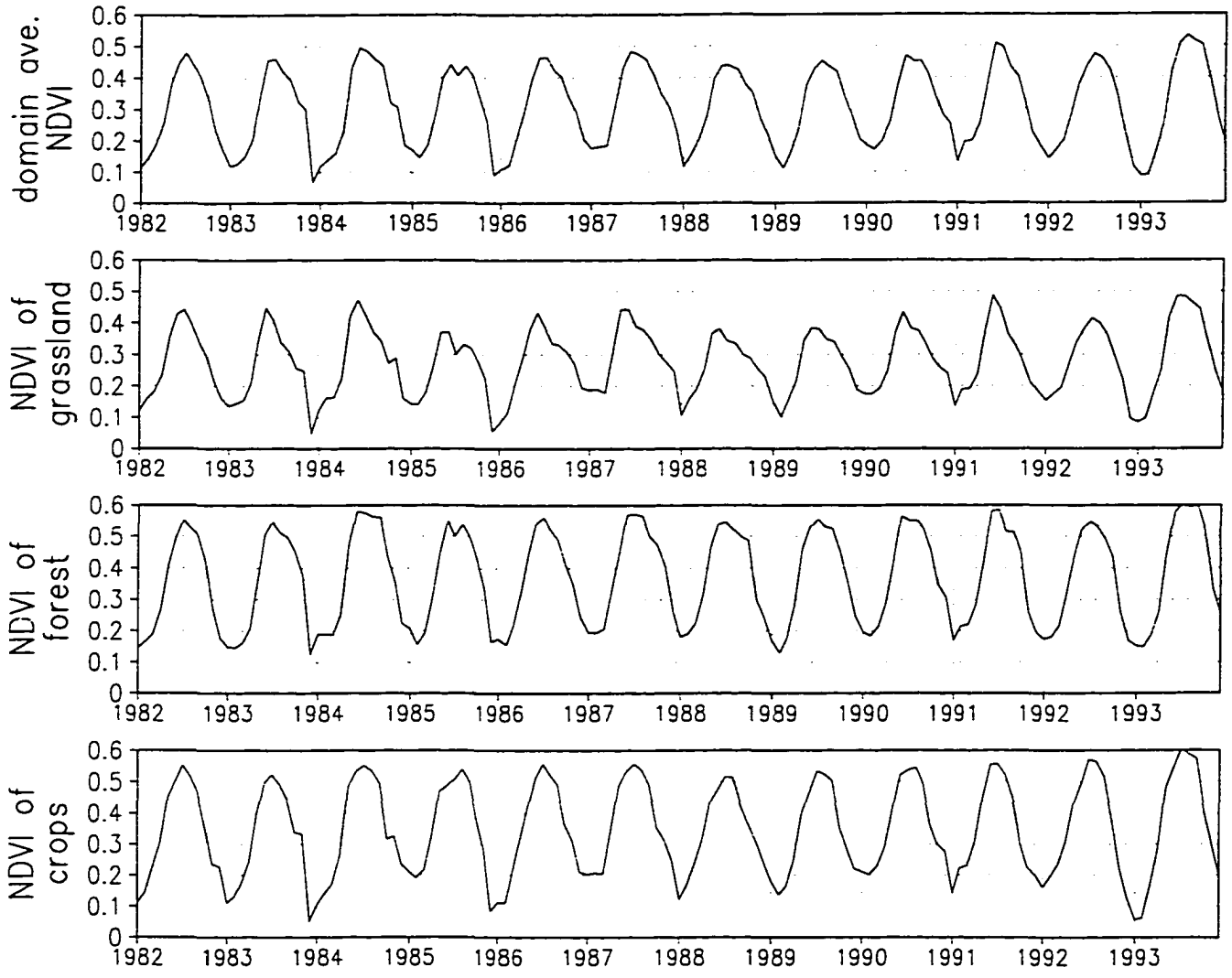

Figure 5.5 Time series of monthly NDVI averaged over the grid 2 domain and different vegetation types for the period of January 1982 through December 1993.

interannual NDVI variability of grasslands contrasts with the limited variability of trees and crops, which is in line with expectation. The rapid growth in spring and early summer, and the prompt senescence in fall, is another striking feature of the central United States NDVI record.

5.3 The Correlation Between Vegetation Index and Atmospheric Variables

In order to study the correlation between NDVI and atmospheric forcings in terms of interannual variation triggered by an El Niño or monsoon phenomena over our study area, we further processed both SOD and NDVI data sets. The monthly, domain-averaged Tmax, Tmin, precipitation, and NDVI were averaged over June, July, and August (JJA), the maximum vegetation growing months in mid-latitudes, to represent the variables' amplitudes during the peak growing season. The times series of JJA domain-averaged climate forcings and NDVI from 1982 to 1993 are shown in Figure 5.6. The following observations can be made: (1) The Tmin time series closely follows the Tmax time series, but the variation magnitude was half that of Tmax. (2) The temperatures and precipitation time series are negatively correlated. (3) The domain-averaged NDVI time series resembles the domain-averaged precipitation time series, with the driest year (1988) having the lowest NDVI value and the wettest year (1993) having the highest. The NDVI and rainfall in the central United States are positively correlated. The physical basis behind this is that vegetation growth strongly depends on soil moisture availability, which is in turn directly affected by the rainfall amount and frequency. This also explains why the NDVI of grassland has larger

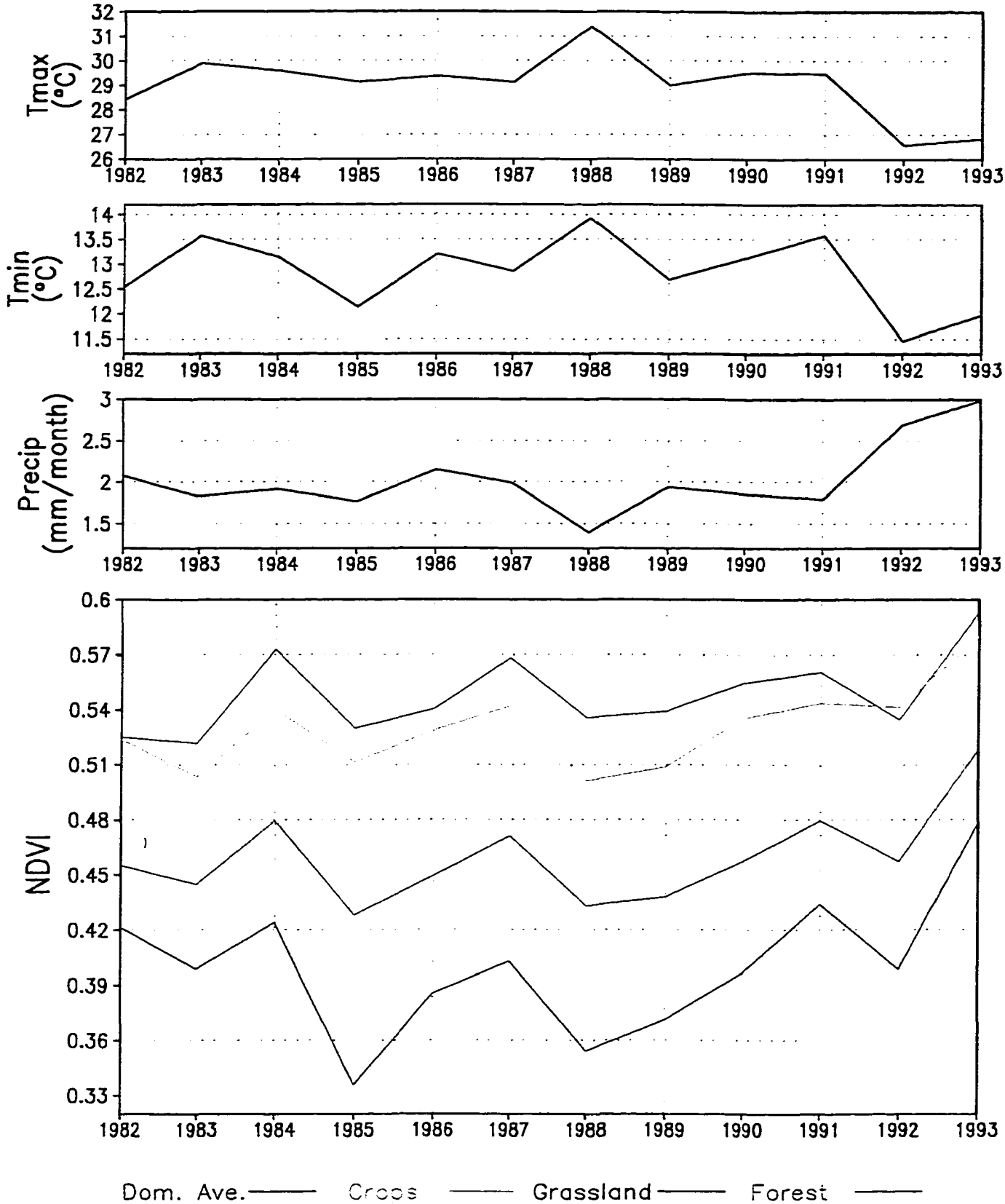

Figure 5.6 Times series of domain-averaged NDVI and climate variables for the period of 1982 through 1993. Shown are the June, July and August averaged values chosen to represent the peak growing season of the year.

interannual variability when compared with trees and crops. The deeper and more extensive rooting system of trees, and irrigation programs for crops, allow them to access more soil moisture than grasslands. Focusing on the bottom panel of Figure 5.6, natural grasslands have the smallest NDVI values, trees have the largest, and the crops lie between the two.

Fu and Wen (1993) examined the correlation between NDVI and precipitation for a shorter time span and higher temporal resolution. Shown in Figure 5.7 is the time series of weekly NDVI and precipitation over eastern China from 31 October 1988 through 29 October 1989. It shows that vegetation dynamics are closely related to monsoon activities in Eastern China. The response time of vegetation growth to the precipitation events is about 6 weeks. The question can be asked here is "Does the precipitation maxima lead to a NDVI maxima in later weeks?" Our coupled modeling system is an ideal tool to answer this question.

5.4 The Algorithm Used to Convert NDVI to LAI

Several algorithms exist to derive LAI from NDVI data sets (Sellers 1996; Nemani et al. 1996). The algorithm introduced by Sellers et al. (1996) was applied to our study. First, a look-up table to convert vegetation type from CENTURY to SiB2 was created. Then a simple ratio (SR) was calculated based on the relation, SR=(1+NDVI)/(1-NDVI). Fractional photosynthetic active radiation (FPAR) is given by

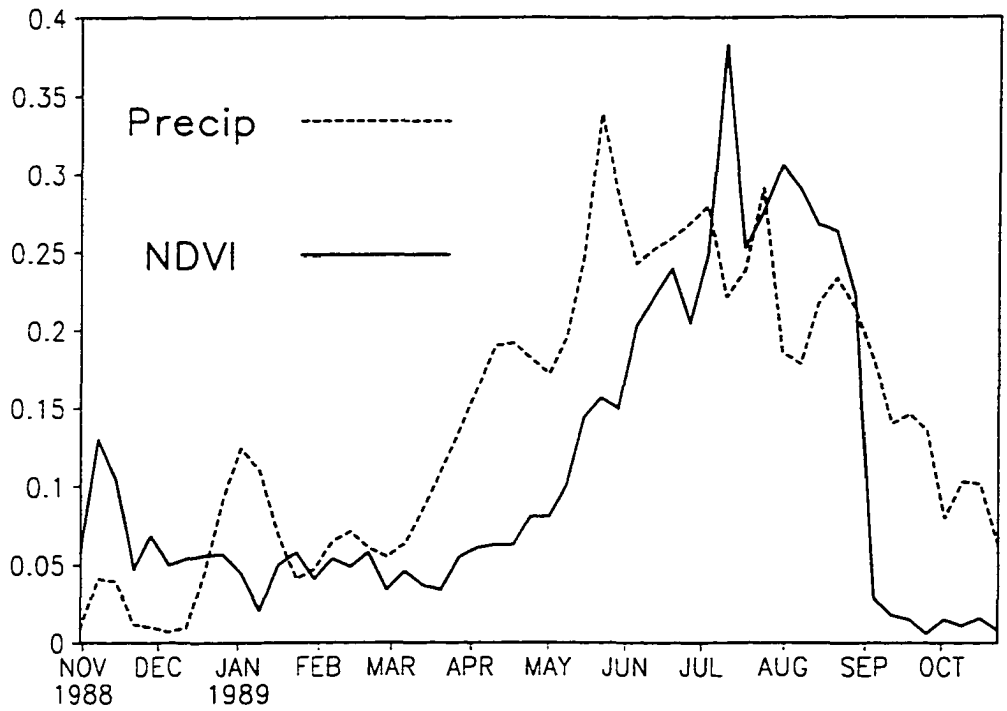

Figure 5.7 The time series of weekly NDVI and precipitation over China for the period of 31 October 1988 through 29 October 1989 (Fu and Wen 1993).

$$FPAR = \frac{(SR - SR_{i,\min})(FPAR_{\max} - FPAR_{\min})}{(SR_{i,\max} - SR_{i,\min})} + FPAR_{\min} \quad (5.1)$$

Where $FPAR_{max}$ = 0.950; $FPAR_{min}$ =0.001; $FPAR_{max}$ and $FPAR_{min}$ are independent of vegetation type; $SR_{i,max}$ is equal to the SR value corresponding to 98% of the NDVI population i; and $Sr_{i,\ min}$ is equal to the SR value corresponding to 5% of NDVI population *i*.

The relationship between *FPAR* and the leaf area index (LAI) for evenly distributed vegetation at a regional scale can be described by an exponential equation (Monteith and Unsworth 1990)

$$LAI = LAI_{i,\max} \frac{\log(1 - FPAR)}{\log(1 - FPAR_{\max})} \quad (5.2)$$

where $LAI_{i,\ max}$ is the maximum green leaf area index defined for vegetation type *i*.

For clustered vegetation, for example coniferous trees and shrubs, the equation becomes (Huenrich and Goward 1992)

$$LAI = LAI_{i,\max} \frac{FPAR}{FPAR_{i,\max}} \quad (5.3)$$

In cases where there is a combination of clustered and evenly distributed vegetation,

$$LAI = (1 - F_{cl}) LAI_{i,\max} \frac{\log(1 - FPAR)}{\log(1 - FPAR_{\max})} + F_{cl} \frac{LAI_{i,\max} FPAR}{FPAR_{\max}} \quad (5.4)$$

where F_{cl} is the fraction of clumped vegetation in the grid area. The value of F_{cl} for each land-cover class can be found in Sellers et al. (1996).

Using the algorithm introduced above, an LAI time series has been derived from the NDVI data set and will be used in Chapter 6 to validate the DayCENT model.

Chapter 6

PRELIMINARY RESULTS

6.1 Validation of DayCENT

DayCENT was driven by observed atmospheric forcings derived from the United States SOD data set for each grid cell of the fine-grid domain from 1 January 1982 to 31 December 1996. The above-ground live carbon (Aglivc) produced by DayCENT was then converted to LAI following the relationship

$$LAI = \frac{Aglivc}{1000} * R_{leaf} \tag{6.1}$$

where Aglivc, g m^{-2}, is above-ground live carbon; and R_{leaf}, (m^2 leaf area) (kg leaf carbon)$^{-1}$, is the specific leaf area which varies according to the vegetation type. The value of R_{leaf} for each land-cover class is provided in Table 6.1.

Figure 6.1 shows monthly NDVI-derived LAI (red) and DayCENT simulated LAI (green). The LAI for the fine grid was then averaged over the domain, grasslands, trees, and crops. The agreement between the two grassland time series is good, with both the seasonal cycle and interannual variation well captured by the model. The simulated LAI maxima for trees, however, are generally 25% higher than

Table 6.1 Conversion factor (R_{leaf}) between above-ground live carbon and LAI.

Vegetation Type #	Vegetation Type	Specific Leaf Area (m^2 leaf area)(kg leaf carbon)$^{-1}$
1	Tundra	9.6
2	Subalpine Conifer	9.6
4	Continental Temperate Conifer	14.4
5	Cool Temperate Mixed Forest	31.2
6	Warm Temperate/Subtropical Mixed Forest	24
7	Temperate Deciduous Forest	24
10	Temperate Mixed Xeromorphic Woodland	21.6
11	Temperate Conifer Xeromorphic Woodland	14.4
13	Temperate/Subtropical Deciduous Savanna	24
14	Warm Temperate/Subtropical Mixed Savanna	14.4
15	Temperate Conifer Savanna	14.4
17	C3 Grasslands	26
18	C4 Grasslands	26
19	Mediterranean Shrubland	14.4
20	Temperate Arid Shrubland	19.8
21	Subtropical Arid Shrubland	14.4
101	Spring Wheat	26
102	Barley	26
103	Winter Wheat	26
104	Dryland Corn	8.7
105	Southern Corn and Mixed Crops	26
106	Irrigated Corn	8.7
114	Temperate Deciduous and Corn Belt (7+104)	24
115	Temperate Deciduous and Mixed Crop (7+105)	24
116	Warm Temperate/Subtropical Mixed Forest & Southern Corn (6+105)	24
118	Winter Wheat	26

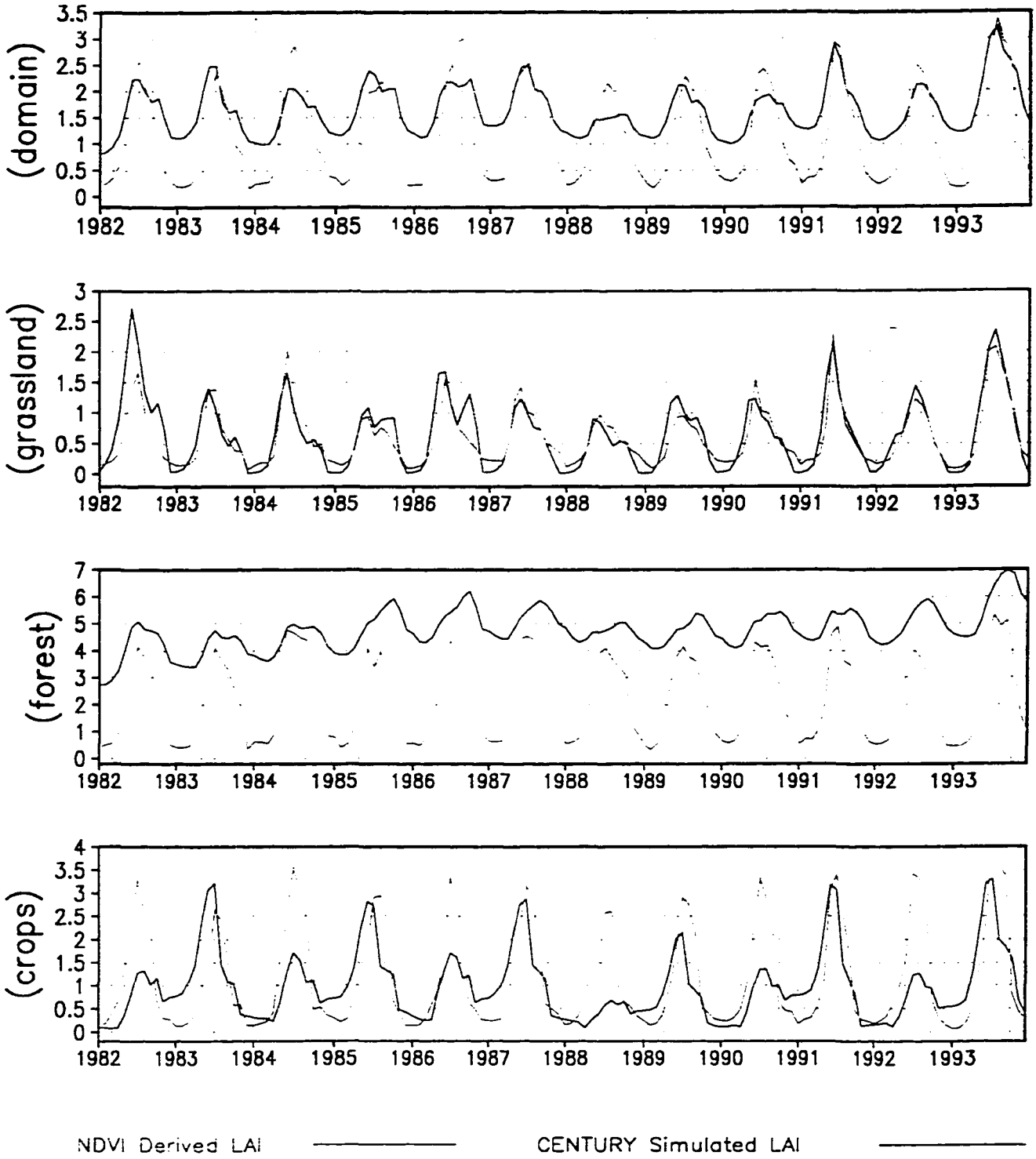

Figure 6.1 Monthly NDVI-derived LAI and DayCENT-simulated LAI over the fine grid for the period 1982 through 1993, averaged over the domain, grasslands, trees, and crops.

observed. The simulated minima are around 4 LAI units, while the observed minima are around 0.5 LAI units. A possible explanation is that the NDVI data might have been contaminated by snow-cover during the winter months so that the evergreen forest can not be detected by the satellite sensors. The large forest-LAI interannual variation in the NDVI data set may not exist at all for this reason. The model-simulated crop LAI clearly shows an alternating "low-high" pattern, which may have been introduced by DayCENT's management practices. For instance, field fallow and crop rotation have been scheduled every other year for a large number of croplands. The LAI time series simulated by the DayCENT crop sub-model appears to have larger interannual variability than the NDVI-derived LAI time series.

Despite the fact that the domain-averaged LAI simulation appears to be negatively affected by DayCENT's forest sub-model, in general, the comparison of domain-averaged LAI between the model and observations show that DayCENT is capable of representing seasonal and interannual biomass variabilities.

Differences between LAIs simulated by DayCENT and those derived from NDVI exist. However, this can result from deficiencies in either (or both) DayCENT or the NDVI data sets. First, the NDVI data set we used is the Pathfinder AVHRR archived land-surface data set. It has been corrected for sensor degradation, viewing and solar zenith angles, Rayleigh scattering, and ozone absorption. A cloud mask and a quality control flag were included when processing the Pathfinder data. No corrections were applied for aerosol and water vapor effects. No inter-sensor calibration has been performed. There are some artifacts in the Pathfinder data set

that are not yet well understood. Also, after processing the entire data set it became apparent that the effects of ozone absorption and Rayleigh scattering were only partially accounted for (Los 1998). Second, any problem existing in the NDVI-to-LAI conversion algorithm can make the comparison even more uncertain. Third, differences between the NDVI-derived LAI and DayCENT-simulated LAI can result from the aggregation method used in defining the land-cover type. The NDVI value for each grid cell (2,500 km^2) is the averaged NDVI values of pixels (64 km^2) located within that grid cell. The land-cover type for each model grid cell is assigned according to the predominant vegetation class. Therefore, DayCENT is simulating the dominant biomass feature while the algorithm that derive LAI from the NDVI data set tends to represent the grid-cell average. A 2,500 km^2 gridded NDVI dataset having homogeneous grid cells would not have this problem.

A reliable NDVI data set and a valid NDVI-to-LAI conversion algorithm would enable ecologists to modify the ecosystem models to produce correct biomass at a regional scale and, at the same time, would allow atmospheric scientists to calibrate climate models based on realistic LAI specifications. This is a crucial next step for the study of climate simulations, regional- to large-scale ecosystem dynamics, and atmosphere-vegetation interactions.

6.2 Validation of ClimRAMS

A comprehensive model description and evaluation of ClimRAMS can be found in Liston and Pielke (1999). The major difference between the control run

performed by a standard ClimRAMS simulation and the one conducted in this section lies in the vegetation-cover initialization, where the former distribution is derived from an International Geosphere-Biosphere Programme (IGBP) data set and the later one is from the VEMAP database (Kittel 1996). Compared to a standard ClimRAMS simulation, minor differences in results exist due to the difference in vegetation-cover specification.

Figure 6.2 through Figure 6.5 summarize the simulation results from the ClimRAMS control run. The model's ability to reproduce the domain-averaged daily maximum (Tmax) and minimum (Tmin) screen-height air temperature and daily precipitation are shown in Figure 6.2, where these variables have been averaged over the 50-km grid given in Figure 4.2. The difference between the model simulation and the observation are also plotted, including a 30-day running mean of the daily values. The model is found to capture the synoptic signals as well as the seasonal temperature evolutions. The total amount of the precipitation simulated by the model is impressively close to the observations considering the simple "dump-bucket" scheme used as the trade-off between the computational time and long-term integration. However, the model tends to rain more frequently and misses the observed precipitation peaks. The spatial patterns of Tmax, Tmin, and precipitation for winter months of January, February, and March (shown in Figure 6.3) and summer months of June, July, and August (shown in Figure 6.4) is found to generally capture the observed spatial patterns. The temperature fields presented here have not been corrected for the elevation difference between model and observation. A comparison

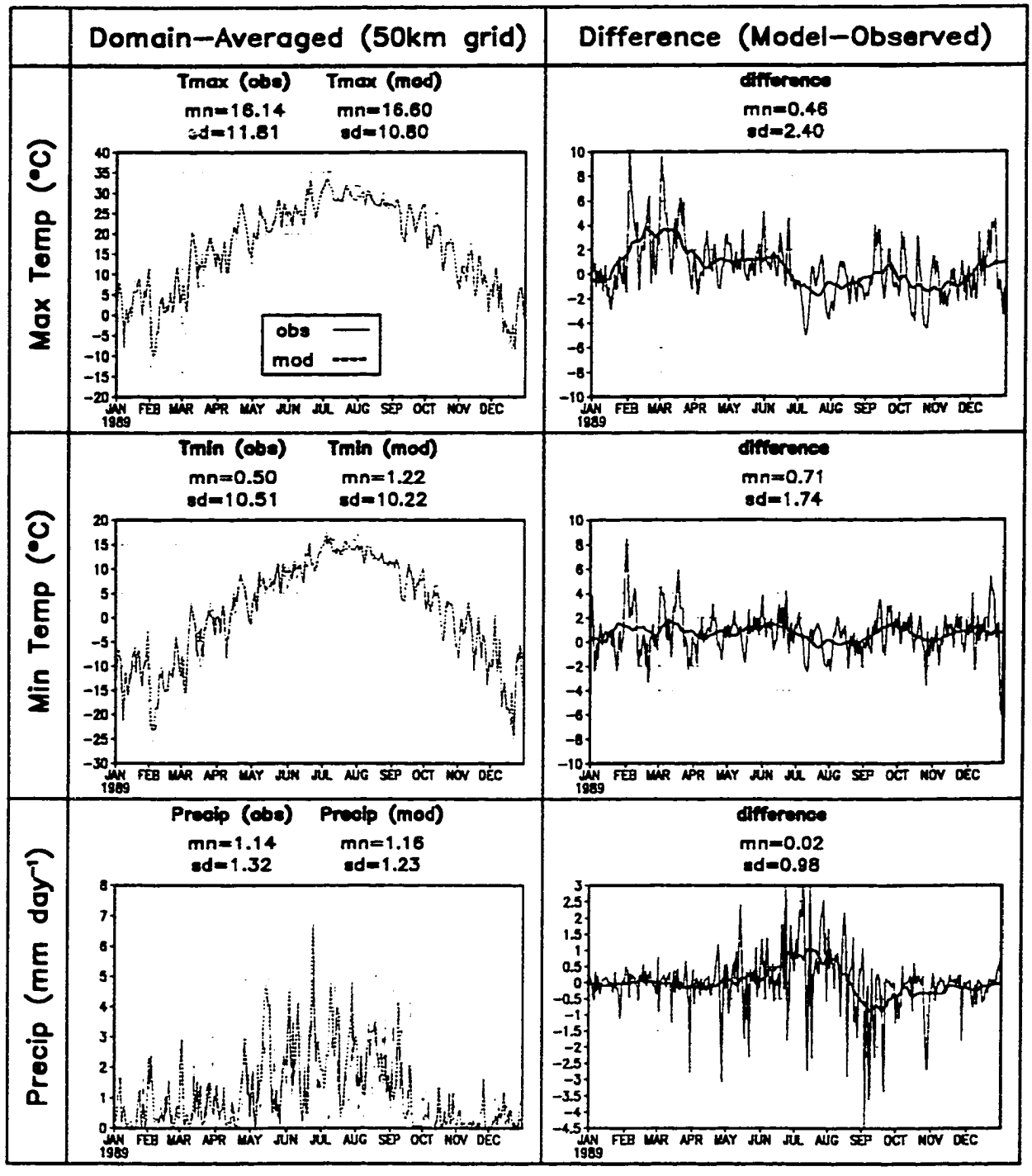

Figure 6.2 Modeled and observed, domain-averaged daily maximum and minimum screen-height air temperature and daily precipitation for 1989, where these variables have been averaged over the 50-km grid given in Figure 4.2. Also shown is the difference between the model and observations, and the 30-day running mean of the difference values. Included are the mean (mn) and standard deviation (sd) for each panel and variable.

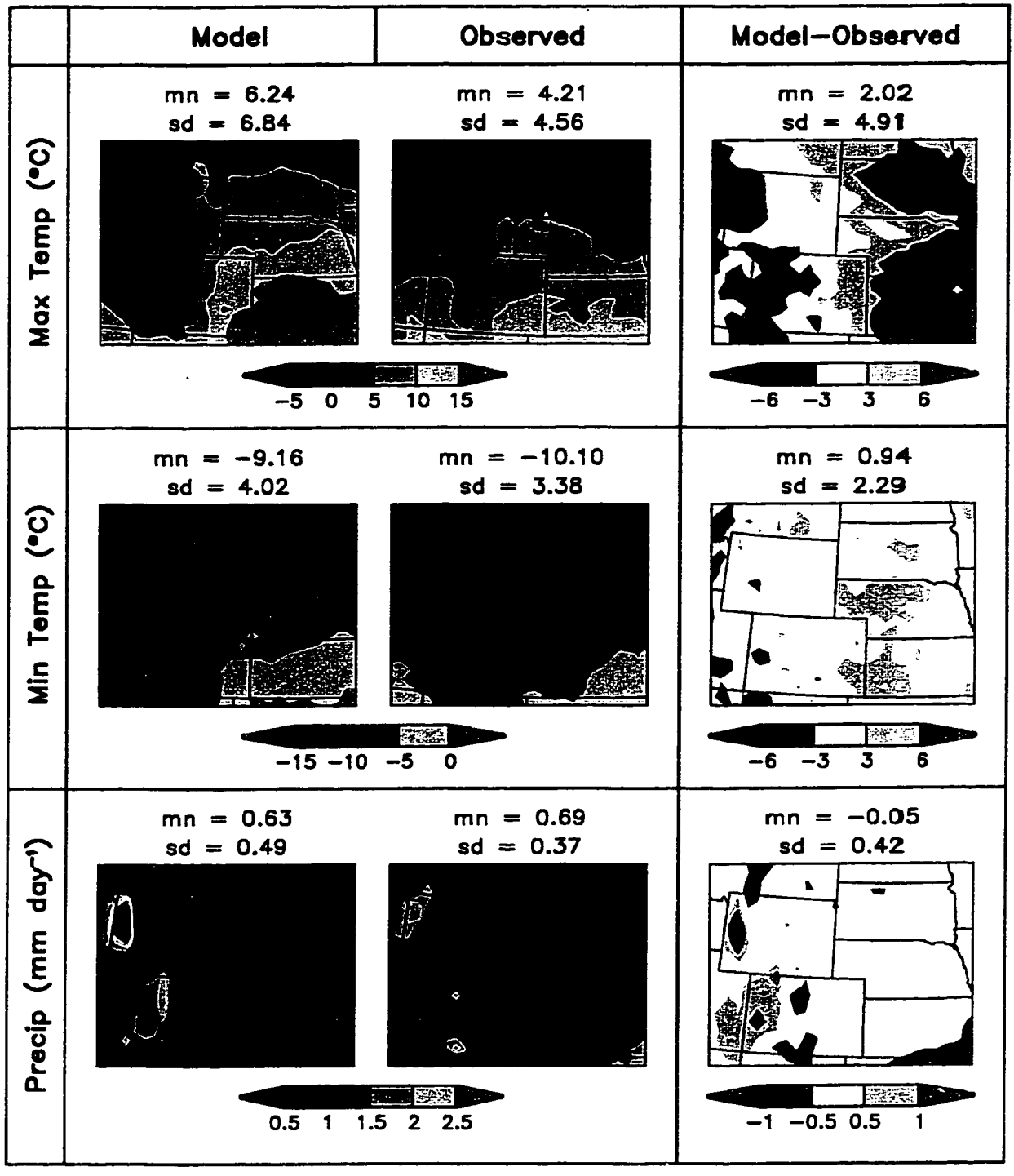

Figure 6.3 The winter spatial patterns of maximum and minimum daily screen-height temperature and daily precipitation, averaged over January through March of 1989. Shown are the modeled and observed fields, and the differences between the two. Also included are the mean (mn) and standard deviation (sd) for each panel and variable.

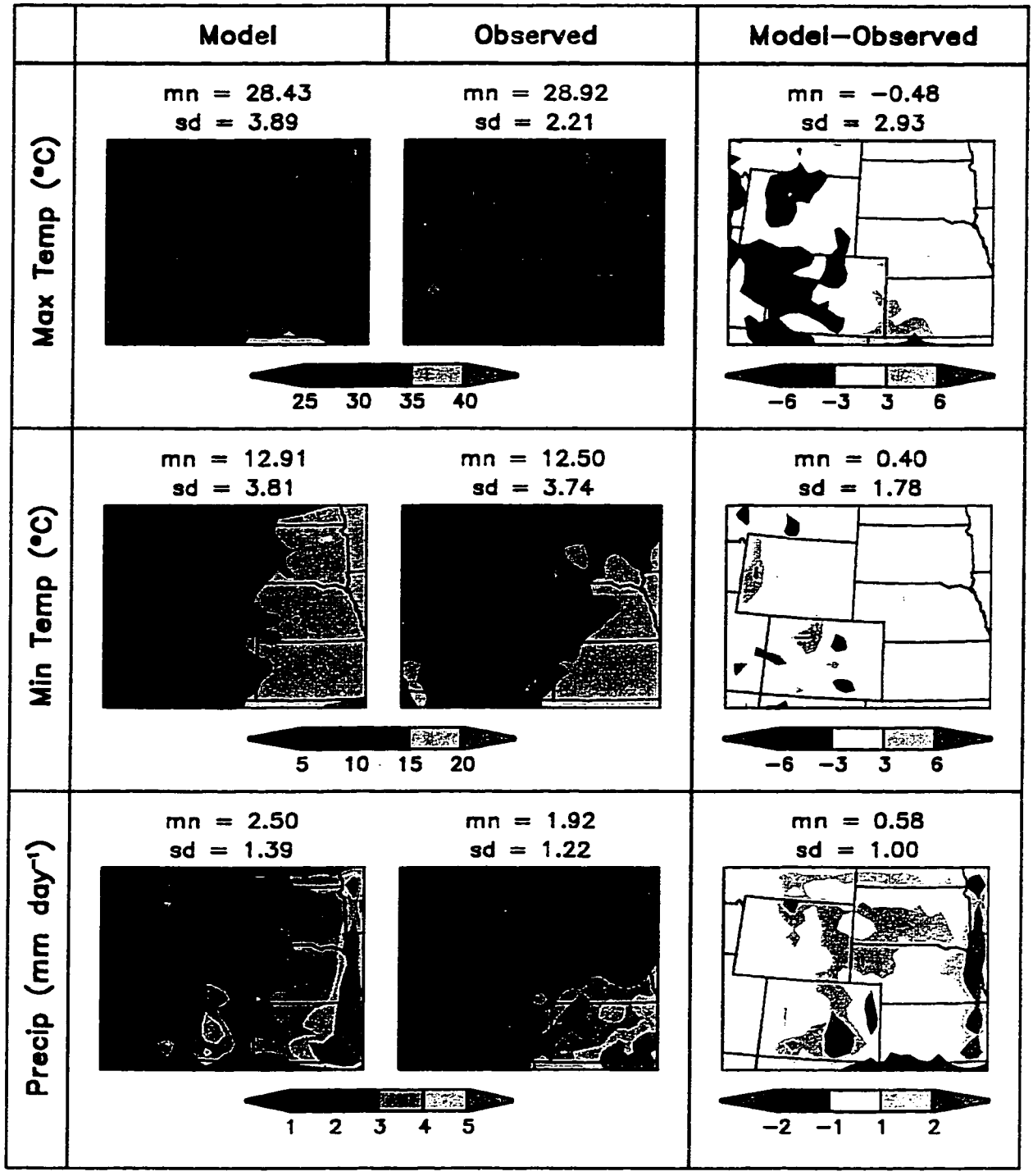

Figure 6.4 Same as Figure 6.3, but for summer, averaged over June through August 1989.

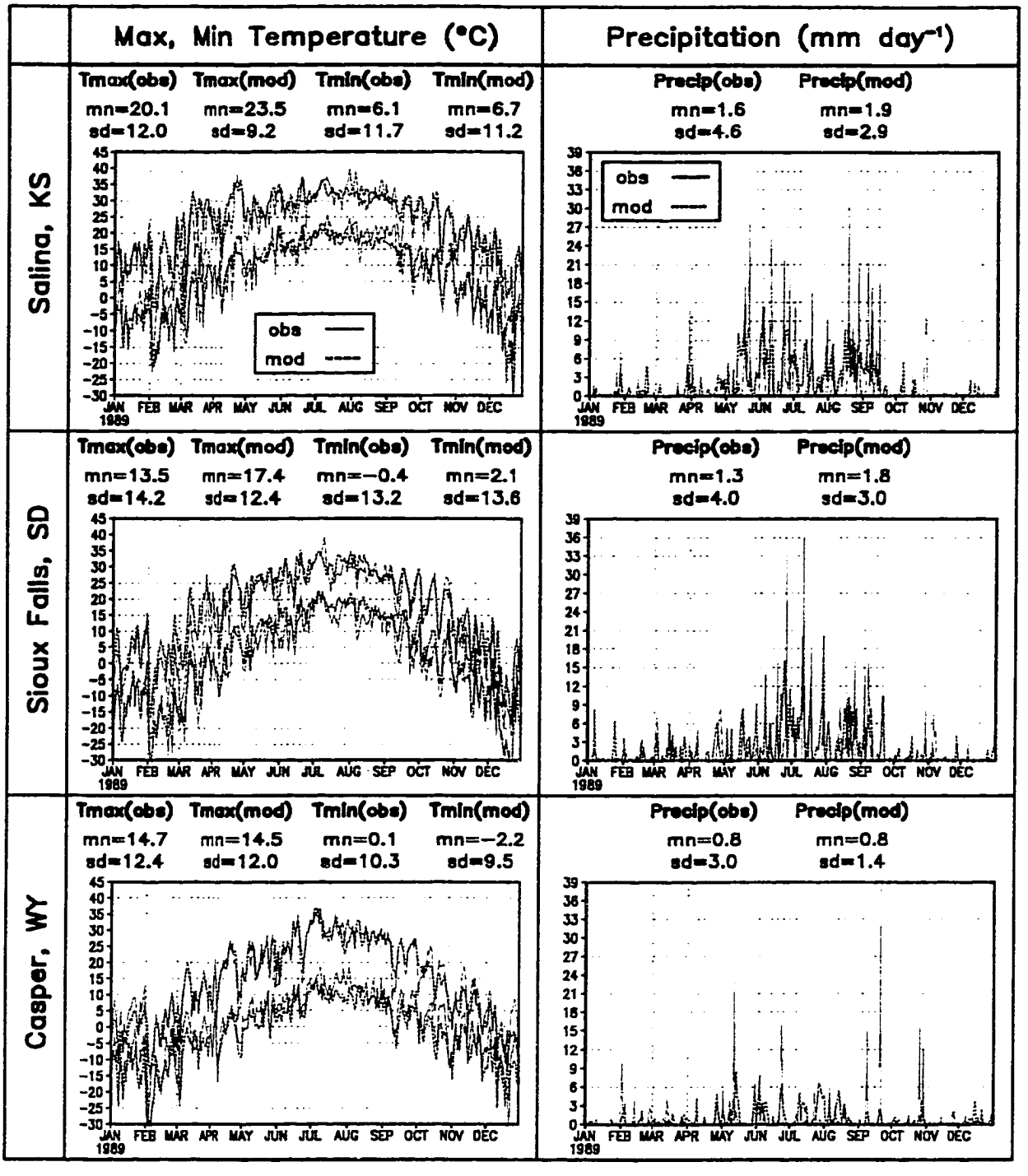

Figure 6.5 The annual cycle of daily maximum and minimum screen-height temperature and daily precipitation for 1989 at the model grid cells corresponding to three cities identified by the markers in Figure 6.6. Also included are the mean (mn) and standard deviation (sd) for each panel and variable.

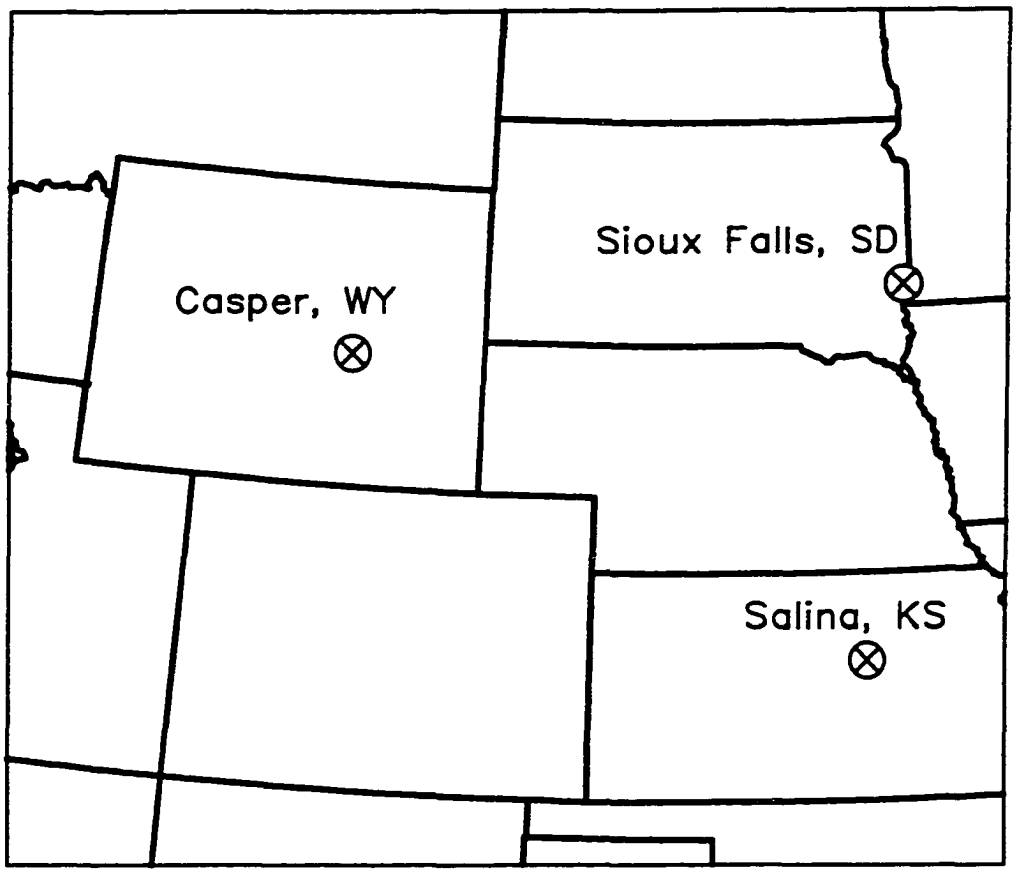

Figure 6.6 The locations of cities (or grid cells) of interest for the fine grid used in Figure 6.5.

of the annual cycle of Tmax, Tmin, and daily precipitation at the model grid-cell level, corresponding to three cities within the fine-grid domain, are given in Figure 6.5. The locations of the three cities can be found in Figure 6.6, and they are: Salina, Kansas; Sioux Falls, South Dakota; and Casper, Wyoming. The model is able to capture the regional variabilities in both temperatures and precipitation fields of these sites. Although the model generally does not capture the peak magnitudes of precipitation events, but the timing of the individual synoptic events and seasonal cycles are well simulated.

A legitimate question to ask at this point is "why not run ClimRAMS with the observed LAI?" First, prior to the work presented in this dissertation, the vegetation specification in ClimRAMS traditionally follows the BATS scheme with the modification that allows LAI to vary according to the time of the year. Second, ClimRAMS has been adjusted to closely match the observations, by making changes to such things as, the soil moisture initialization and the precipitation coefficients. Thus, using a different vegetation specification may lower the model's skill in reproducing the observed climate, even though the new representation is more physically realistic. Third, the observed LAI was derived from the NDVI data set. Lots of uncertainties and errors exist with regard to the NDVI data retrieval processes and the NDVI-to-LAI conversion algorithm. Therefore, it is premature to run the ClimRAMS with the observed LAI since currently only limited insight can be gained by doing so.

6.3 Results From the Coupled RAMS/CENTURY Modeling System

Three numerical experiments will be repeatedly referred to henceforth. They are: (1) the offline ClimRAMS, where the prescribed LAI specification following the BATS scheme was used; (2) the offline DayCENT, where the DayCENT is driven by either observed atmospheric forcings or by the climate produced by ClimRAMS; (3) the coupled model or the coupled RAMS/CENTURY, where the ClimRAMS and DayCENT are two-way interactive on a weekly time step.

6.3.1 Simulated LAI

The coupled model was integrated from 1 January to 31 December 1989. The three curves shown in Figure 6.7 are the domain-averaged LAI prescribed in offline ClimRAMS, simulated by the coupled model, and simulated by the offline DayCENT. These curves are seven-day running means. At the first glance, the three curves are very different in both patterns and magnitudes. Recalling the LAI curve derived from the NDVI data set (Figure 6.1), the DayCENT-simulated LAI is closer to the observation both in value and curve shape. The LAI prescribed in ClimRAMS is too high both in winter and summer, demonstrating an unrealistic vegetation growth phenology for our domain. The coupled-model-simulated LAI is generally higher than that simulated by the offline DayCENT. This can be explained later by the fact that the coupled model produces more summer precipitation than the offline ClimRAMS simulation (to be discussed in the next section).

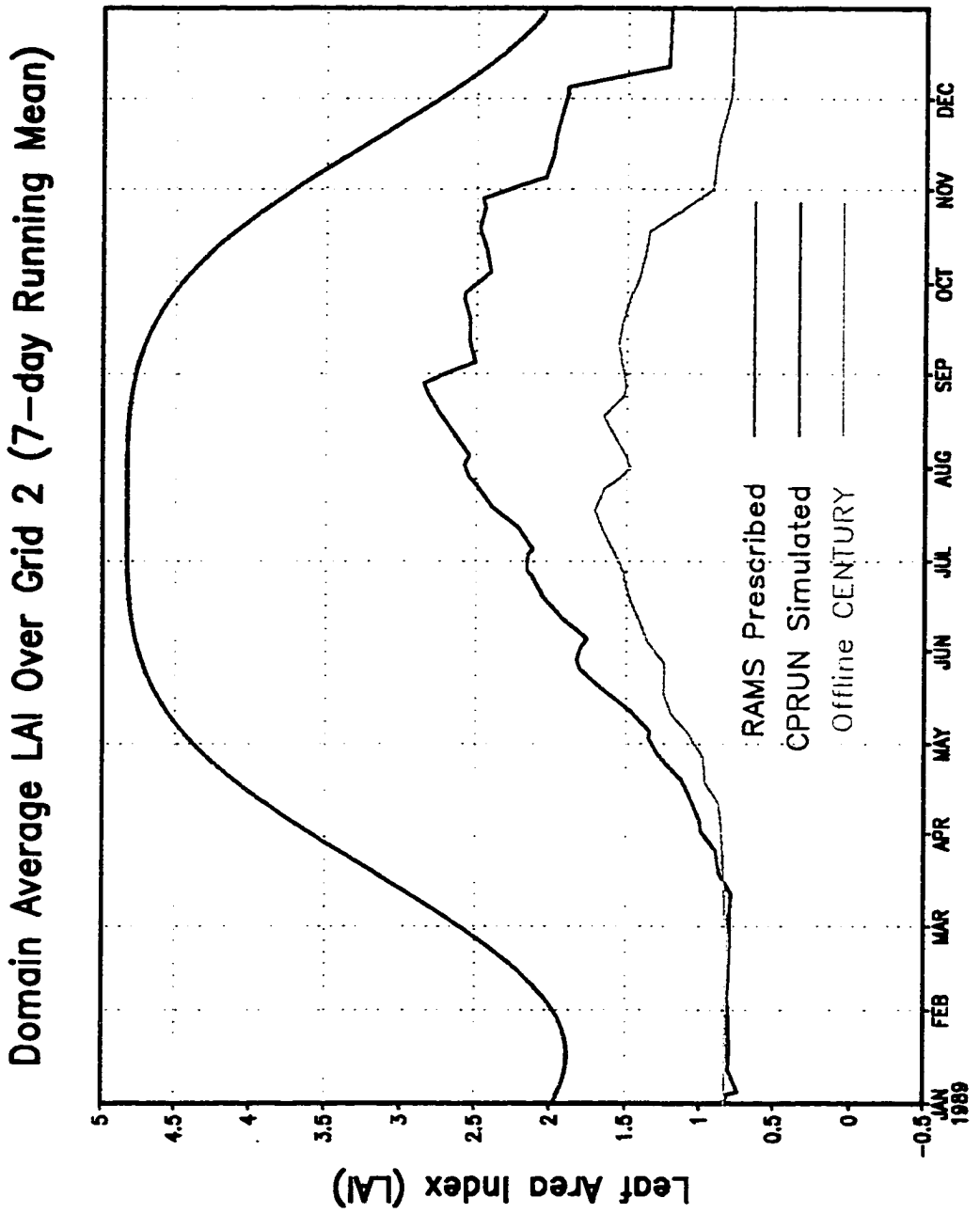

Figure 6.7 Domain-averaged LAI prescribed in offline ClimRAMS (RAMS Prescribed), simulated by the coupled model (CPRUN Simulated), and simulated by offline DayCENT (Offline CENTURY) for the fine grid.

6.3.2 Simulated Climate

The primary purpose of conducting the coupled model simulation is to study the two-way interactions between the atmosphere and the vegetation. The intent is not to tune the coupled model close to the observation. We should not be surprised if the offline ClimRAMS produces better agreement with the observed climate than the coupled model, since ClimRAMS has been adjusted to match the observations. Little insight can be found by comparing offline ClimRAMS and the coupled model's forecast skills. Therefore, we will focus on analyzing the differences between the coupled and the offline ClimRAMS simulation and what causes them.

Shown in Figure 6.8 are the daily maximum screen-height air temperature (Tmax) averaged over the fine grid from the offline ClimRAMS, the coupled model and the observations, respectively. The differences between the coupled model and the offline ClimRAMS simulation are also plotted, including a 30-day running mean of the difference values. The coupled and offline model are very close in simulating Tmax for November, December, January, and February. The coupled model is in better agreement with the observation from March to the end of June compared to offline ClimRAMS run. A much more realistic spring and early summer vegetation green-up description from DayCENT may contribute to the improved simulation during that period. A coupled model cold bias was found in Tmax from July to October when compared to the observations and the offline ClimRAMS simulation due to the excessive rainfall simulated by the coupled model.

Figure 6.9 displays the same information as Figure 6.8 except that it is for the

daily minimum screen-height air temperature (Tmin). The coupled run is warmer than the offline run for the winter months, but colder for the summer months, where Tmin can be as much as 3 °C colder. This is also closely related to the excessive precipitation produced by the coupled model during the summer period.

Figure 6.10 presented the same information as Figure 6.8 except that it is for the daily precipitation. The coupled model produces more rain than the offline simulation throughout the year, especially in the summer, which means that the vegetation phenology from DayCENT enhances the coupled model's ability to capture the precipitation event peaks. But the coupled model tends to rain more frequently and overestimate the total rainfall amount compared to the observations.

In general, the coupled model's temperature and precipitation simulation captures the synoptic signals as well as the seasonal evolution. The coupled model simulated more precipitation in summer, which led to a colder summer compared to the offline ClimRAMS simulations.

Then why does the coupled run differ from the offline run the way it does? First, instead of using prescribed LAI, the coupled simulation uses the LAI generated by DayCENT model, which is only about half the value of LAI traditionally used in ClimRAMS (Figure 6.7). At the same time, the representation of vegetation phenologies between the two models are quite different. Second, the vegetation transmissivity was dynamically coupled to ClimRAMS for the coupled control run. Since in the coupled model LAI is smaller than the prescribed ClimRAMS LAI, the vegetation transmissivity of the coupled model is larger and allows more solar

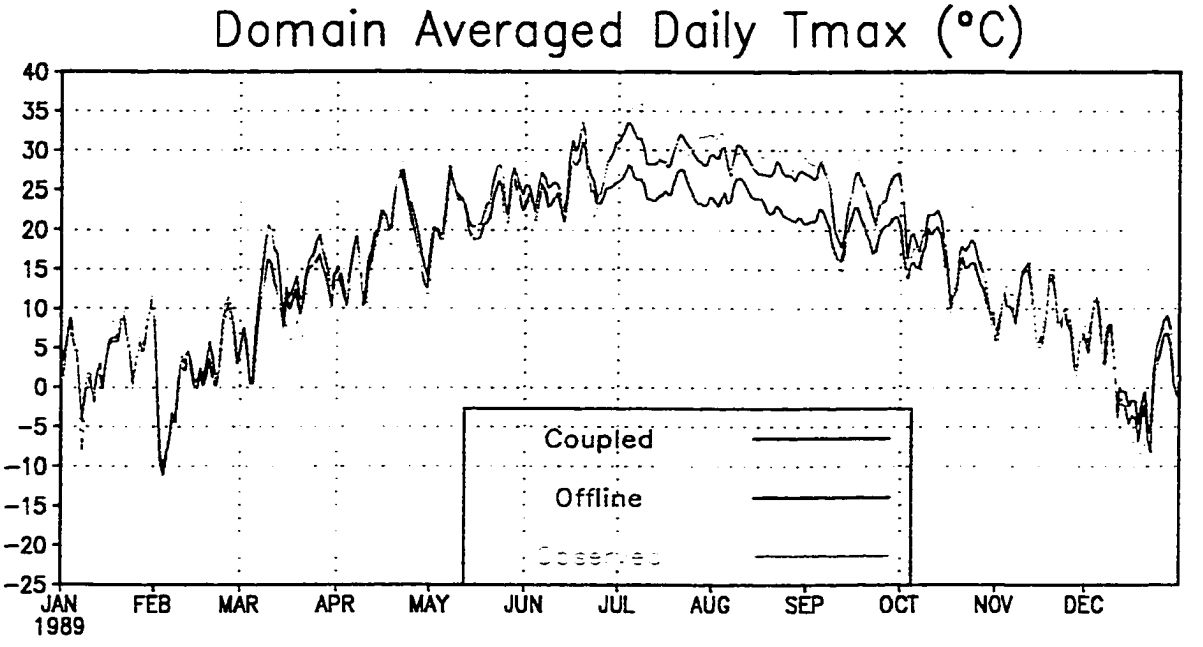

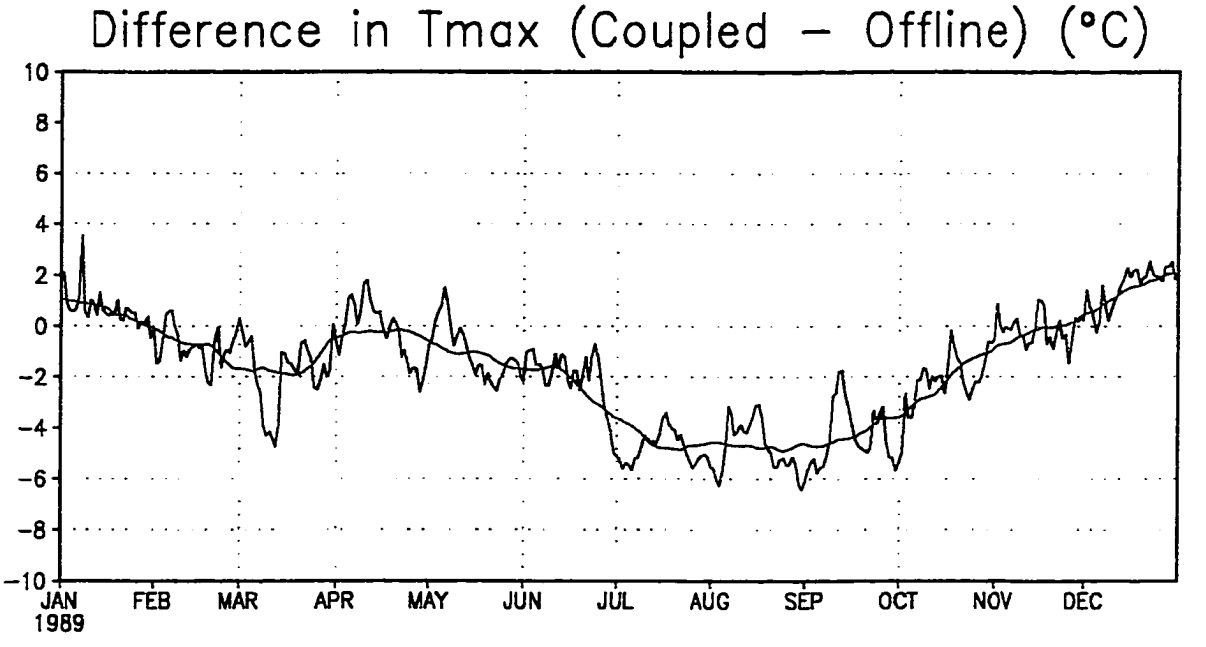

Figure 6.8 The daily maximum screen-height air temperature averaged over the fine grid from offline ClimRAMS (Offline), the coupled model (Coupled) and the observations (Observed), respectively, for the time period 1 January through 31 December 1989. Also shown is the difference between the coupled model and the offline ClimRAMS, and the 30-day running mean of the difference values.

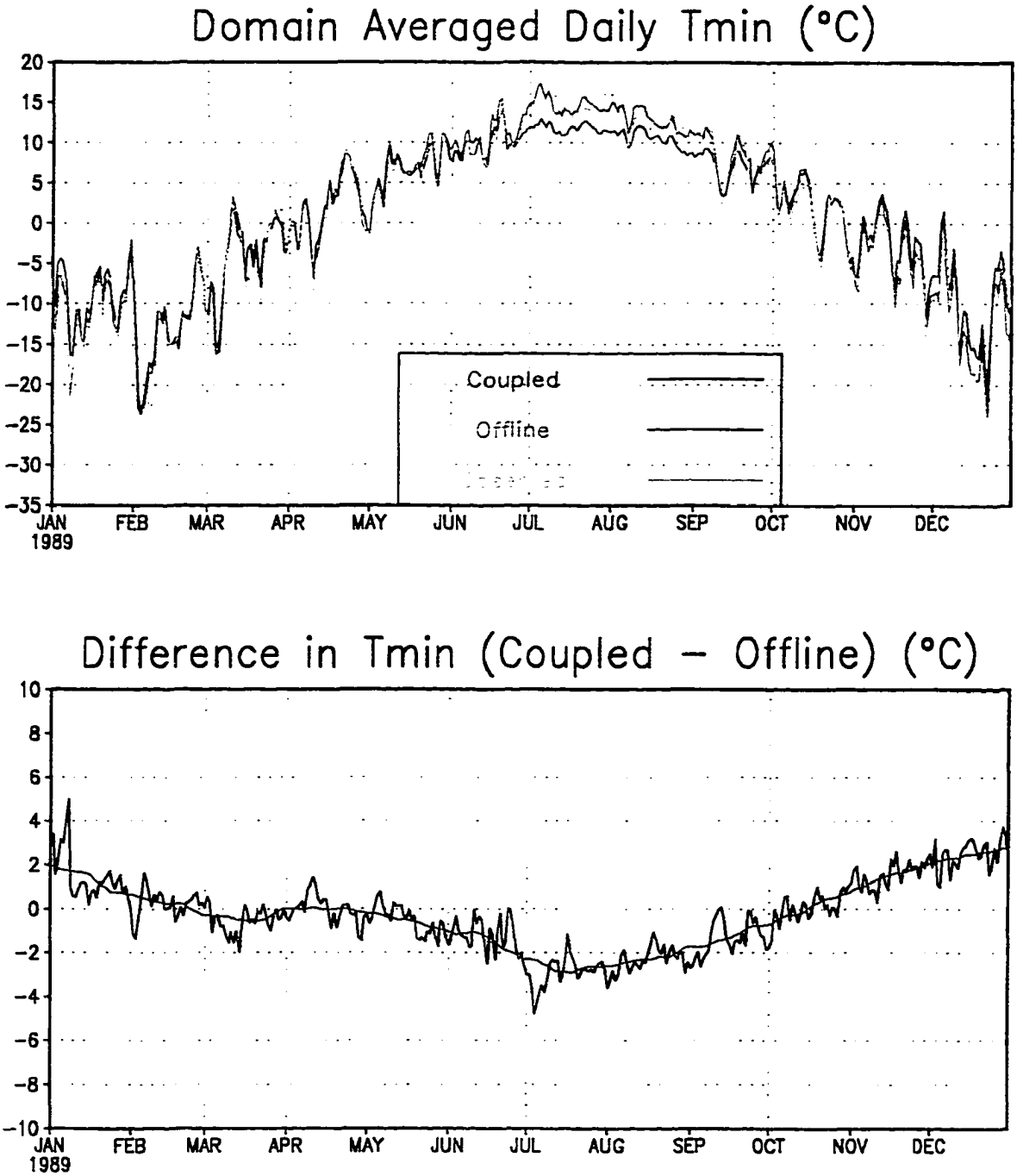

Figure 6.9 The same as Figure 6.8, but for daily minimum screen-height air temperature.

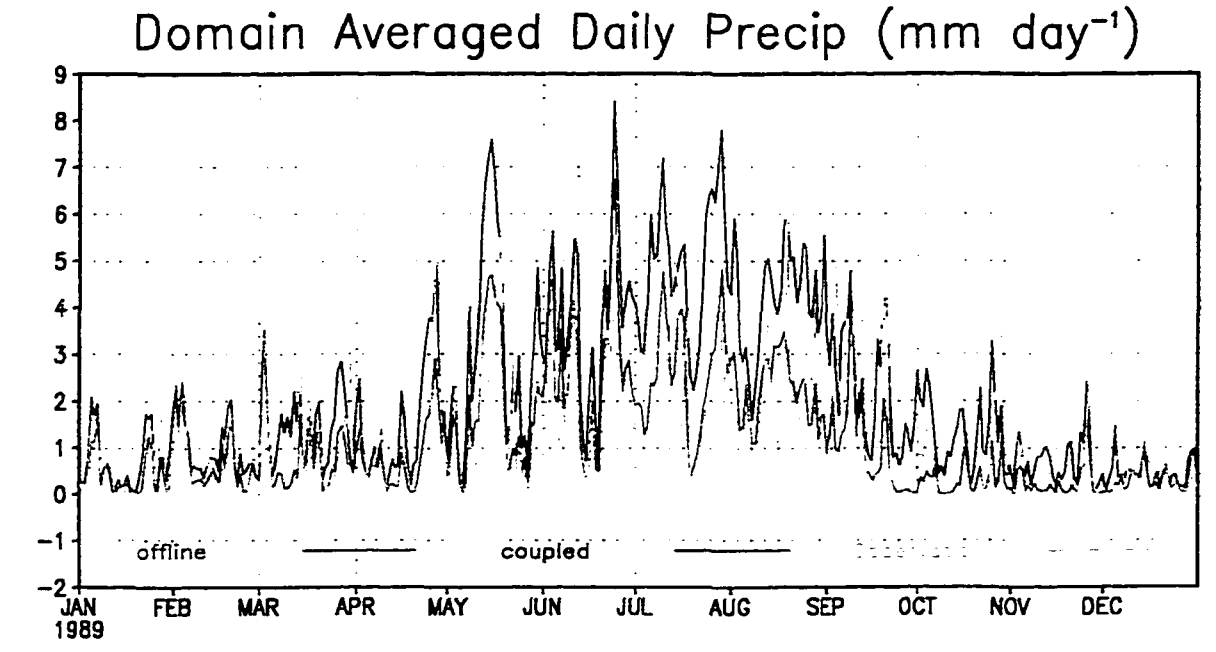

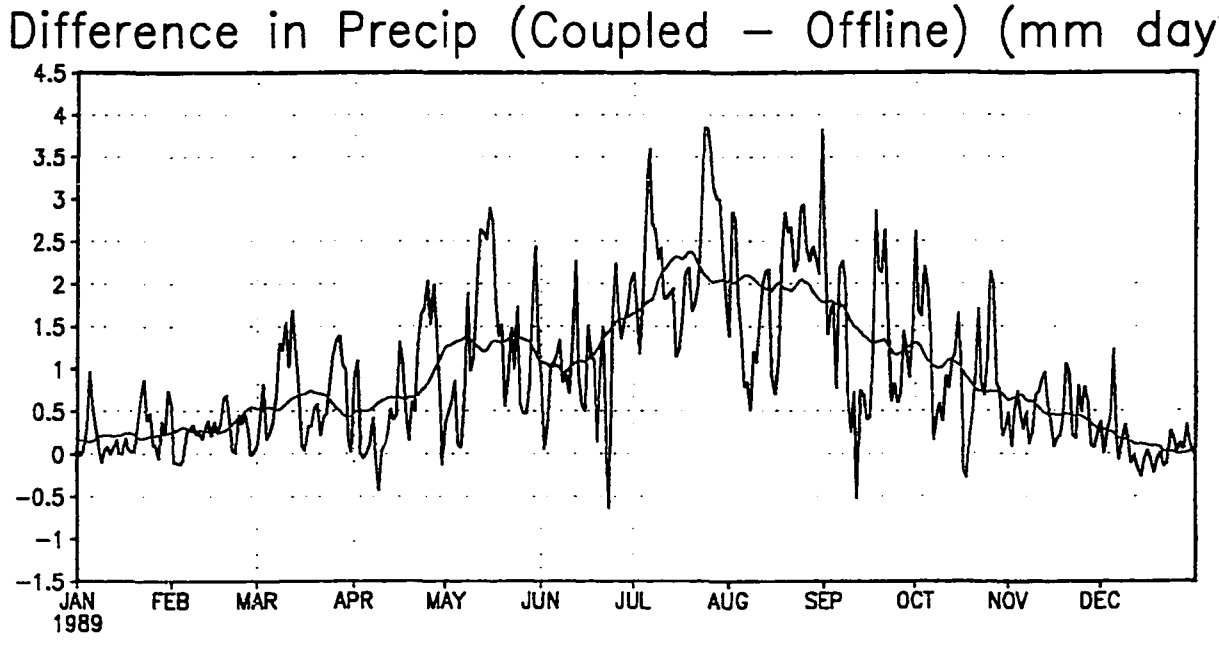

Figure 6.10 The same as Figure 6.8, but for daily precipitation.

radiation to reach the land surface. Initially, extra surface heating (Figure 6.11) increases the instability, which can in turn triggers more convective precipitation. Soon the wetter surface condition becomes important and the transpiration and evaporation from the vegetated surface and bare soil greatly increases. This is accompanied by decreased Bowen ratios and increased latent heat fluxes (Figure 6.12). Although the lateral atmospheric boundary conditions used in the coupled and the offline ClimRAMS simulations are identical, there is more local moisture available in the coupled simulation. This process leads to the increase of moist static energy which favors the generation of more precipitation. Thus, a positive feedback mechanism exists between the LAI and precipitation, which may contribute to the increase of local moisture and, in turn, cause more precipitation. This point will be further discussed in the next sub-section.

Furthermore, the vegetation specification from the coupled model is simulated by DayCENT, while in ClimRAMS it is defined by the BATS classification and varied only based on the Julian day according to a sine function. DayCENT provides the domain with much more heterogeneities both in vegetation classes and their evolution patterns. Land surface inhomogeneities can induce atmospheric solenoidal circulations which not only influence the surface layer above the vegetation but can also act as triggers for moist convection and precipitation in preferred areas, with obvious strong feedbacks to vegetation.

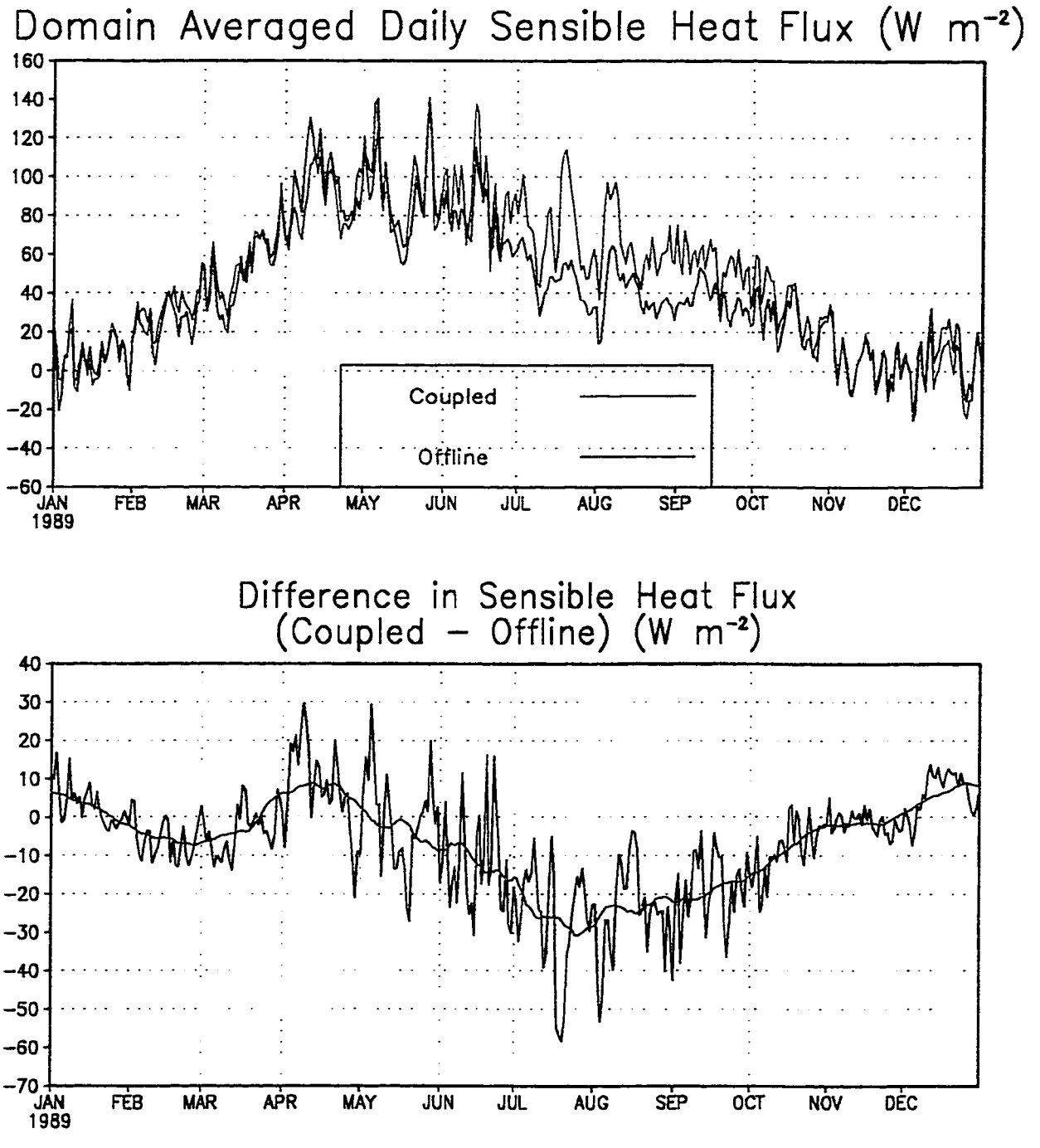

Figure 6.11 Domain-averaged daily sensible heat flux from offline ClimRAMS (Offline) and the coupled model (Coupled) for the time period 1 January through 31 December 1989. Also shown are the differences between the offline and the coupled model, and a 7-day running mean of the difference values.

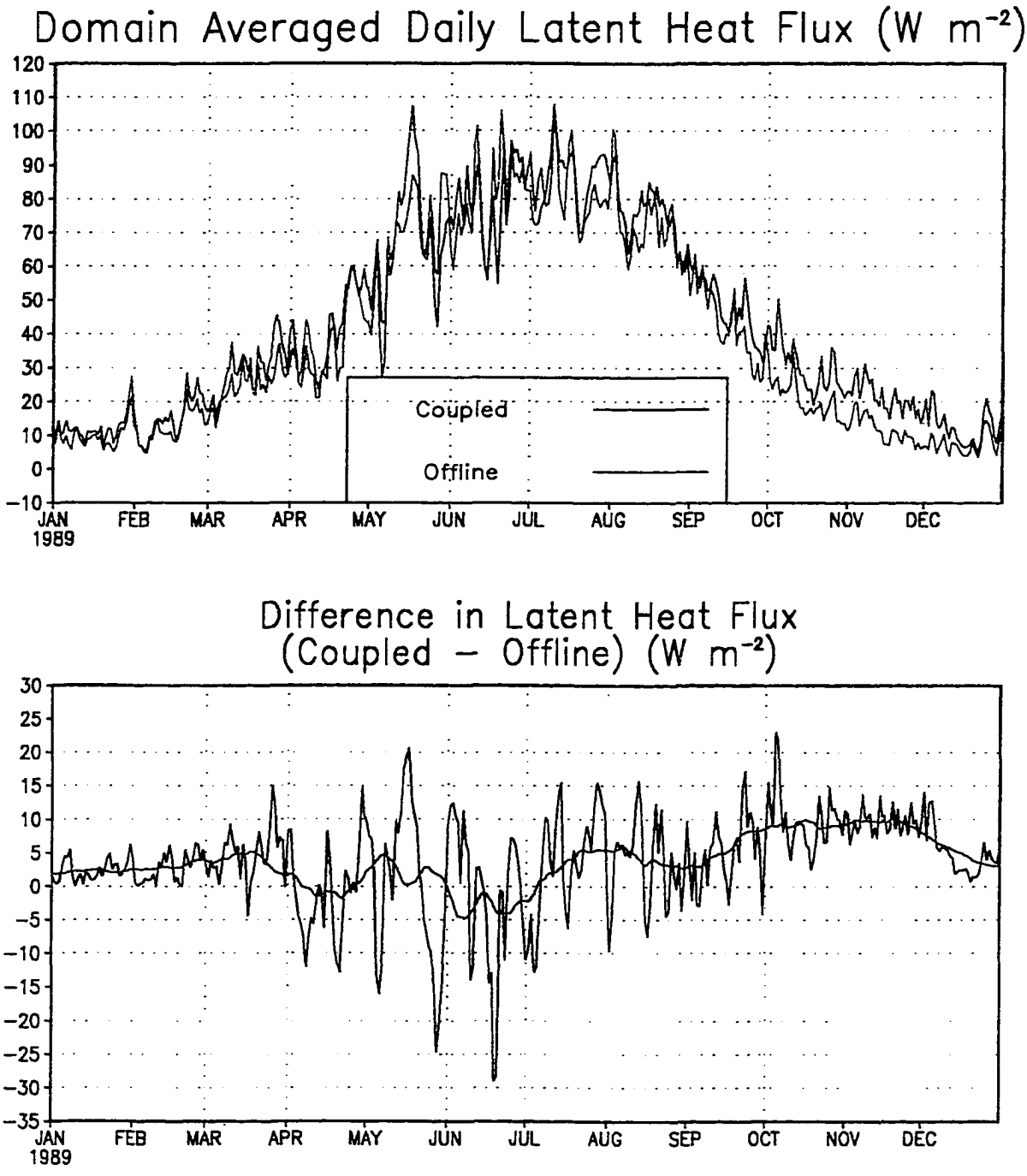

Figure 6.12 Domain-averaged daily latent heat flux from offline ClimRAMS (Offline) and the coupled model (Coupled) for the time period 1 January through 31 December 1989. Also shown are the differences between the offline and the coupled model, and a 7-day running mean of the difference values.

6.3.3 Simulated Atmosphere and Vegetation Feedbacks

The coupled model allows us to look into the feedback dynamics between atmosphere and vegetation in a much more detailed manner.

Figure 6.13 shows the daily LAI prescribed by ClimRAMS, generated by DayCENT and simulated by the coupled model, for a single grid cell. Also shown is the precipitation difference between the coupled and offline simulation, and the 30-day running mean. The land-use type for this grid cell is winter wheat. The location of the grid cell corresponds to Salina, Kansas. At the beginning of August, the winter wheat harvest occurred which brought the LAI down to near zero. Corresponding to the harvest event, the coupled model has a dramatic precipitation decrease from August to mid-September due to the sudden shutdown of vegetation transpiration which greatly reduced the local moisture availability. Accordingly, the offline DayCENT starts another year's winter wheat growth with less precipitation and drier soil than the offline ClimRAMS, resulting in less biomass growth in the coupled model than the offline DayCENT which is driven by the offline ClimRAMS climate.

Figure 6.14 shows the daily LAI prescribed by the offline ClimRAMS, generated by offline DayCENT, and simulated by the coupled model, over a C3 grassland near Casper, Wyoming. There are dramatic differences between the LAI curves generated by DayCENT and the one originally used in the offline RAMS simulations (the long-dash line). The seasonal evolution of LAI is realistically represented in the coupled model. The growing season starts rapidly in late April, peaks in late summer, and senesces in the fall. The coupled model (the solid line)

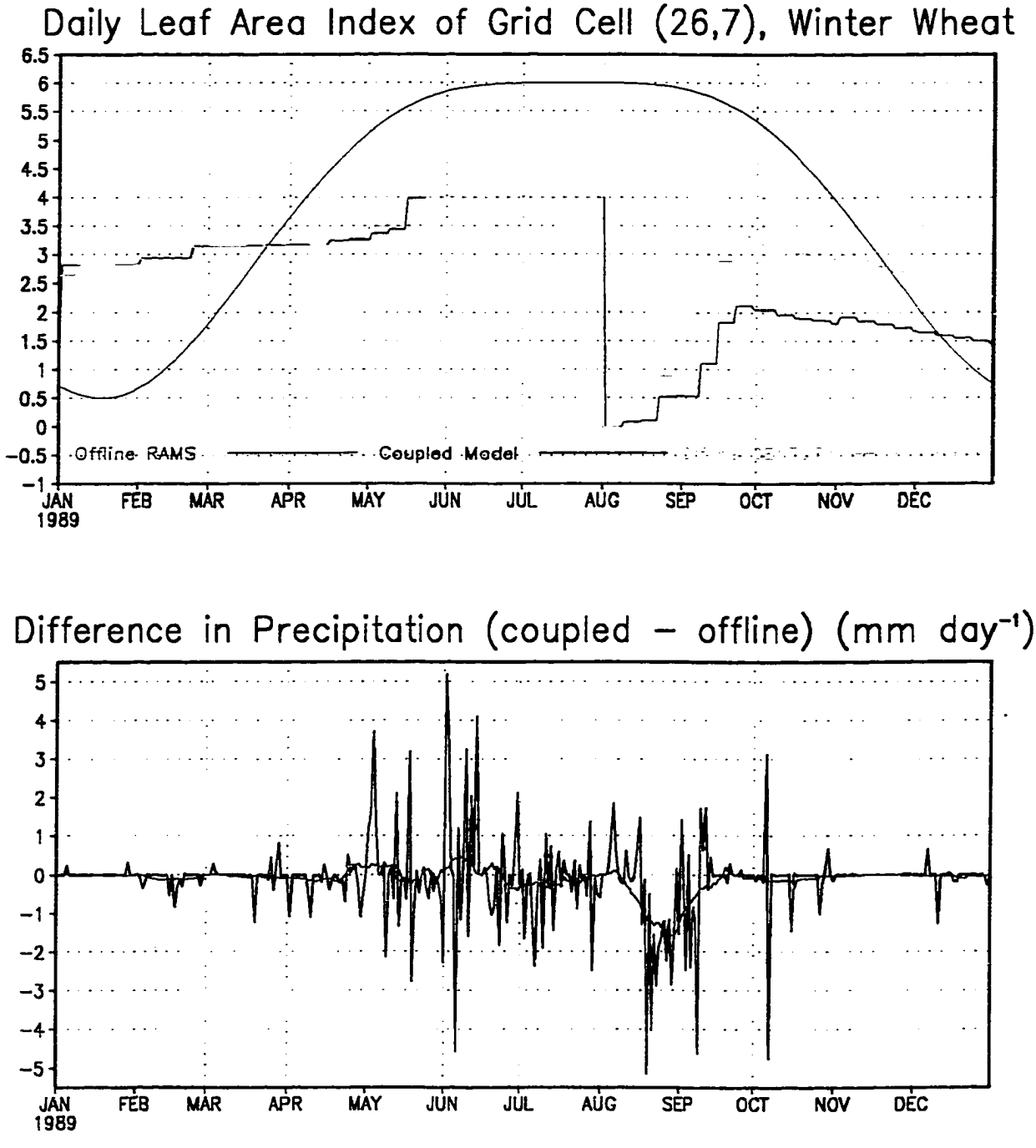

Figure 6.13 Daily LAI prescribed by ClimRAMS (Offline RAMS), simulated by DayCENT (Offline CENTURY) and simulated by the coupled model (Coupled Model), respectively, for a single grid cell near Salina, Kansas. Also shown is the precipitation difference between the coupled and off-line simulation, and the 30-day running mean. The land-use type for this grid cell is winter wheat.

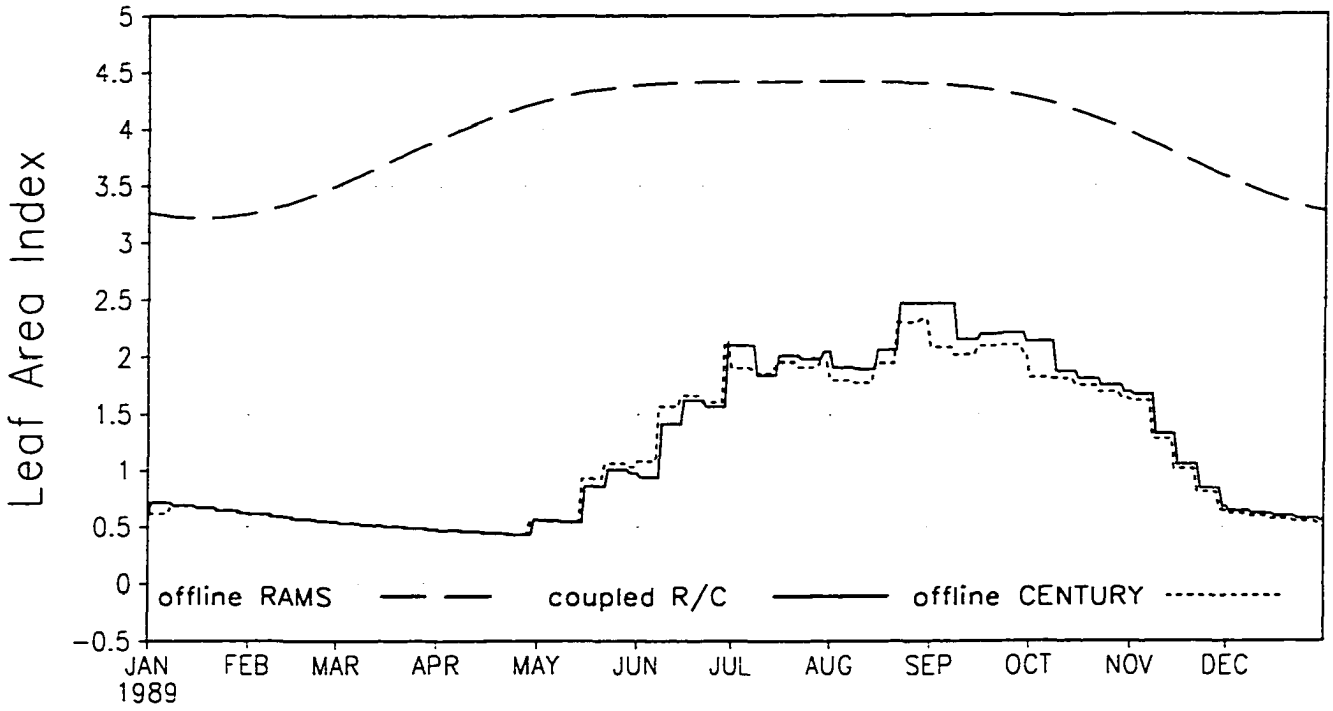

Figure 6.14 Daily LAI prescribed by the offline ClimRAMS (offline RAMS), generated by offline DayCENT (Offline CENTURY), and simulated by the coupled model (Coupled R/C), respectively, over a C3 grassland near Casper, Wyoming.

produces less LAI at the beginning of the growing season due to the lower minimum temperature and less precipitation compared to the offline DayCENT run. The surface heating brought about by the higher Tmax can, in turn, trigger precipitation if enough lower-level moisture convergence is available. Correspondingly, though with a time lag, the vegetation begins to grow more biomass in the early summer. This extra biomass increases the latent heat flux and leads to more rain by transpiring water vapor into the air. A short-term, positive but nonlinear, feedback between LAI and precipitation exists when no other limiting factors, such as temperature, nutrients, etc., are causing stress. Another interesting feature is that the LAI evolution simulated by the coupled model clearly shows an accumulated effect on plant growth. Though sometimes the coupled run receives less rain than the offline run, once the vegetation develops, it tends to remain until the end of the year as shown in Figure 6.14. The positive feedback between LAI and precipitation seems to be one of the vegetation's mechanism to modify the environment, and to adjust to the atmospheric conditions in order to maximize their prospects of growth and survival.

To further explore the feedback dynamics between the vegetation and climate, the 7-day running means of domain-averaged precipitation and LAI were plotted in Figure 6.15. Following each rainfall maximum, an LAI maximum occurred one or two weeks later. This phenomena lasts until the vegetation enters September, when senescence processes take over. This comprehensively demonstrates that the coupled model is able to represent the two-way feedbacks between the weather and vegetation.

Potential longer-term feedbacks from the soil nutrient cycle and roots need to

be explored using multi-year simulations.

In the coupled RAMS/CENTURY modeling system, ClimRAMS provides the atmospheric forcings required by DayCENT to decribe the plant environment, while DayCENT provides vegetation characteristics of direct importance to the atmosphere that develop in response to plant life-cycles and evolution. The simulation results described above provide evidence that two-way feedbacks between the atmosphere and land surface can cause significant changes in atmospheric conditions that, in turn, influence vegetation growth and evolution. Therefore, current land surface models that do not consider the two-way feedbacks between the atmosphere and vegetation neglect a significant component of the Earth-atmosphere system.

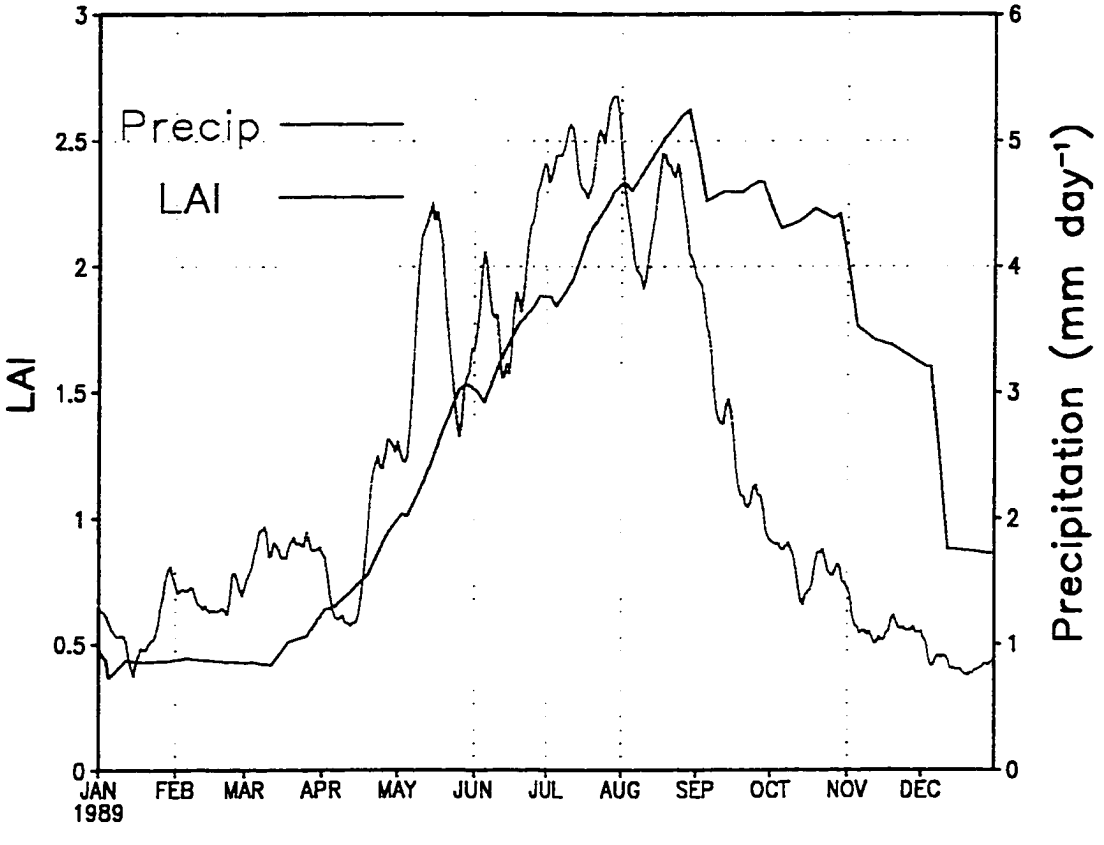

Figure 6.15 7-day running means of precipitation and LAI, averaged over the fine grid.

Chapter 7

COUPLED-MODEL SENSITIVITY EXPERIMENTS

7.1 Simulating Interannual Variations

Computational resources limit our ability to perform long-term simulations with the current model configurations. To investigate the coupled model's sensitivity to interannual climate variations, an alternative approach is to perform simulations one year at a time for both average and anomalous years instead of running continuous multi-year simulations.

7.1.1 Simulating Dry and Wet Years With ClimRAMS

In Section 4.4.2 of Chapter 4, 1988, 1989, and 1993 were identified as dry, average, and wet years, respectively, according to the analyses of the domain-averaged climate variables. The results of the 1989 ClimRAMS simulation have been presented in Section 6.2 of Chapter 6, where the model's skill of representing the climatology of an average year has been demonstrated. In this section, ClimRAMS will be further applied to 1988 (dry year) and 1993 (wet year), and the model's ability to reproduce the seasonal and annual cycles of extreme years will be examined. The land-cover specification and topographic distribution are identical for all three years' integrations,

whereas the model's initialization and boundary conditions are defined by using NCEP reanalysis products corresponding to each of the three years. Since the results from these ClimRAMS simulations will be used to spin-up DayCENT to ClimRAMS climate for three years before the coupled runs start, they should be viewed not only as ClimRAMS sensitivity tests, but also as a prelude for the coupled model simulations.

The performance of ClimRAMS in simulating the climate of 1988 (dry year) is illustrated in Figure 7.1 through Figure 7.4 by comparing against the observations. Shown in Figure 7.1 are domain-averaged daily maximum (Tmax) and minimum (Tmin) temperature and daily precipitation. Also plotted are the differences between the modeled and observed values, including a 30-day running mean of the daily values. The model is found to capture the annual cycles as well as the synoptic events of these primary atmospheric variables. Throughout 1988, the model-simulated daily Tmax and Tmin averaged 0.06 °C lower and 0.54 °C higher than those observed, respectively. The precipitation averaged 0.05 mm day^{-1} lower than the observed with the greatest underestimation occurring in spring and fall. The greatest overestimation of rainfall happened in the summer, which unfortunately demonstrates the fact that the model is not capable of reproducing the extremely dry summer. The model generally captured the spatial patterns of Tmax, Tmin, and precipitation in both winter months (Figure 7.2) and summer months (Figure 7.3). The model tends to have a large warm bias for the eastern portion of the domain and a cold bias for the western region of the domain, especially in winter where the model-simulated Tmax can deviate from

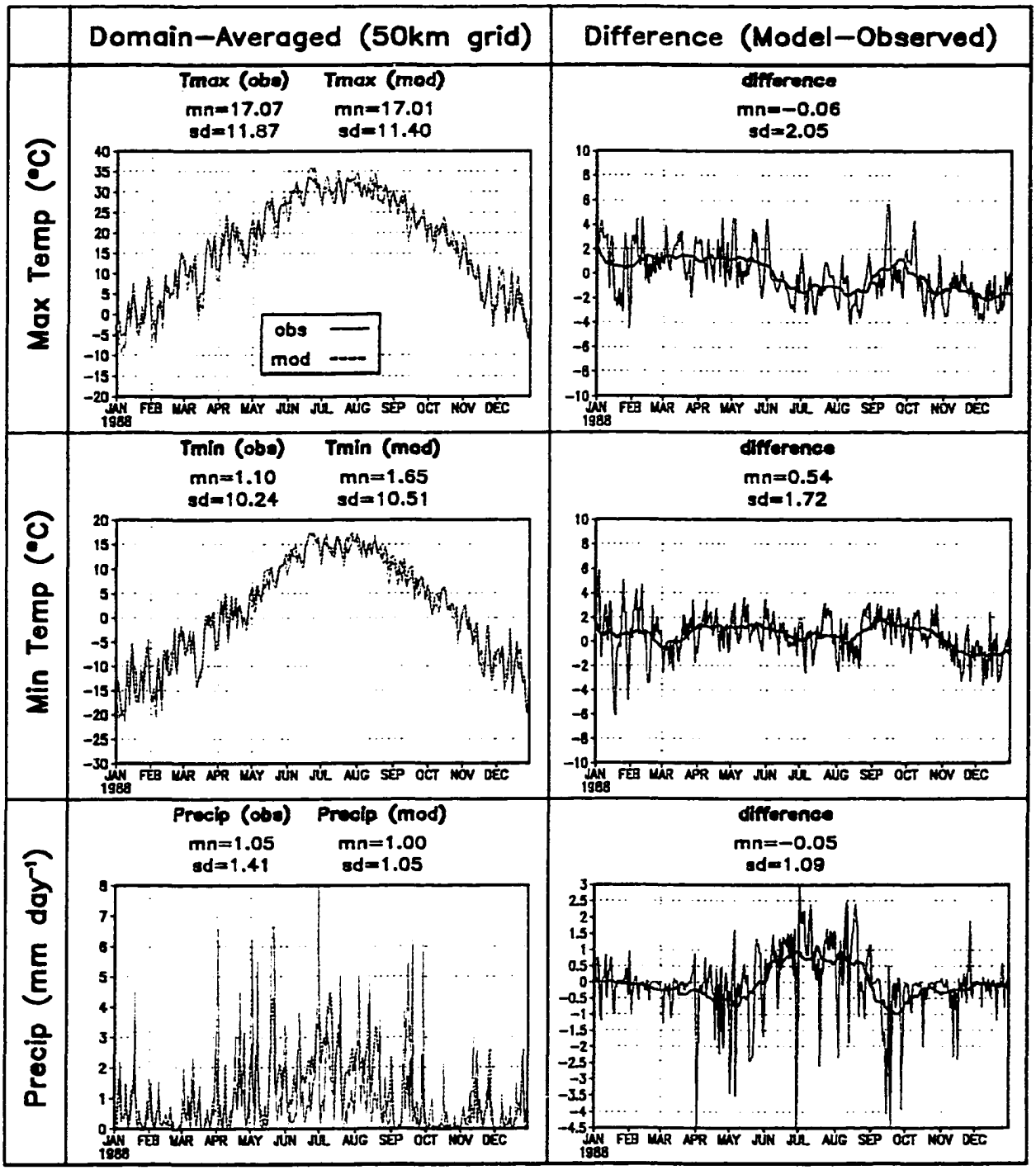

Figure 7.1 Modeled and observed, domain-averaged daily maximum and minimum screen-height air temperature and daily precipitation for 1988, where these variables have been averaged over the 50-km grid given in Figure 4.2. Also shown is the difference between the model and observations, and the 30-day running mean of the difference values. Included are the mean (mn) and standard deviation (sd) for each panel and variable.

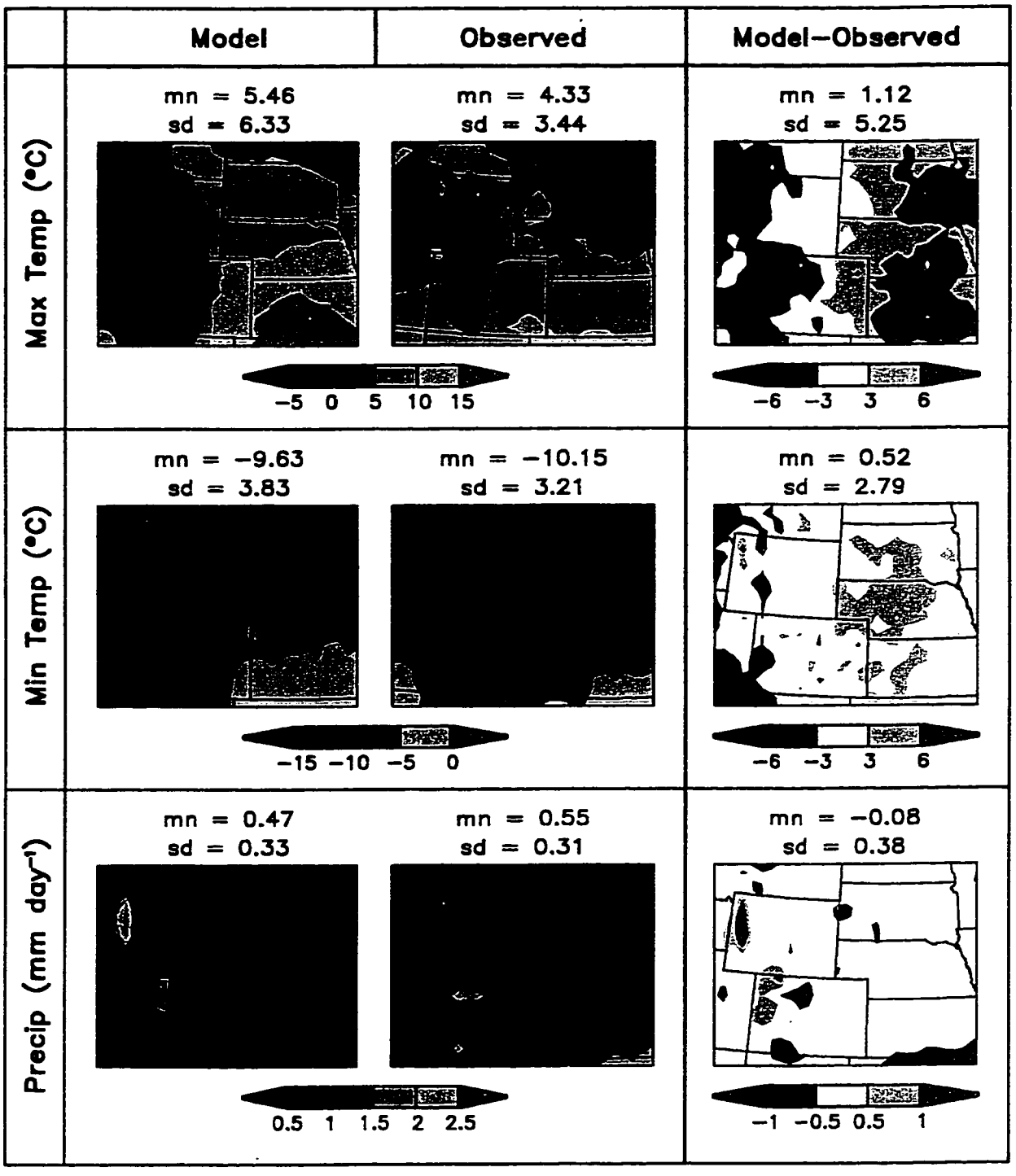

Figure 7.2 The winter spatial patterns of maximum and minimum daily screen-height temperature and daily precipitation, averaged over January through March of 1988. Shown are the modeled and observed fields, and the differences between the two. Also included are the mean (mn) and standard deviation (sd) for each panel and variable.

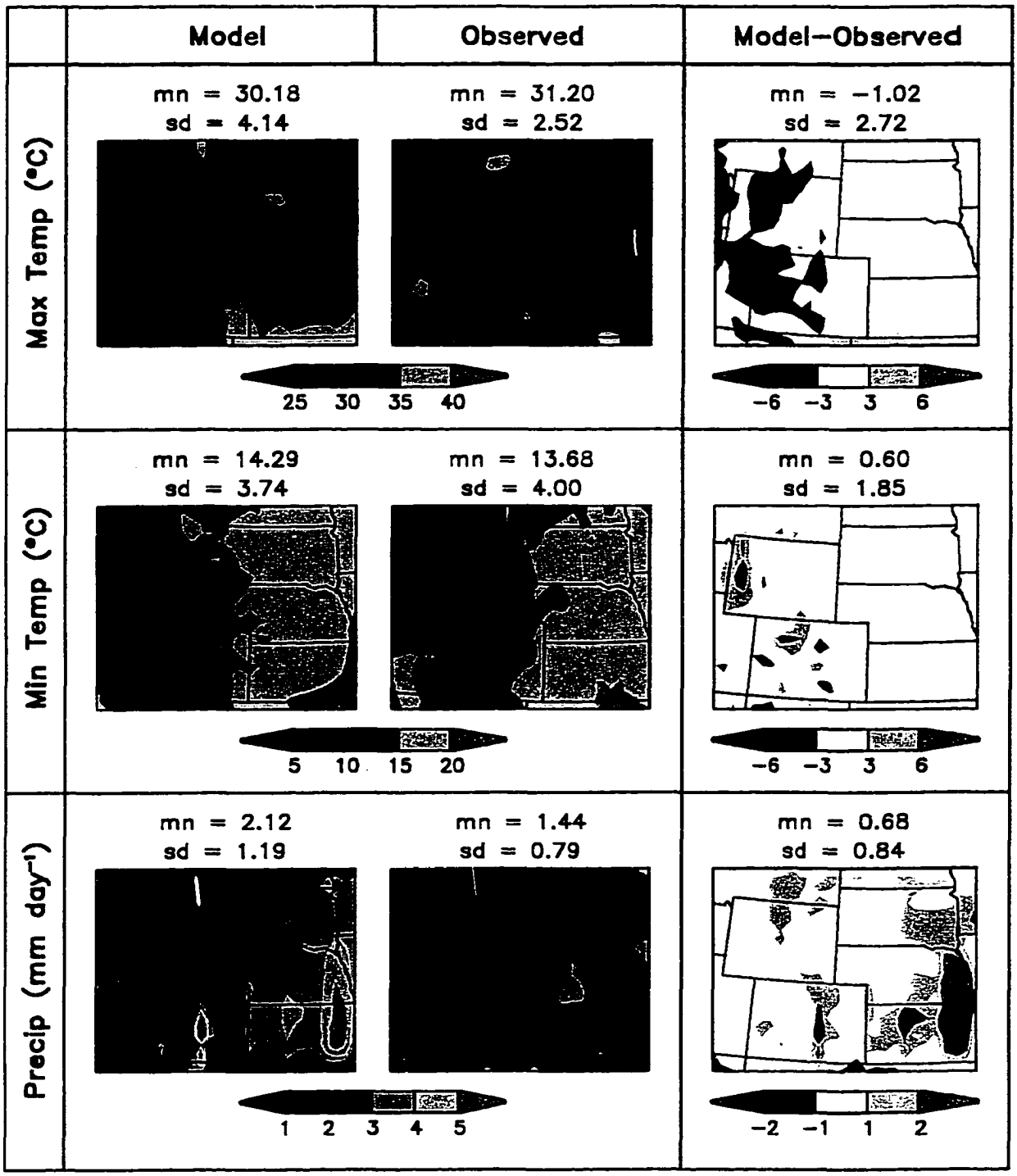

Figure 7.3 Same as Figure7.2, but for summer, averaged over June through August of 1988.

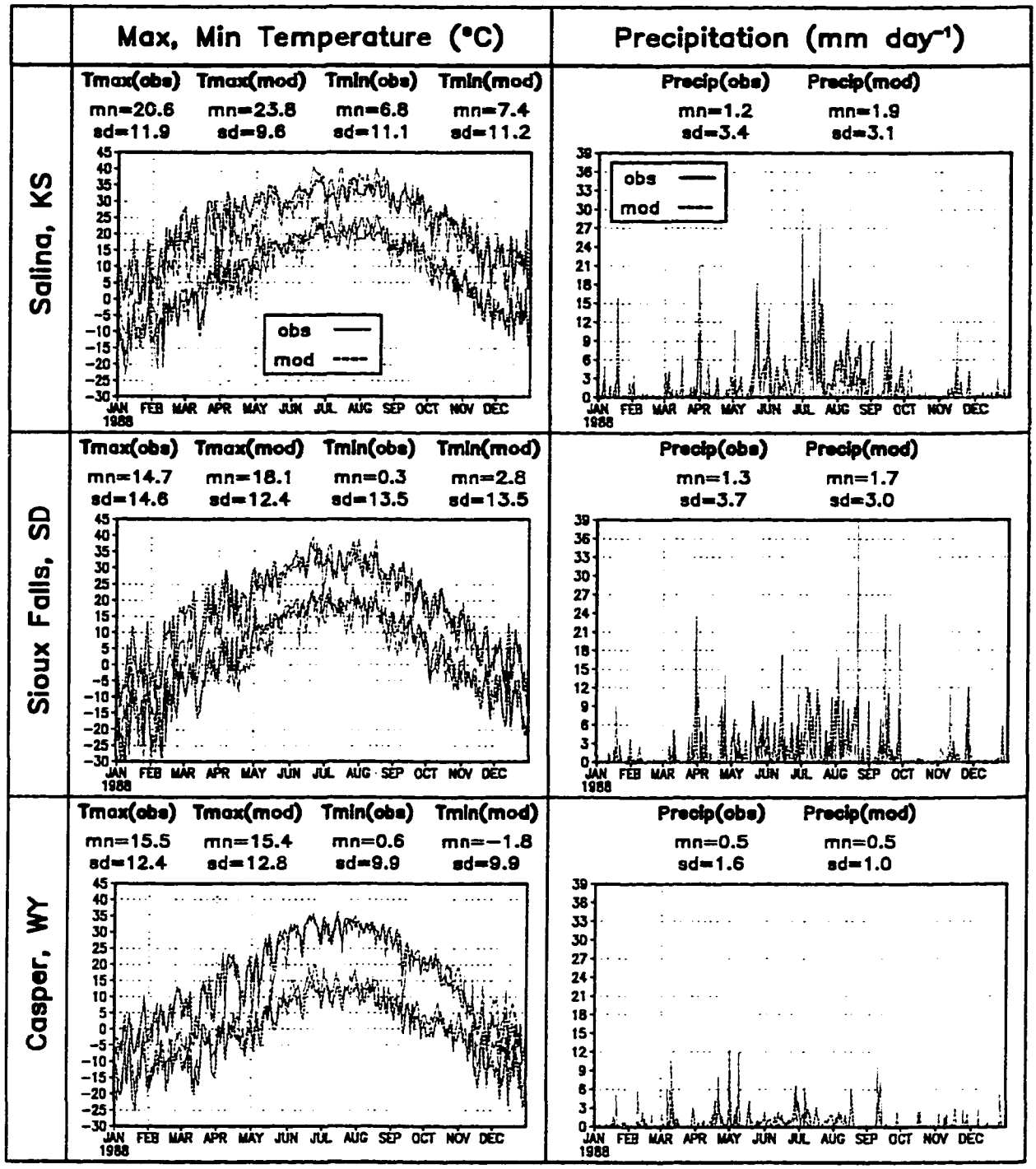

Figure 7.4 The annual cycle of daily maximum and minimum screen-height temperature and daily precipitation for 1988 at the model grid cells corresponding to three cities identified by the markers in Figure 6.6. Also included are the mean (mn) and standard deviation (sd) for each panel and variable.

observation as much as ± 6 °C. The temperature biases could presumably be reduced greatly in the western mountainous areas if the temperature fields were corrected for the elevation differences between model and observation (Liston and Pielke 1999). Snowfall over the Teton mountain range in northwestern Wyoming has been overestimated. The greatest rainfall overestimation happened in the Rocky Mountain Front Range and southeast corner of the domain. The annual cycles of daily Tmax, Tmin, and precipitation at the model grid cells corresponding to the three cities within the fine-grid domain (Figure 6.6), are given in Figure 7.4, in which the model is able to simulate the regional variability of these sites.

Figure 7.5 through 7.8 demonstrates the ability of ClimRAMS to simulate the 1993 climate (wet year). Shown in Figure 7.5 are domain-averaged daily maximum (Tmax) and minimum (Tmin) temperature and daily precipitation, for the time period 1 January through 31 December 1993. Also plotted are the differences between the modeled and observed values, including a 30-day running mean of the daily values. The model is found to capture the annual cycles as well as the synoptic events of these primary atmospheric variables. During 1993, the model-simulated daily Tmax and Tmin averaged 2.01 °C and 0.75 °C higher than the observed, respectively, with the greatest Tmax bias occurring in March and April. The total precipitation averaged 0.02 mm day^{-1} higher than the observed, while at the same time, the precipitation was underestimated from mid-June to mid-August. This again emphasizes the fact that the model is not capable of reproducing the rainfall of the extremely wet summer. The model generally captures the spatial patterns of Tmax, Tmin and precipitation in both

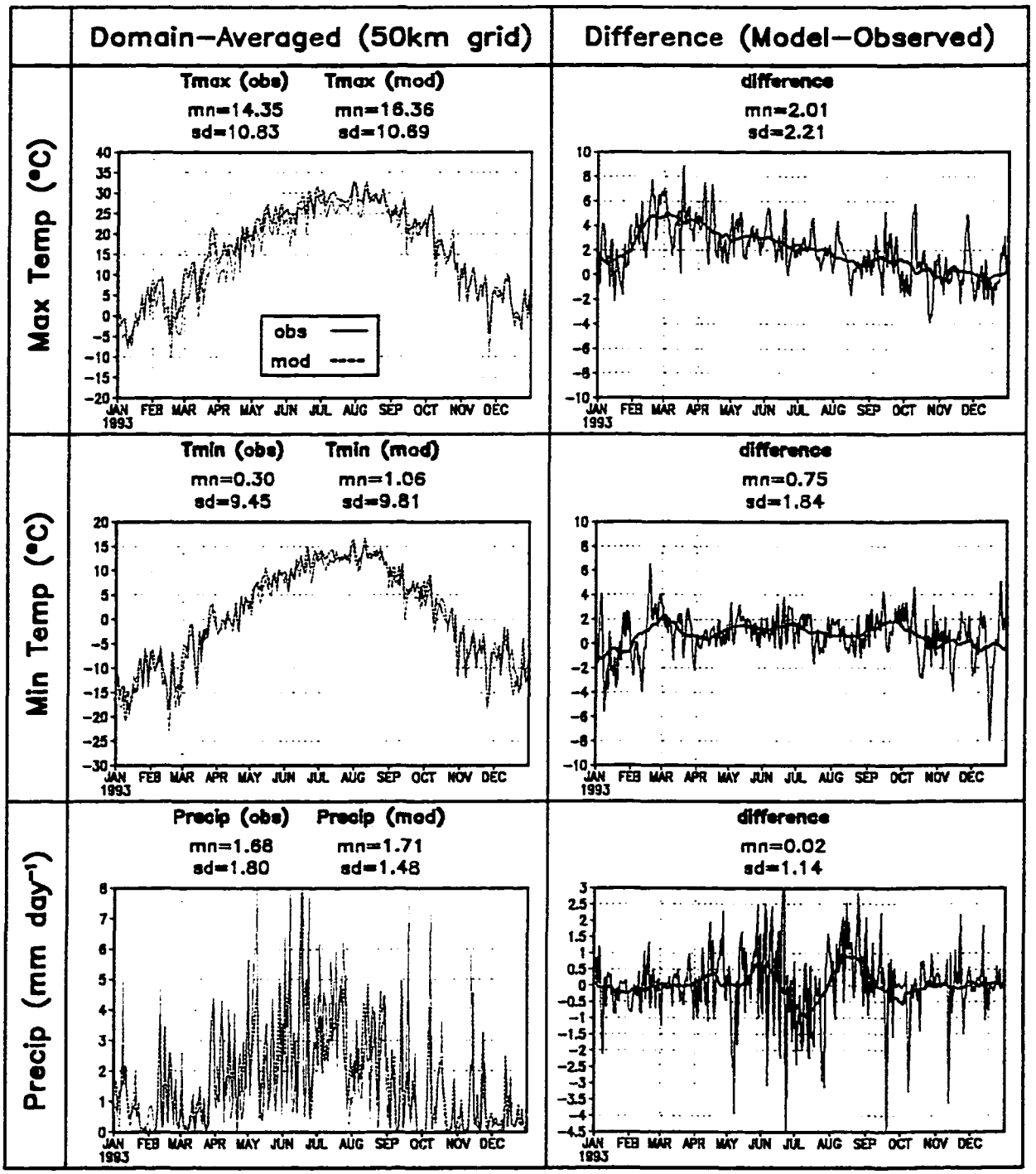

Figure 7.5 Modeled and observed, domain-averaged daily maximum and minimum screen-height air temperature and daily precipitation for 1993, where these variables have been averaged over the 50-km grid given in Figure 4.2. Also shown is the difference between the model and observations, and the 30-day running mean of the difference values. Included are the mean (mn) and standard deviation (sd) for each panel and variable.

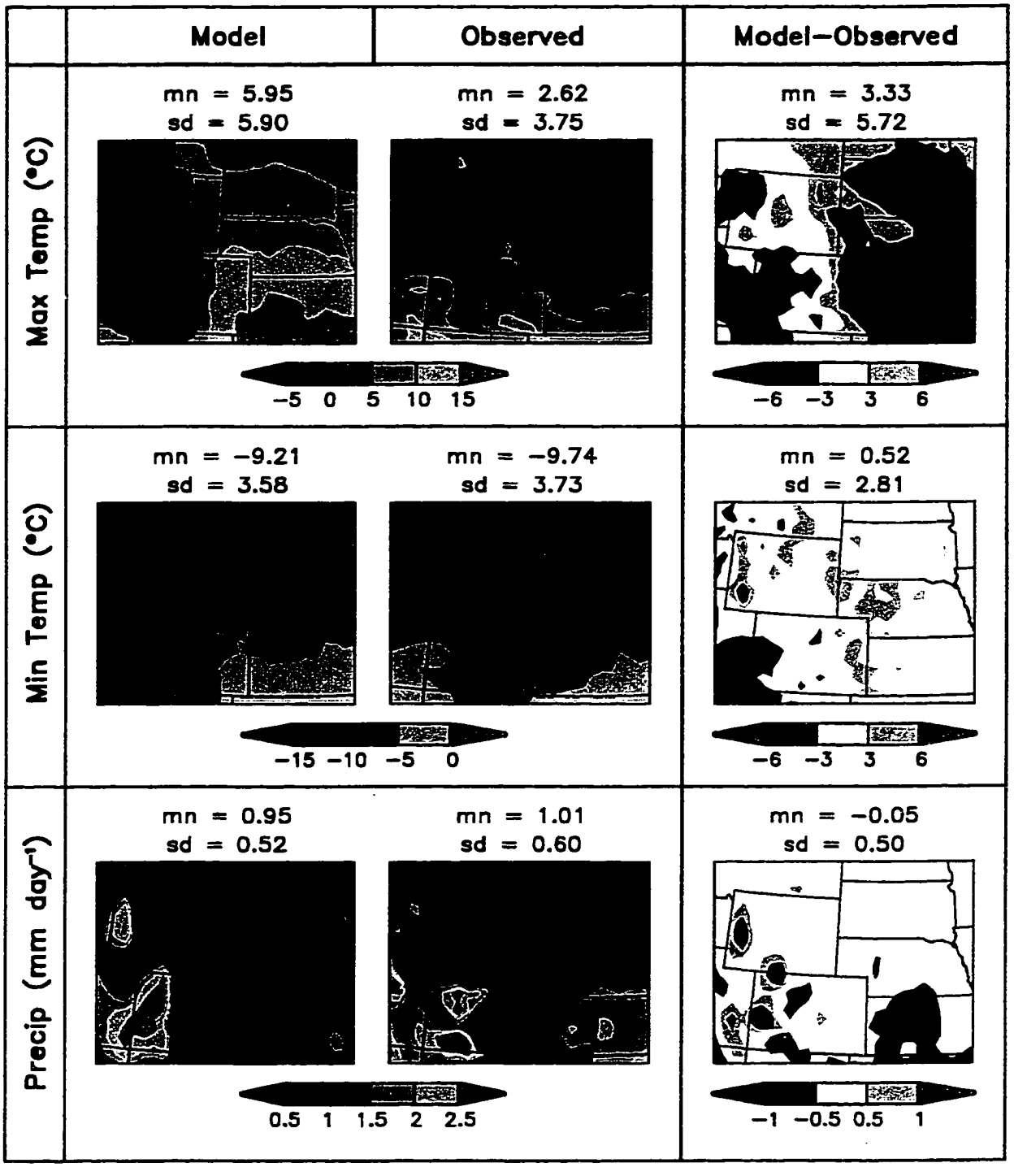

Figure 7.6 The winter spatial patterns of maximum and minimum daily screen-height temperature and daily precipitation, averaged over January through March of 1993. Shown are the modeled and observed fields, and the differences between the two. Also included are the mean (mn) and standard deviation (sd) for each panel and variable.

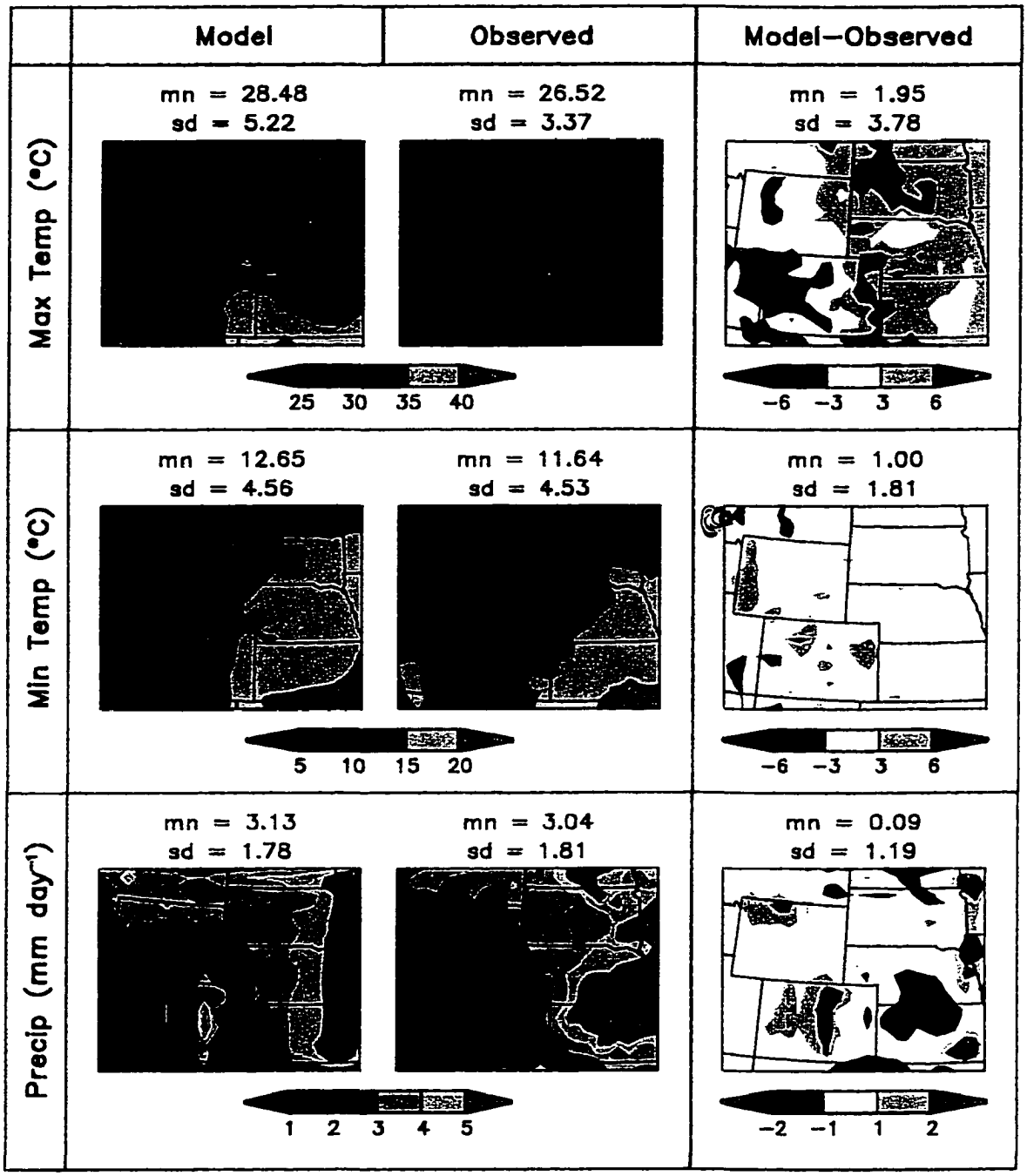

Figure 7.7 Same as Figure 7.6, but for summer, averaged over June through August of 1993.

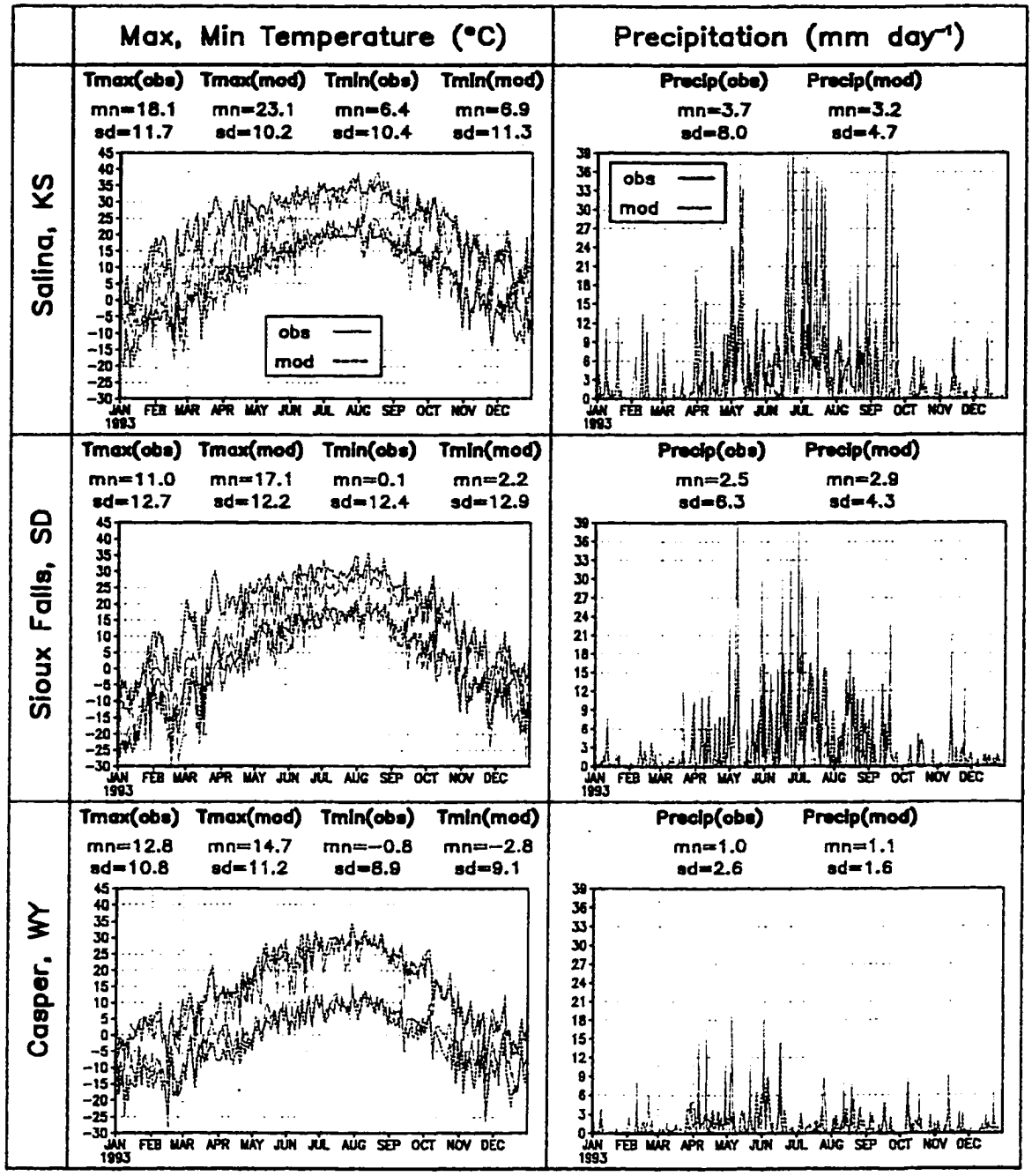

Figure 7.8 The annual cycle of daily maximum and minimum screen-height temperature and daily precipitation for 1993 at the model grid cells corresponding to three cities identified by the markers in Figure 6.6. Also included are the mean (mn) and standard deviation (sd) for each panel and variable.

winter months (Figure 7.6) and summer months (Figure 7.7). The model tends to have a large warm bias for the eastern portion of the domain and a cold bias for the western region of the domain, especially in winter where the model-simulated Tmax can deviate from observation as much as ± 6 °C. The model-simulated temperature fields for the mountainous areas would presumably be closer to those observed if they were corrected by the elevation differences between the model and observations. The overestimation of snowfall in the Teton mountain range and overestimation of rainfall in the Rocky Mountain Front Range happened again in the wet year simulation. The annual cycles of daily Tmax, Tmin, and precipitation, at the model grid cells corresponding to the three cities within the fine-grid domain (Figure 6.6), are given in Figure 7.8. Again it is clear that the model is able to simulate the regional variability of these sites.

In conclusion, ClimRAMS is generally capable of capturing the annual and seasonal variations of primary atmospheric variables. Although the model is able to represent the average precipitation amount for the year and differentiate the dry, average, and wet years, the overestimation of the rainfall in the dry year (1988) and the underestimation of the rainfall in the wet year (1993) demonstrate that ClimRAMS is not capable of reproducing the extremes of individual rainfall events under the 1989 model configuration and therefore model modifications are required in order to completely represent the magnitude of interannual precipitation variations.

7.1.2 The Sensitivity of the Coupled Model to Interannual Variations

This series of experiments is designed to investigate the coupled model's ability to represent interannual variations in terms of both atmospheric variables and biomass. The coupled model was integrated from 1 January through 31 December, for 1988, 1989 and 1993, representing the dry, average, and wet years, respectively.

A comparison of the domain-averaged Tmax between the offline ClimRAMS, the coupled model, and the observations for 1988 is displayed in Figure 7.9. The differences between the coupled model and the offline ClimRAMS simulation are also plotted, including the 30-day running mean of the difference values. Figure 7.10 and Figure 7.11 display the same information as Figure 7.9, but for the daily minimum screen-height air temperature (Tmin) and daily precipitation, respectively. For the year of 1993, the coupled model's performance can be found in Figure 7.12 through Figure 7.14. Shown in Figure 7.12 are the daily maximum screen-height air temperature (Tmax) averaged over the fine grid from the offline ClimRAMS, the coupled model, and the observation, respectively, for the period 1 January through 31 December 1993. The differences between the coupled model and the offline ClimRAMS simulation are also plotted, including the 30-day running mean of the difference values. Figure 7.13 and Figure 7.14 display the same information as 7.12, but for the daily minimum screen-height air temperature (Tmin) and daily precipitation, respectively.

In general, the coupled model is found to capture the interannual, annual and seasonal cycles as well as the synoptic events. Compared to the offline run, Tmax and Tmin of the coupled run are colder from late May to early October, and warmer

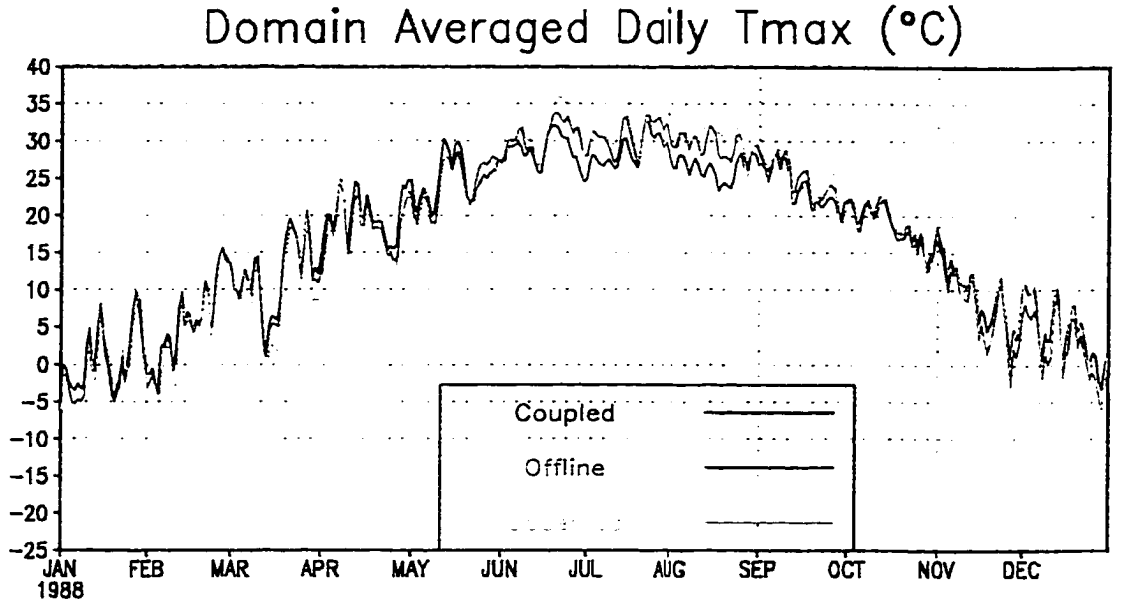

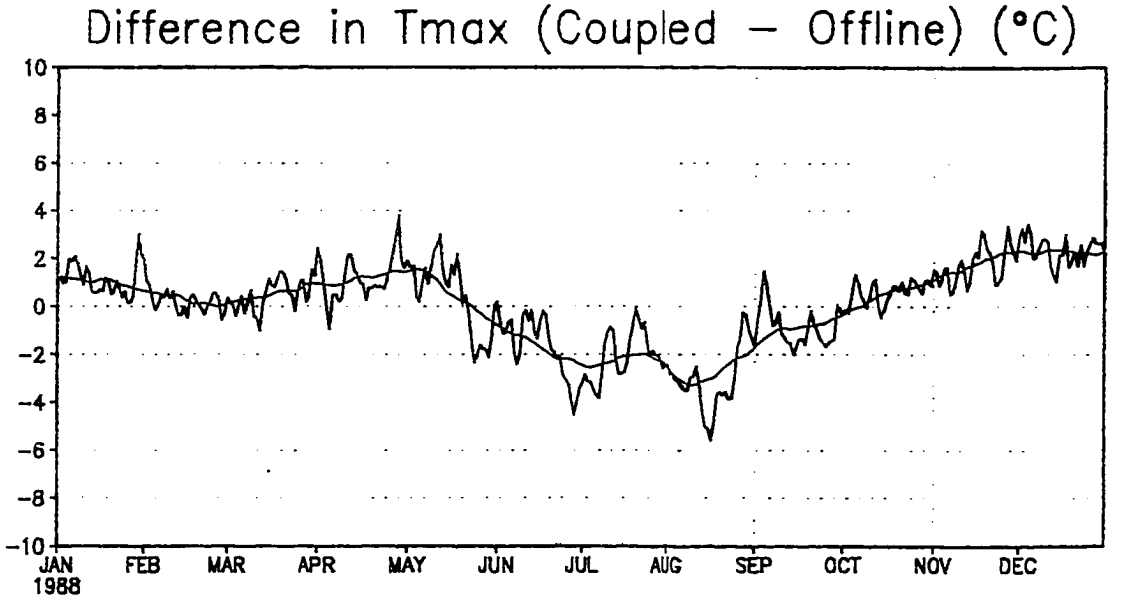

Figure 7.9 The daily maximum screen-height air temperature averaged over the fine grid from off-line ClimRAMS (Offline), the coupled model (Coupled) and the observation (Observed), respectively, for the time period January 1 through December 31, 1988. Also shown is the difference between the coupled model and the off-line ClimRAMS, and the 30-day running mean of the difference values.

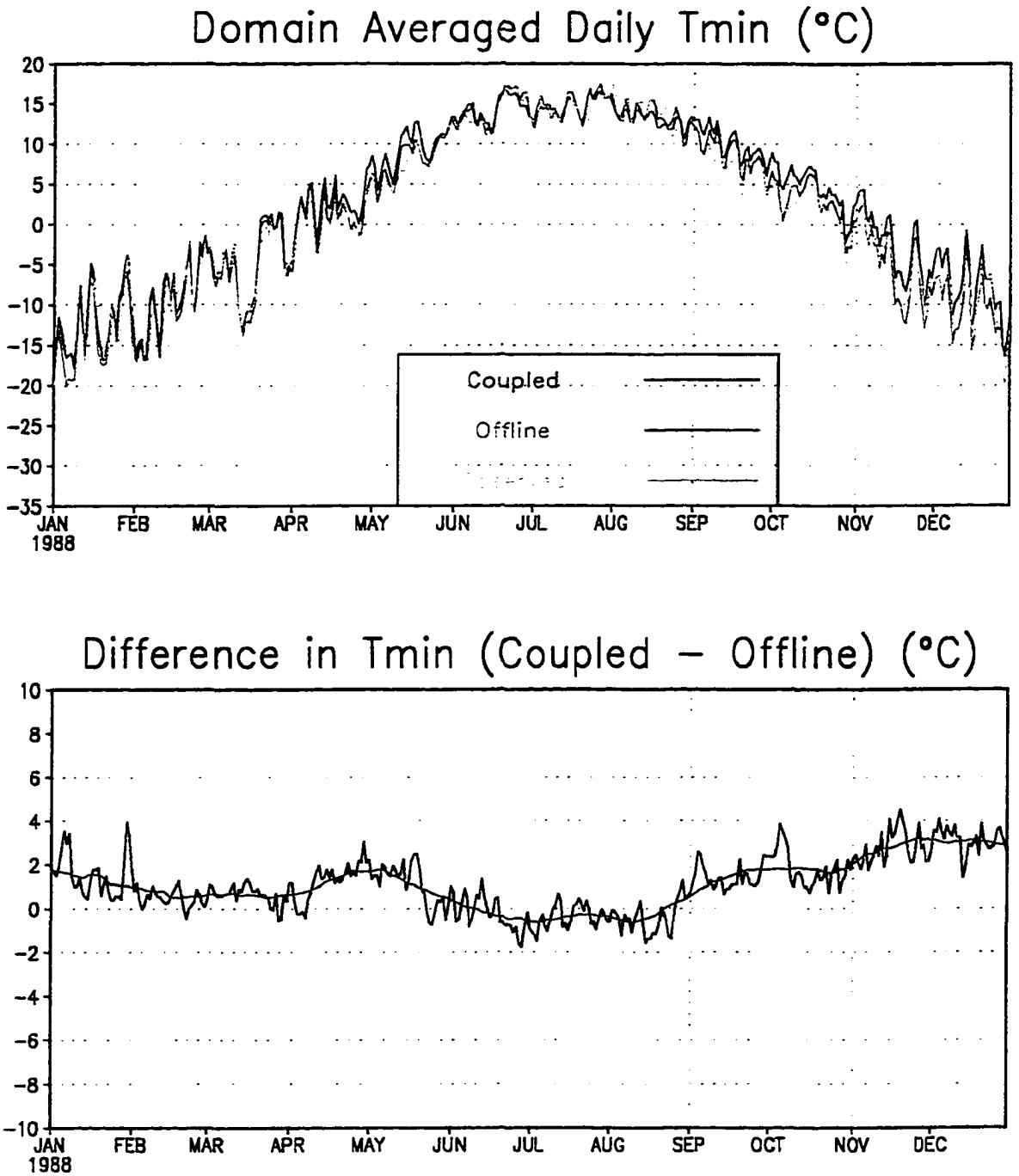

Figure 7.10 The same as Figure 7.9, but for daily minimum screen-height air temperature.

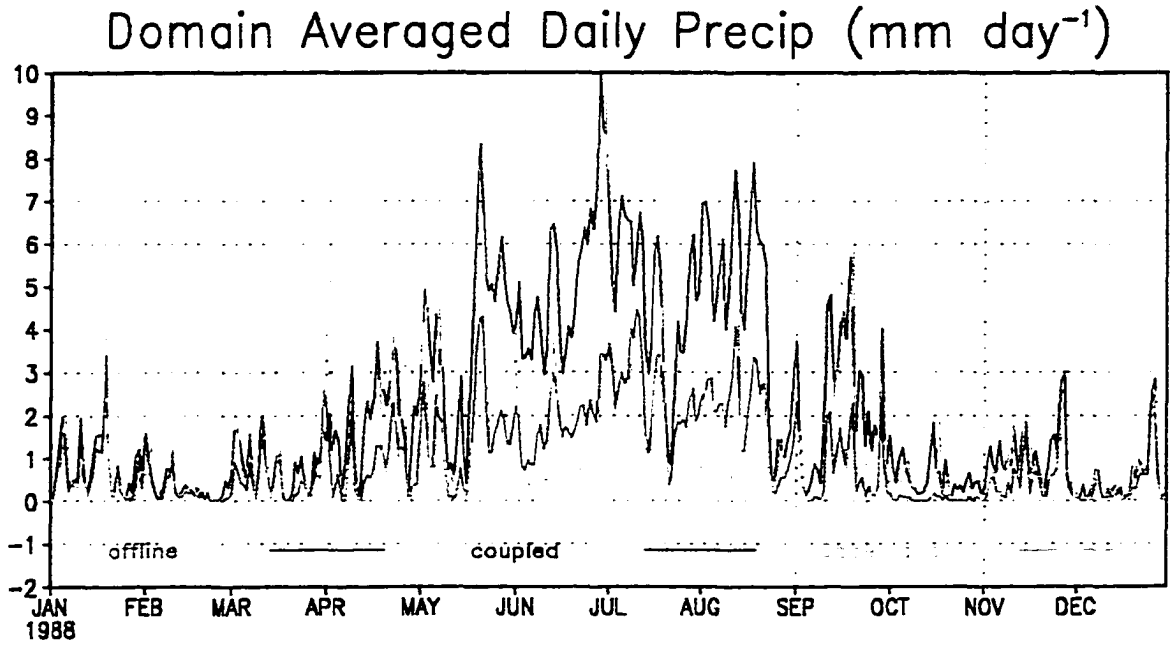

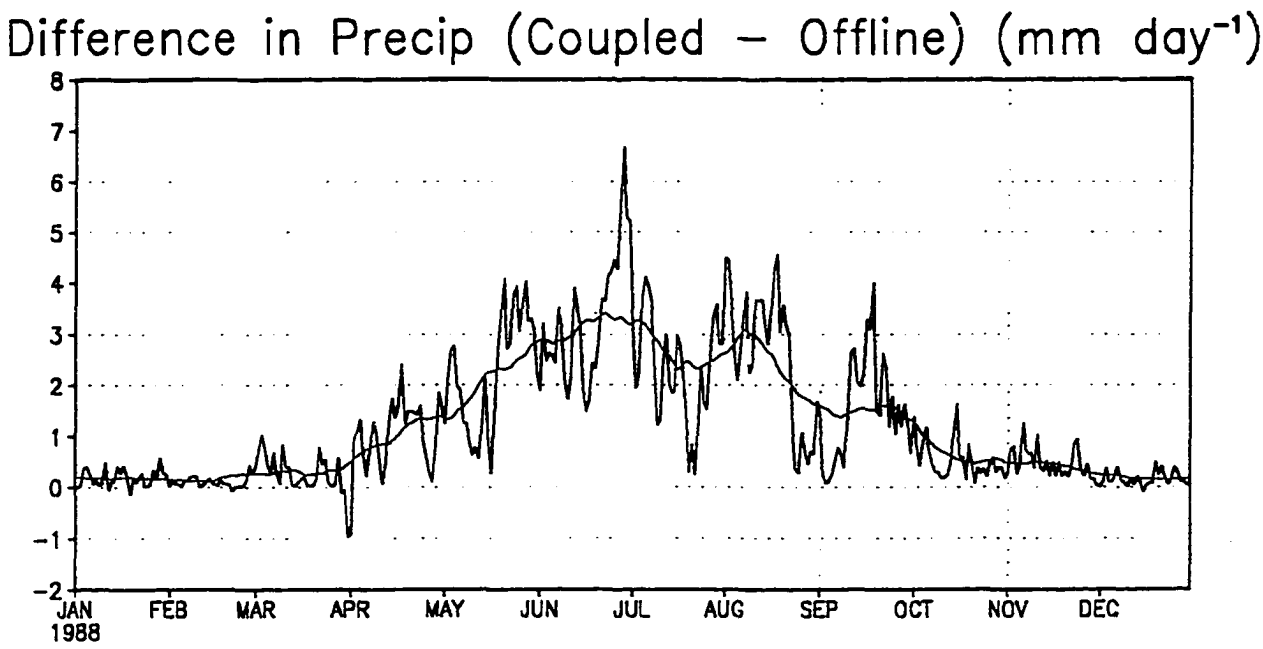

Figure 7.11 The same as Figure 7.9, but for daily precipitation.

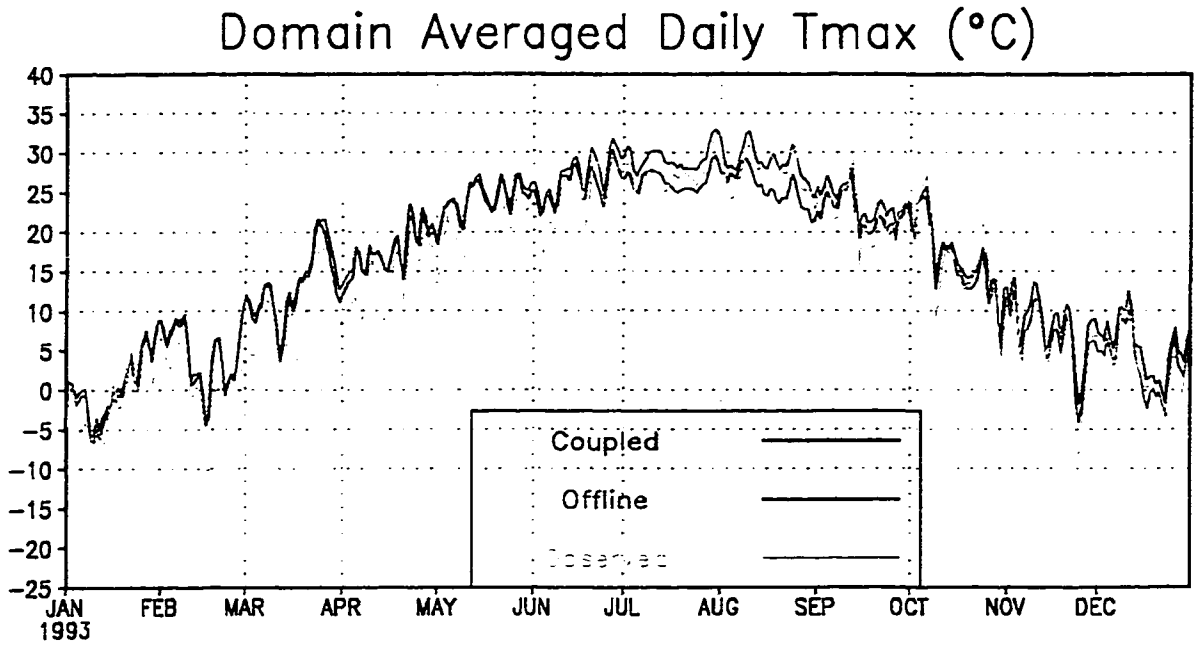

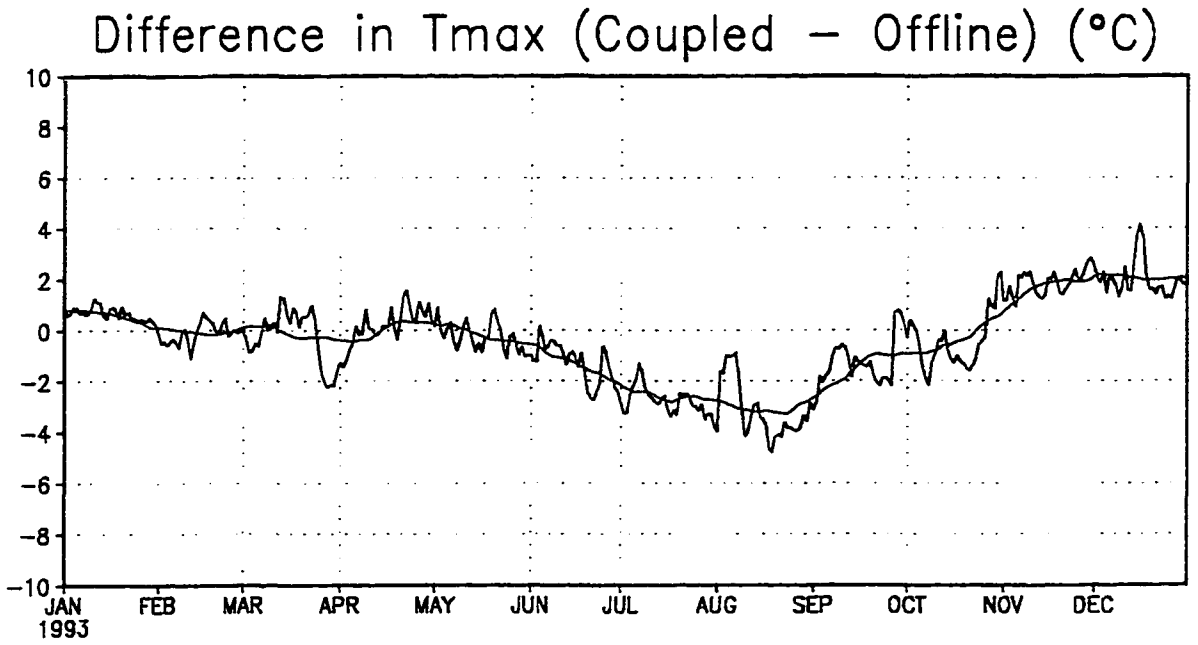

Figure 7.12 The daily maximum screen-height air temperature averaged over the fine grid from offline ClimRAMS (Offline), the coupled model (Coupled) and the observation (Observed), respectively, for the time period 1 January through 31 December 1993. Also shown is the difference between the coupled model and the offline ClimRAMS, and the 30-day running mean of the difference values.

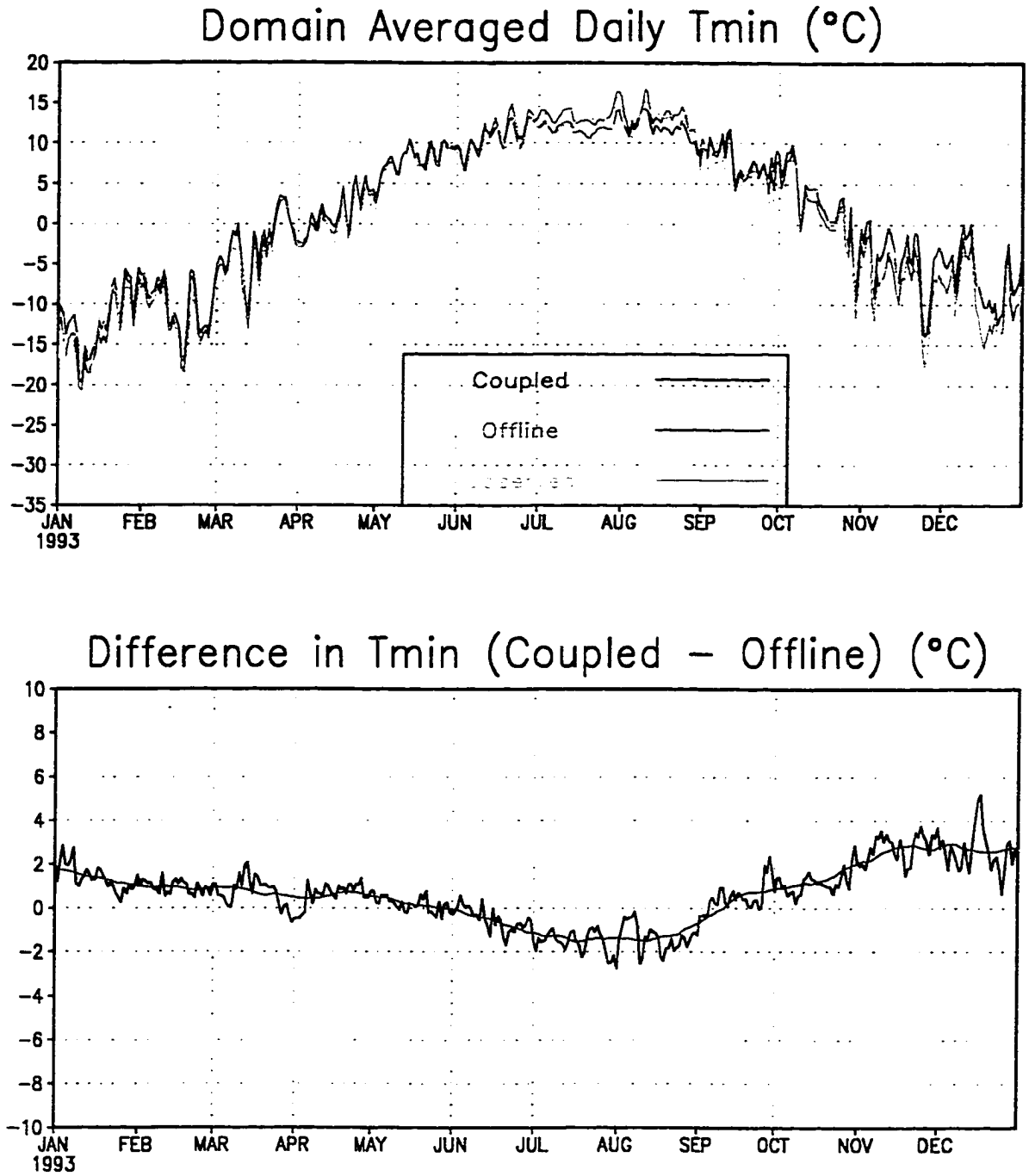

Figure 7.13 The same as Figure 7.12, but for daily minimum screen-height air temperature.

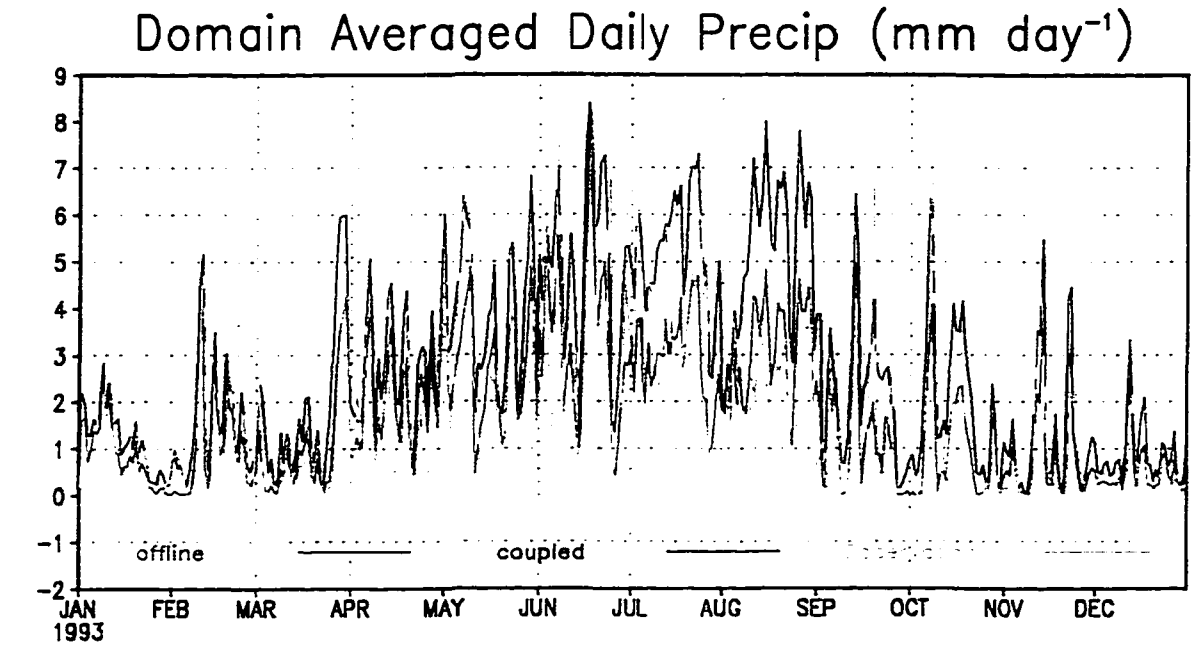

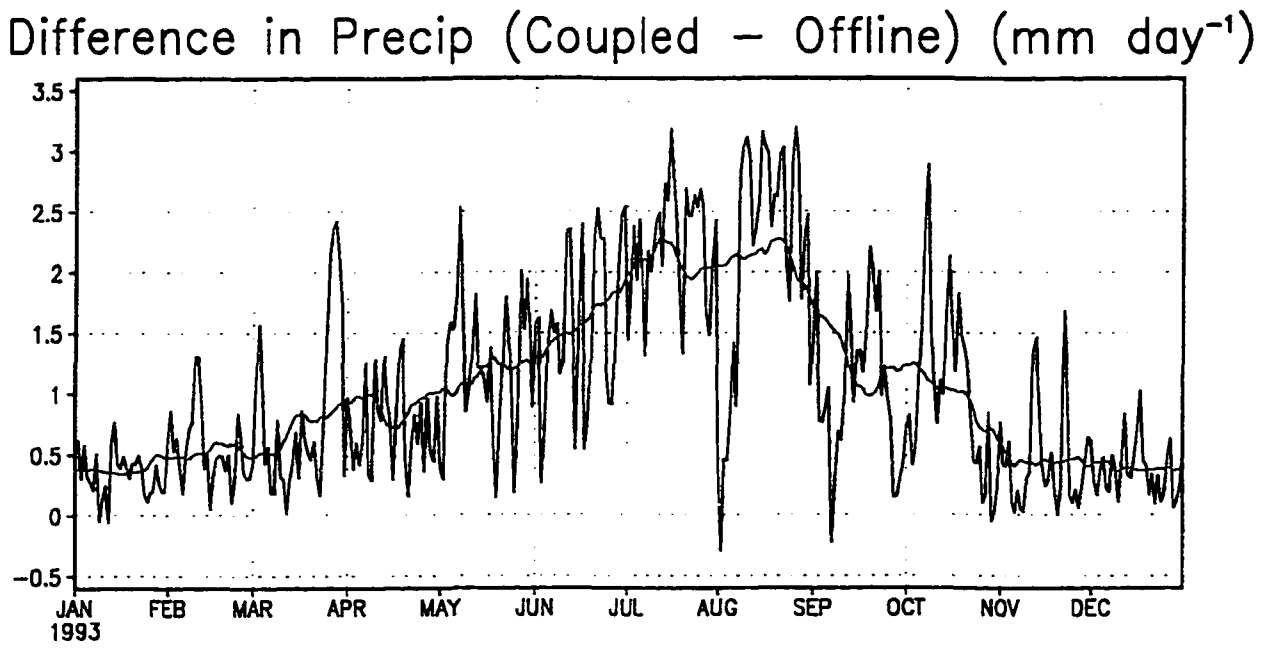

Figure 7.14 The same as Figure 7.12, but for daily precipitation.

the rest of the year. The coupled model's forecast skill can be seen from the same figures by comparing the coupled run against the observations. Although the coupled model rains more from April to mid-October, which enhances the model's ability to capture the peaks of precipitation events, it tends to rain more frequently and overestimate the total rainfall amount compared to the observation. The coupled model has correctly picked up the higher air temperature and lower precipitation of 1988 compared to 1989 and 1993, which demonstrates some skill in its ability to represent the interannual variability of primary atmospheric variables. All three years show that the coupled model produced more precipitation and led to lower summer temperatures than those simulated by the offline ClimRAMS.

Figure 7.15 shows the domain-averaged LAI simulated by the coupled model for the dry, average, and wet years. Also shown are the 7-day running means of LAIs averaged over grasslands, trees, and crops for the same time period. The domain-averaged LAI clearly shows that the wet year had the greatest vegetation biomass growth, which was followed by the average year. The dry year has the least accumulated amount of LAI. This demonstrates that the coupled model is able to represent the domain-averaged interannual biomass variability. However, the offline DayCENT-simulated LAI (Figure 6.1) shows a much larger magnitude of interannual biomass variation. One of explanations is that since ClimRAMS has not simulated the magnitude of variations observed in the anomalous years, such as the extremely dry or wet years, this results in smaller-amplitude LAI interannual variations. Despite its deficiencies in simulating the observed interannual variability, the coupled model is

clearly able to distinguish a wet year from a dry year in both biomass and atmospheric variables.

The domain-averaged LAI can be a little bit misleading since different vegetation types react differently to interannual variability. For instance, the forest is least sensitive to the dry condition due to its deep rooting depth. The crops are insensitive to the dry and wet condition due to the irrigation in many locations. The grasslands are most susceptible to summer rainfall and responses strongly to interannual precipitation variations. Therefore, it would be helpful to know the area-fraction of each vegetation type in order to better understand the real meaning of the domain-averaged features. The trees compose 14.2% of the simulation domain and have maximum LAI values of 6 units in the growing season. The crops and mixed farming account for 31.3%, while the grasslands make up 30.0% and shrublands cover 13.3% of the domain. The rest of vegetation types together covers 11.2% of the domain and will not be discussed here.

Looking at the LAI at a single grid cell (Figure 7.16), vegetation growth phenology is found to respond strongly to seasonal and interannual atmospheric variations. Changes in atmospheric forcings not only alter the maximum LAI value, but also affect when the peak occurs and the growing season length. For instance, a strong LAI sensitivity to interannual climate variability was simulated for the C3 grassland, with the maximum LAI value as low as 2.1 for 1988 and as high as 4.2 for 1993. The timing of the peak shifted from October in 1988 to November in 1993. The simulated LAI changes modify the surface heat and momentum fluxes, and feed

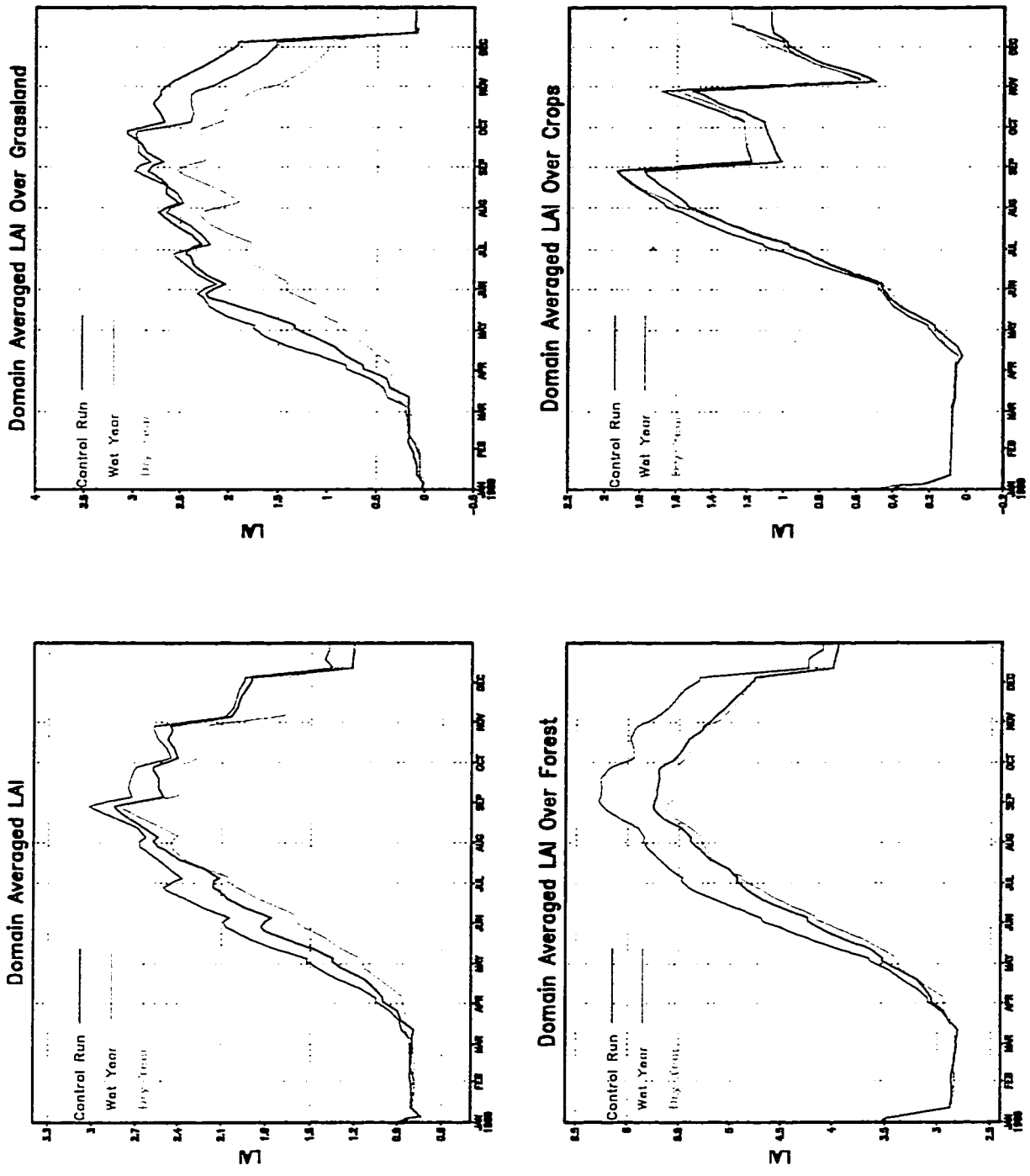

Figure 7.15 The domain-averaged LAIs simulated by the coupled model for dry (1988), control (1989), and wet (1993) years. Also shown are the LAIs averaged over grasslands, trees, and crops for the same time periods. All the LAIs are 7-day running means.

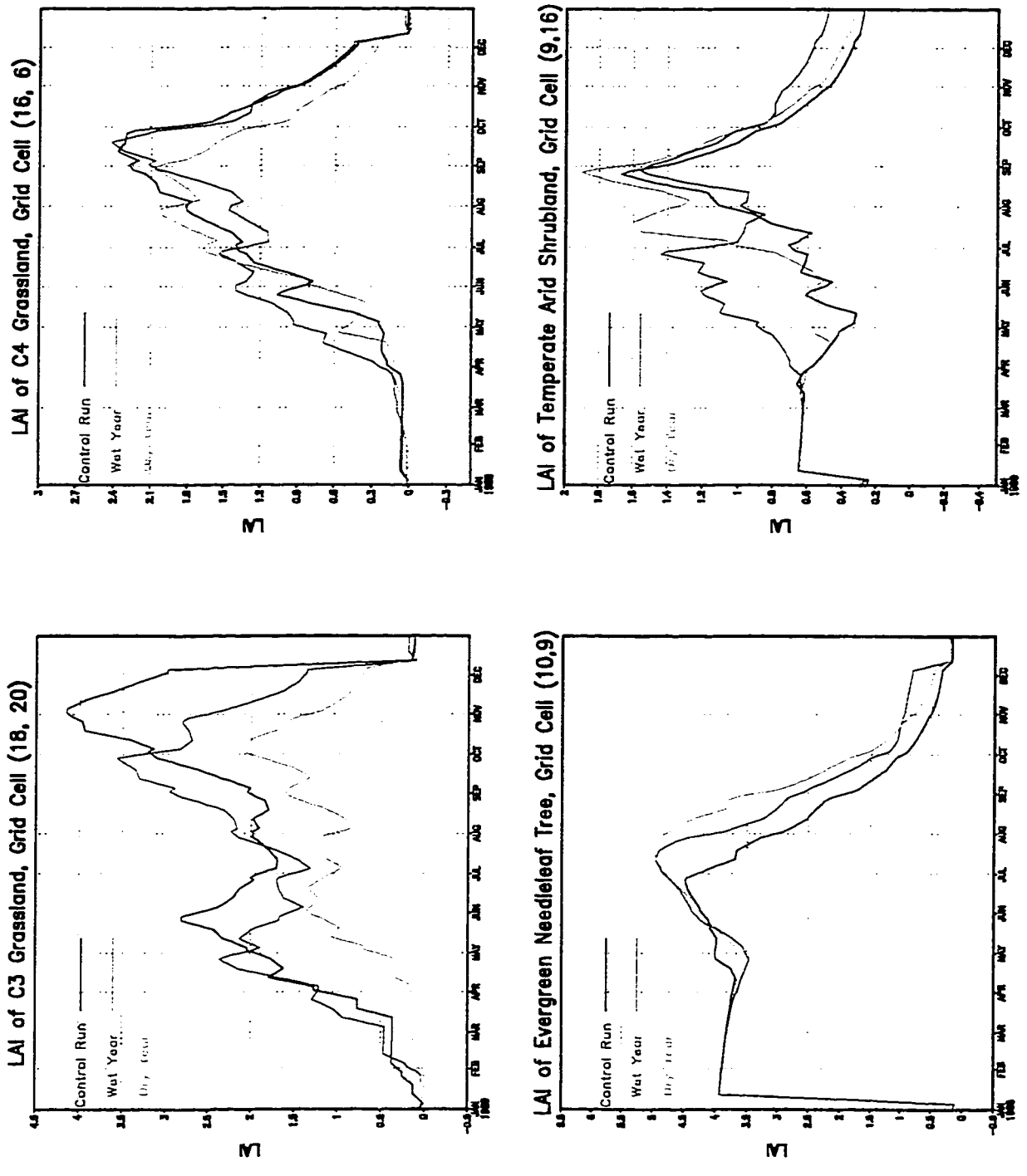

Figure 7.16 The LAIs simulated by the coupled model for dry (1988), control (1989), and wet (1993) years for single grid cells with different land cover types. All the LAIs are 7-day running means.

back to the atmosphere.

In summary, these experiments demonstrate that the coupled RAMS/CENTURY modeling system is sensitive to interannual variations. Therefore, it has the potential of realistically representing interannual differences in atmospheric- and vegetation related processes and interactions.

7.2 Simulating Seasonal Variations

7.2.1 Creating Dry and Wet Springs

Two perturbation runs were carried out under identical conditions used in the 1989 coupled control simulation, except that the relative humidity of the atmospheric lateral boundary conditions were decreased by 50% of their original values in one case and increased by 50% in the other. When the increase causes the relative humidity to exceed saturation, 100% is applied to the boundary condition. The perturbation time period starts on 1 March and ends on 31 May 1989. Figures 7.17 and 7.18 show that the boundary condition perturbation creates a dry spring for the former case and a wet spring for the later case. Accordingly, the temperature fields have been altered, where the dry spring is accompanied by increased Tmax and Tmin (Figure 7.17), and the wet spring is accompanied by decreased Tmax and Tmin (Figure 7.18).

7.2.2 The Sensitivity of the Coupled Model to Seasonal Variations

The goal of this series of experiments is to investigate the sensitivities of the coupled model to seasonal variations in both the atmosphere and biosphere.

For the dry spring case (Figure 7.17), Tmax and Tmin increased about 2 °C and 0.5 °C, respectively. The precipitation was reduced up to 1.2 mm day^{-1} during the perturbation time period. For the wet spring case (Figure 7.18), Tmax and Tmin decreased about 2.5 °C and 1.5 °C, respectively, while the precipitation increased up to 0.9 mm day^{-1} during the perturbation time period.

The atmospheric and soil moisture status at the end of the perturbation period appears to work as an initial condition for the rest of the year. The perturbation effects begin to disappear immediately after the perturbation period ends. The perturbed run and the control run appear to converge immediately after the perturbation period ends, as the boundary effects dominate the results.

Figure 7.19 shows the 7-day running mean, domain-averaged LAIs for the dry, control, and wet springs. From the biosphere perspective, the dry spring exerts stress on biomass growth. But since the synoptic-scale systems, defined by the prescribed lateral boundary conditions, did not change after the perturbation period ends, the vegetation gradually recovered from the dry spring and the LAIs of the three cases begin to converge in late summer.

The other conclusion we can draw from this experiment is that the regional climate model is always constrained by the prescribed lateral boundary conditions, which are not modified by the model solution in the interior domain. This prohibits the model from representing a more realistic feedback mechanisms where the lateral boundary conditions are allowed to evolve two-way interactively with the model solution from the inner domain. This partially accounts for why the LAIs of the dry,

wet, and average spring cases converge soon after the perturbation period ends. In the late summer, senescent processes begin to take over and the three LAI curves tend to converge as they approach the end of the year.

In addition, the reaction of biomass growth to the spring precipitation perturbation are vegetation-type dependent (Figure 7.20). The C3 grassland has a major growing period in late spring and early summer. Thus, it is most sensitive to the spring precipitation perturbation. In contrast, the C4 grassland biomass growth peaks in late summer, so that spring water availability is less important. The temperate arid shrubland thrives with the extra moisture brought in by the spring precipitation. For the forest, the spring precipitation greatly affected the LAI value throughout the growing season, that starts in early summer due to its higher elevation.

To summarize this experiment, we conclude that the coupled RAMS/CENTURY modeling system is sensitive to seasonal atmospheric variations. Therefore, it is capable of representing seasonal variations in both atmospheric and biospheric processes and interactions. Because the lateral atmospheric boundary conditions are defined by a one-way nudging procedure, the current climate model configuration does not allow the coupled system to fully address the two-way feedback problems involving the lateral boundary condition perturbations.

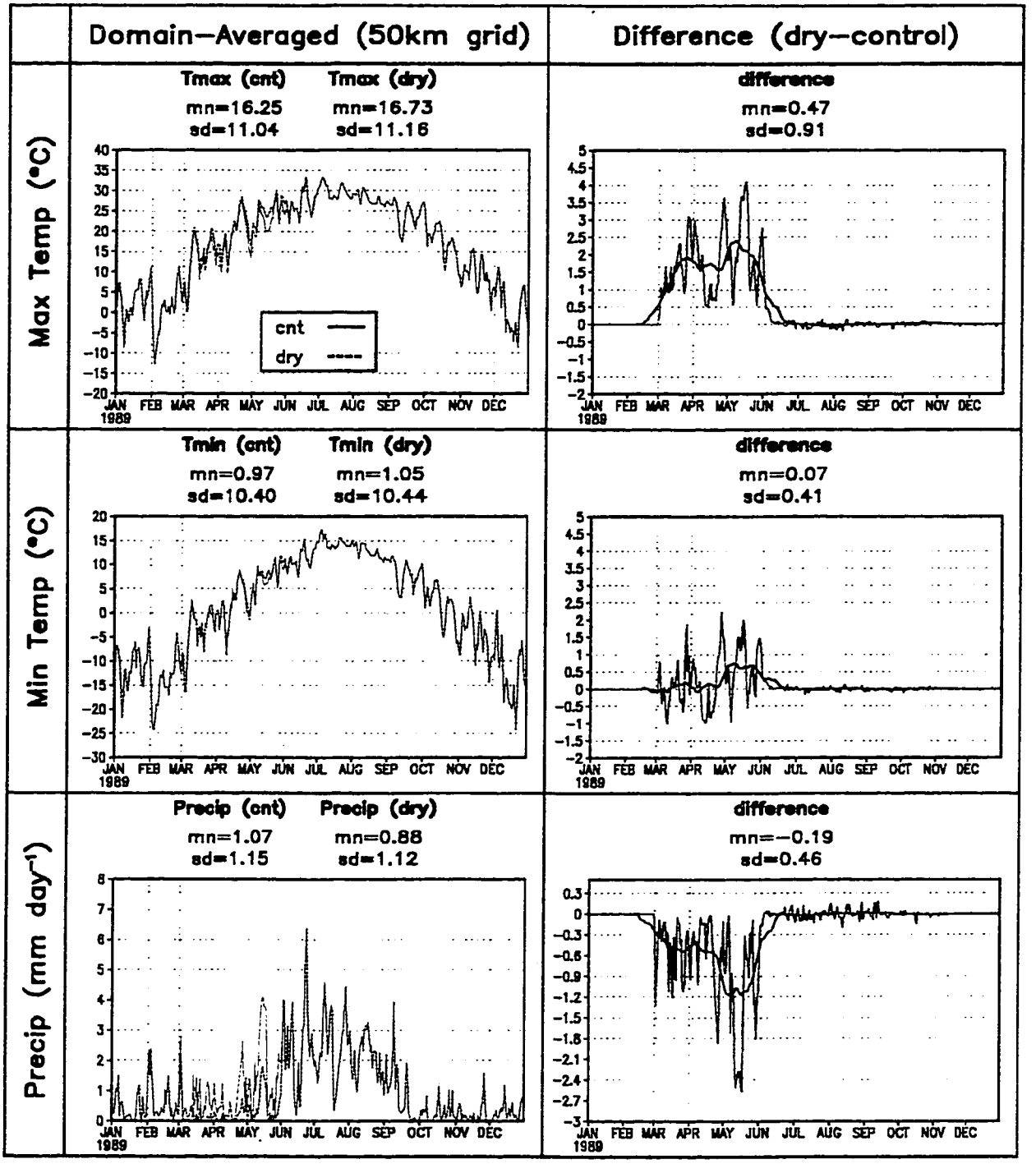

Figure 7.17 Domain-averaged daily maximum and minimum temperatures and precipitation from the perturbed offline ClimRAMS simulation for the time period 1 January through 31 December 1989. The relative humidity of the lateral boundary conditions have been reduced to 50% of its original value from 1 March to 31 May 1989. Also shown are the differences between the perturbed run and the control run, and a 7-day running mean of the difference values.

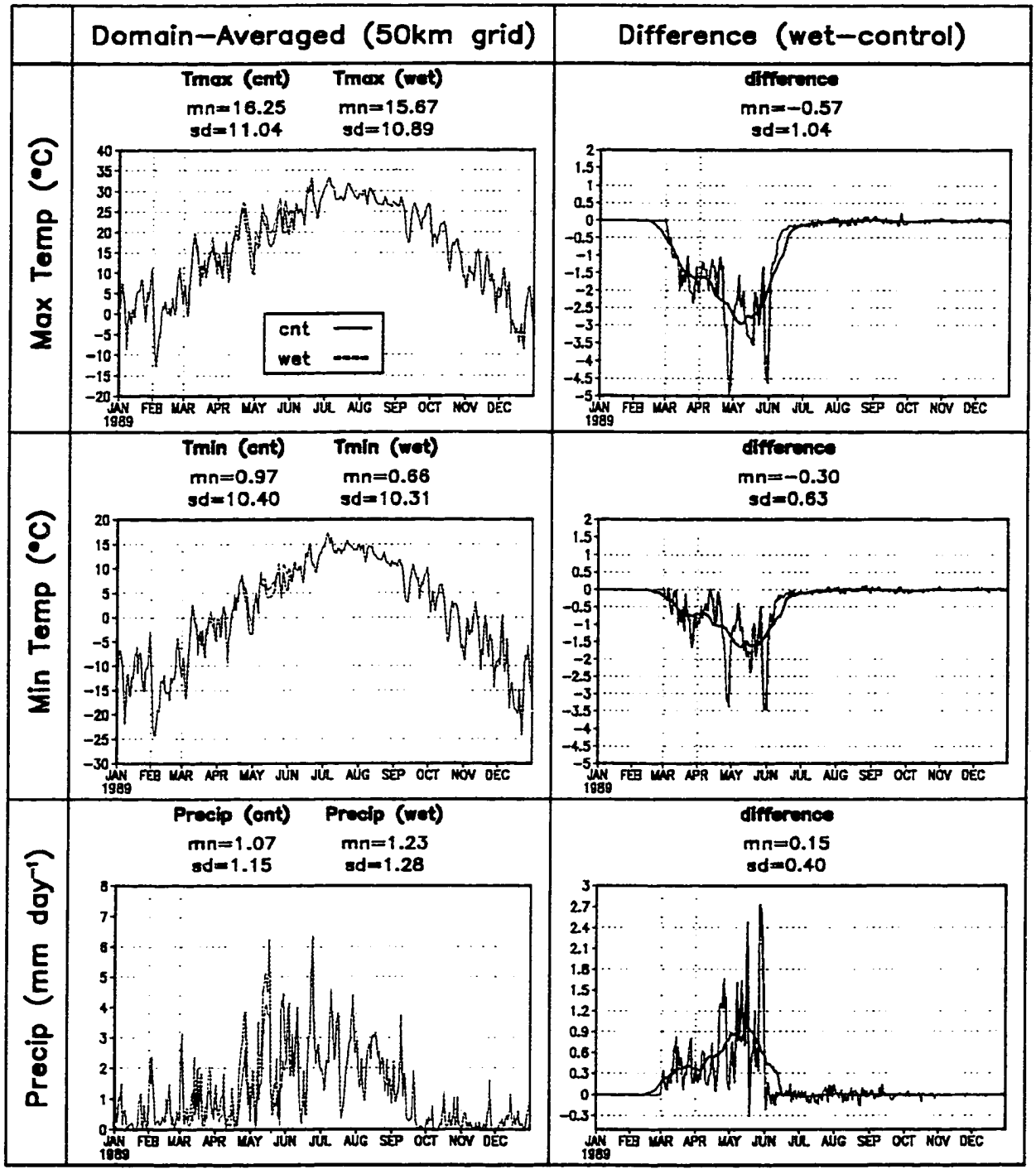

Figure 7.18 Domain-averaged daily maximum and minimum temperatures and precipitation from the perturbed offline ClimRAMS simulation for the time period 1 January through 31 December 1989. The relative humidity of the lateral boundary conditions have been increased by 50% of its original value from 1 March to 31 May 1989. Also shown are the differences between the perturbed run and the control run, and a 7-day running mean of the difference values.

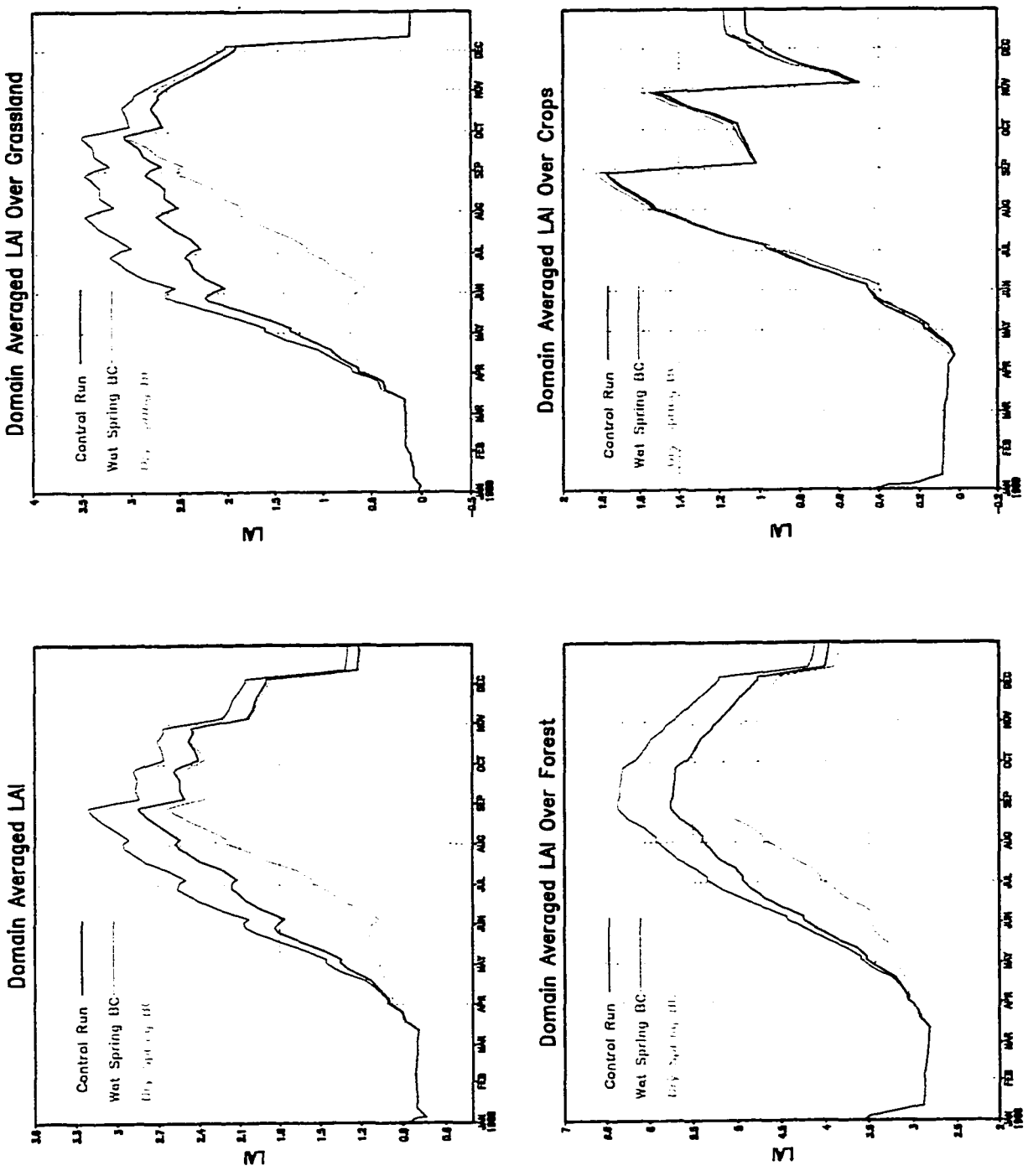

Figure 7.19 The domain-averaged LAIs simulated by the coupled model for dry, average, and wet springs, respectively. Also shown are the LAIs averaged over grassland, trees, and crops for the same time periods. All the LAIs are 7-day running means.

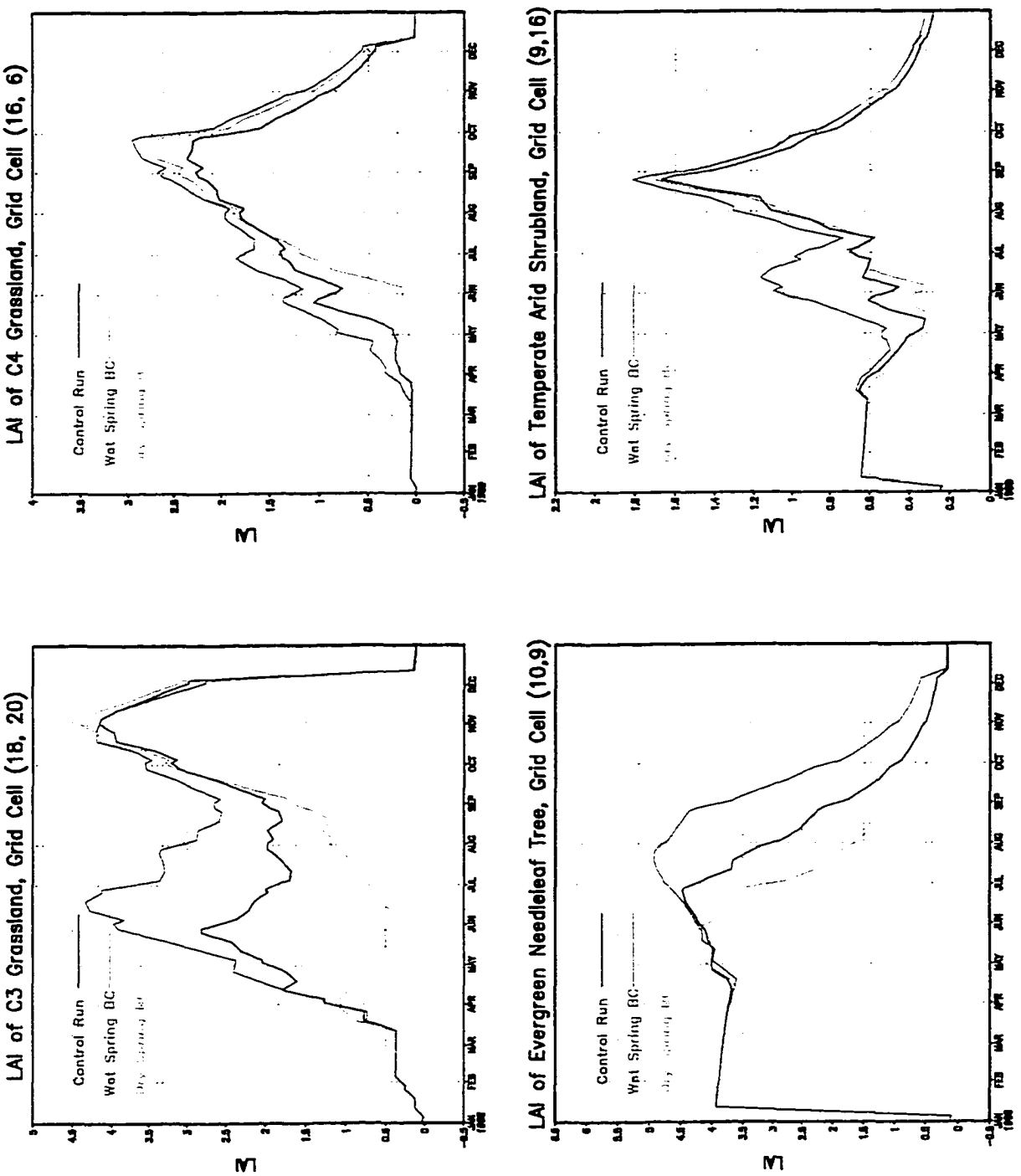

Figure 7.20 The LAIs simulated by the coupled model for dry, average, and wet springs for single grid cells with different land-cover types. All the LAIs are 7-day running means.

Chapter 8

SUMMARY, DISCUSSION AND SUGGESTIONS FOR FUTURE WORK

8.1 Summary and Discussion

The coupled RAMS/CENTURY modeling system has been developed to study the two-way interactions between the atmosphere and land surface. Both atmospheric forcings and ecological parameters (LAI, etc.) are prognostic variables in the linked system. The coupled model was integrated from 1 January through 31 December, for 1988, 1989 and 1993, which represent dry, average and wet years, respectively, focusing on the central United States. Validation is performed for the atmospheric portion of the model by comparing with over 3,800 meteorological station observations over the entire domain, and for the ecological component by comparing to the Pathfinder AVHRR remote-sensing NDVI data sets. A series of sensitivity experiments has been conducted to highlight interactions and feedbacks between the atmosphere and land surface processes. The control run atmospheric lateral boundary conditions have been perturbed to create dry and wet springs. The model's ability to represent the interannual and seasonal variations in both weather and biomass has been

examined. The results show that seasonal and interannual vegetation phenological variability strongly influences regional atmospheric patterns through its control over land-surface water and energy exchange. The coupled model captures the key aspects of weekly, seasonal, and annual feedbacks between the atmospheric and ecological systems. In addition, the coupled model has demonstrated its usefulness as a research tool for studying the complex interactions between the atmosphere, biosphere, and hydrosphere.

Although the coupled RAMS/CENTURY modeling system provides an approach to represent the two-way feedbacks between the atmosphere and the biosphere, due to limitations in our ability to numerically model the complete dynamics of the two systems, and the nonlinear features of the feedbacks, our efforts may not directly or immediately improve the model's forecast skill. In spite of this, the coupled model provides a valuable tool to study the physical and biological processes and interactions within the climate system. The coupled model and the simulations presented herein, also provide guidance on the limits imposed on climate prediction as a result of the identified nonlinear feedbacks.

New computer science technologies, such as the internet stream socket and client/server mechanisms, provide the scientific community with an innovative and feasible method to accomplish large-scale model integration and data assimilation. It is particularly efficient and convenient when the linkage involves diversified models running at different temporal and spatial resolutions. Each model involved can be run completely independent of the other models. Sending and receiving required

information between the models at scheduled times can be easily achieved through this mechanism. This implementation of the coupled RAMS/CENTURY modeling system is the first successful attempt of utilizing this technology in earth science, and should be viewed as a pilot project which explores a new dimension in model integrations.

8.2 Suggestions for Future Work

In the current configuration of the coupled modeling system, RAMS and CENTURY use their own soil sub-models. The use of different soil models may cause inconsistencies in the coupled model's hydrological cycle. Developing a common soil model for the coupled modeling system would solve this problem. However, this can be a difficult task, not only because the temporal and spatial resolution utilized by the two soil models are different, but also because other components of both RAMS and CENTURY are highly interwoven with their soil water budget sub-models. To correct these inconsistencies, a consistent unified soil model is required. Any change made to the soil model must meet the requirement that other processes simulated by both models will not be adversely affected.

The computer network communication mechanism used in the coupling allows the relevant information to pass back and forth between the two models rather efficiently. While the above-ground live carbon has been the only variable utilized in RAMS after conversion to LAI, we plan to include other variables generated by CENTURY in the coupled system. For example, RAMS can assimilate information, such as below-ground live carbon (Bglivc), from CENTURY to provide the rooting

profile. However, the conversion algorithm to allocate Bglivc to each vertical soil level has yet to be developed. At the same time, the cloud cover generated from RAMS could be used by CENTURY but has not been implemented into the coupled system yet.

CENTURY is a biogeochemistry model where its strength lies in simulating long-time-scale nutrient dynamics. Instead of a physical-process based approach, it uses atmospheric conditions, such as precipitation and temperature, to empirically infer above-ground live carbon. This limits its ability to run simulations at finer temporal resolution than its current one-day time step. Because the physical and biological processes are described empirically, there is little justification for applying CENTURY at higher temporal resolutions. A physical-process based vegetation model would allow the coupled system to represent the atmosphere and vegetation feedbacks at diurnal, or even finer time scale.

Recent advances in satellite remote sensing technologies have provided us with unprecedented and invaluable observational information for the study of earth science. An improved NDVI data set and a valid NDVI-to-LAI conversion algorithm would enable ecologists to modify ecosystem models to produce correct biomass at regional scales and, at the same time, would allow atmospheric scientists to calibrate climate models based on realistic LAI specifications. This is a crucial next step for studying climate simulations, regional- to large-scale ecosystem dynamics, and atmosphere-vegetation interactions.

Because of the difficulties in developing a valid NDVI-to-LAI conversion

algorithm, scientists in remote sensing area are designing new sensors that can observe LAI information in a more direct manner. If they succeed, all the uncertainties and complexities caused by NDVI-to-LAI conversion algorithm can be avoided.

While conducting sensitivity experiments with the coupled modeling system, we concluded that regional atmospheric models are highly constrained by their prescribed lateral boundary conditions. Since the boundary condition does not interact with the model's evolving inner domain, a portion of the ecosystem feedback information is lost. A possible solution for this problem is to make a regional atmospheric model two-way interactive with a global model (e.g., GCM) and simply let the regional model represent a relatively high resolution element within that global model. This would allow the regional weather, which has been altered by the land processes, to feed back to the larger-scale, and in turn to incorporate this feedback into the next time step of the regional atmospheric model's evolution. Computationally, this nesting approach is easy to achieve since we can focus on a specific region instead of running the GCM globally at very high-resolution; something that is limited by available computer resources.

With the emergence of parallel programming techniques, high-resolution, long-term regional atmospheric simulations are becoming feasible. A parallelized version of ClimRAMS that can be used to run the model at 10 km resolution for multiple years is being developed. This new modeling system will be able to resolve mesoscale circulations generated by land surface heterogeneities, and at the same time represent the possible long-term feedbacks from the soil nutrient cycle and roots.

Finally, only static vegetation species and community structures have been used in the coupled RAMS/CENTURY modeling system. To simulate longer-term climate or to study climate-change scenarios under specified disturbance, species composition and community structure changes and evolutions should also be considered. Therefore, linking the MAPSS (Neilson 1995) biogeographical model to form an integrated RAMS/CENTURY/MAPSS modeling system promises to be an important contribution to studying the dynamically-coupled Earth-atmosphere system.

REFERENCES

Arakawa, A., and R.V. Lamb, 1977: Computational design of the basic dynamical processes of the UCLA general circulation model. Methods in Computational Physics, Vol. 17, Academic Press, 174-265.

Avissar, R., and Y. Mahrer, 1988: Mapping forest-sensitive areas with a three-dimensional local-scale numerical model. Part I: Physical and numerical aspects. J. Appl. Meteor., 27, 400-413.

Avissar, R., and R.A. Pielke, 1989: A parameterization of heteorogeneous land surfaces for atmospheric numerical models and its impact on regional meteorology. Mon. Wea. Rev., 117, 2113-2136.

Bastable, J.G., W.J. Shuttleworth, R.L. G. Dallarosa, G. Fisc, and C.A. Nobre, 1993: Observations of climate, albedo and surface radiation over cleared and undisturbed Amazonian forest. Int. J. Climatol., 13, 783-296.

Betts, A.K. S.-Y. Hong, and H.-L. Pan, 1996: Comparison of NCEP-NCAR reanalysis with 1987 FIFE data. Mon. Wea. Rev., 124, 1480-1498.

Bonan, G.B, D. Pollard and S.L. Thompson, 1993: Influence of subgrid-scale heteorogeneity in leaf area index, stomatal resistence, and soil moisture on grid-scale land-atmosphere interactions. J. Climate, 6, 1882-1897.

Bonan, G.B., 1995: Land-atmosphere interactions for climate System models: coupling biophysical, biogeochemical, and ecosystem dynamical processes. Remote Sens. Environ., 51: 57-73.

Bonan, G.B., 1996: A land surface model (LSM Version 1.0) for ecological, hydrological, and atmospheric studies: technical description and user's guide. NCAR Technical Note 417, 150pp.

Businger, J.A., J.C. Wyngaard, Y. Izumi, and E.F. Bradley, 1971: Flux-profile relationship in the atmospheric surface layer. J. Atmos. Sci., 28, 181-189.

Chase, T.N., R.A. Pielke, T.G.F. Kittel, R. Nemani, and S.W. Running, 1996, The sensitivity of a general circulation model to global changes in leaf area index. J. Geophys. Res., 101, 7393-7408.

Chase, T.N., R.A.Pielke Sr., T.G.F. Kittel, R. Nemani and S.W. Running, 1999: Simulated impacts of historical land cover changes on global climate in northern winter. Climate Dynamics, accepted.

Charney, J.G., 1975: Dynamics of deserts and drought in the Sahel. Quart. J. Roy. Meteor. Soc., 101, 193-202.

Charney, J.G., W.J. Quirk, S. H. Chow and J. Kornfield, 1977: A comparative study of the effects of albedo change on drought in semi-arid regions. J. Atmos. Sci., 34, 1366-1385.

Chen, C., and W. R. Cotton, 1983: A one-dimensional simulation of the stratocumulus-capped mixed layer, Bound.-Layer Meteor., 25, 289-321.

Chen, C., and W. R . Cotton, 1987: The physics of the marine stratocumulus-capped

mixed layer, J. Atmos. Sci., 44, 2951-2977.

Clapp, R., and G. Hornberger, 1978: Empirical equations for some soil hydraulic properties. Water Resour. Res., 14, 601-604.

Clark, T.L., 1977: A small-scale dynamic model using a terrain-following coordinate transformation. J. Comp. Phys., 24, 186-215.

Clark, T. L., and R. D. Farley, 1984: Severe downslope windstorm calculations in two and three spatial dimensions using anelastic interactive grid nesting: A possible mechanism for gustiness, J. Atmos. Sci., 41, 329-350.

Claussen, M., 1994: On coupling global biome models with climate models. Climate Res., 4, 203-221.

Claussen, M., 1998: On multiple solutions of the atmosphere-vegetation system in present-day climate. Global Change Biology., in press.

Claussen, M., V.Brovkin, A. Ganopolski, C. Kubatzki, and V. Petoukhov, 1998: Modeling global terrestrial vegetation-climate interaction. Phil. Trans. Roy. Soc. London, in press.

Copeland, J.H., R.A. Pielke, and T.G.F. Kittel, 1996: Potential climatic impacts of vegetation change: A regional modeling study. J. Geophys. Res., 101, 7409-7418.

Cotton, W. R., J. F. Weaver, and B. A. Beitler, 1995: An unusual summertime downslope wind event in Fort Collins, Colorado, on 3 July 1993, Wea. Forecasting, 10, 786-797.

Cotton, W.R., and R.A. Pielke, 1995: Human Impacts on Weather and Climate,

Cambridge University Press, New York, 288p.

Cressman, G.P., 1959: An operational objective analysis system. Mon. Wea. Rev., 87, 367-374.

Deardorff, J. W., 1978: Efficient prediction of ground surface temperature and moisture, with inclusion of layer of vegetation. J. of Geophys. Res. 83, 1889-1903.

Deardorff, J. W., 1980: Stratocumulus-capped mixed layers derived from a three-dimensional model, Bound.-Layer Meteor., 18, 495-527.

Dickinson, R., A. Henderson-Sellers, P.J. Kennedy, and M.F. Wilson, 1986: 'Biosphere-atmosphere transfer schemes (BATS) for the NCAR community climate model'. NCAR/TN-275+STR.

Dickinson, R. E., A. Henderson-Sellers, and O.J. Kennedy, 1993: Biosphere-Atmosphere Transfer Scheme (BATS) version 1E as coupled to the NCAR community climate model. Tech. Note NCAR/TN-387+STR, 72 pp.

Dickinson, R. E., 1995: Land processes in climate models. Remote Sensing Environment, 51:27-38.

Dickinson, R. E., Muhammad Shaikh, R. Bryant, and L. Graumlich, 1998: Interactive canopies for a climate model. J. Climate, 11, 2823-2836.

Dirmeyer, P.A., 1994: Vegetation stress as a feedback mechanism in midlatitude drought. Journal of Climate, vol. 7, 1463-1483.

Eastman, J., 1999: Analysis of the effects of CO2 and landscape change using a coupled plant and meteorological model. Ph.D. Dissertation. Department of

Atmospheric Science, Colorado State University, Fort Collins, Colorado, 100pp.

Foley, J.A., 1994: The sensitivity of the terrestrial biosphere to climate change: A simulation of the middle Holocene. Global Biogeochem. Cycles, 8, 505-525.

Foley, J.A., S. Levis, I.C. Prentice, D. Pollard, and S.L. Thompson, 1998: Coupling dynamic models of climate and vegetation. Global Change Biology, 4, 561-579.

Fu C. and G. Wen, 1993: A preliminary study on vegetation dynamics of China by using meteorological satellite. Chinese Science Bulletin, 38, 221-228.

Gal-Chen, T., and R.C. J. Somerville, 1975: On the use of coordinate transformation for the solution of the Navier-Stokes equations. J. Comput. Phys., 17, 209-228.

Gash, J.H.C. and C.A. Nobre, 1997: Climatic effects of Amazonian deforestation: some results from ABRACOS. Bull. Amer. Meteor. Soc., 78, 5, 823-830.

Harrington, J. Y., 1997: The effects of radiative and microphysical processes on simulated warm and transition season Arctic stratus, Ph.D. Dissertation, Atmospheric Science Paper No. 637, Department of Atmospheric Science, Colorado State University, 289 pp., 1997.

Henderson-Sellers, A., Z.L. Yang, and R. E. Dickinson, 1993: The project for intercomparison of land-surface parameterization schemes. Bull. Amer. Meteor. Soc., 74, 7, 1335-1349.

Henderson-Sellers, A., and K. McGuffie, 1995: Global climate model and 'dynamic' vegetation changes. Global Change Biology, 1, 63-75.

Henderson-Sellers, A., A.J. Pitman, P.K. Love, P. Irannejad, and T.H. Chen, 1995:

The Project for Intercomparison of Land Surface Parameterization Schemes (PILPS) Phases 2 and 3. Bull. Amer. Meteor. Soc, 76, 4, 489-503.

Huemmrich, K.F., and S.N. Goward, 1992: Spectral vegetation indexes and the remote sensing of biophysical parameters. Proc. Int. Geosci. Remote Sens. Symp. (IGARSS). Houston, TX, Institute of Electrical and Electronics Engineers, 1017-1019.

Jarvis, P.G., 1976: The interpretation of the variations in leaf water potential and stomatal conductance found in canopies in the field. Philos. Trans. Roy. Soc. London, 273B, 593-610.

Ji, J.J., 1995: A climate-vegetation interaction model: Simulating physical and biological processes at the surface. J. Biogeochem., 22, 2063-2068.

Kalnay, E., M. Kanamitsu, R. Kistler, W. Collins, D. Deaven, J. Derber, L. Gandin, S. Sara, G. White, J. Woollen, Y. Zhu, M. Chelliah, W. Ebisuzaki, W. Higgins, J. Janowiak, K. C. Mo, C. Ropelewski, J. Wang, A. Leetma, R. Renolds, and R. Jenne, 1995: The NMC/NCAR reanalysis project. Bull. Amer. Meteor. Soc., 77, 437-471.

Kelly, R.H., W.J. Parton, M.D. Hartman, L.K. Stretch, D.S. Ojima, and D.S. Schimel, 1999: Intra- and interannual variability of ecosystem processes in shortgrass steppe: new model, verification, simulations. Global Change Biology, Submitted.

Kittel, T.G.F, N.A. Rosenbloom, T.H. Painter, D.S. Schimel, H.H. Fisher, A. Grimsdell, VEMAP Participants, C. Daly, and E.R. Hunt, Jr., 1996: The VEMAP Phase I database: An integrated input dataset for ecosystem and vegetation modeling for the conterminous United States. CDROM and World Wide Web (URL=http://www.cgd.ucar.edu/vemap/).

Kuo, H.L., 1974: Further studies of the parameterization of the influence of cumulus

convection on large-scale flow. J. Atmos. Sci., 31, 1232-1240.

Lee, T. J., 1992: The impact of vegetation on the atmospheric boundary layer and convective storms,Ph.D. dissertation, Atmospheric Science Paper No. 509, Department of Atmospheric Science, Colorado State University, Fort Collins, Colorado, 137 pp.

Linacre, E.T. 1977: A simple formula for estimating evaporation rates in various climates, using temperature data alone. Agric. Meteorol. 18:409-424.

Liston, G. E., R. A. Pielke, Sr., L. Lu, and E. M. Greene, 1998: Central U.S. climate simulations using the Regional Atmospheric Modeling System, GCIP Mississippi River Climate Conference, June 8-12, St. Louis, Missouri.

Liston, G.E. and R.A. Pielke, Sr., 1999: A climate version of the regional atmospheric modeling system. Journal of Climate, Submitted.

Los, S. O., 1998: Linkages between global vegetation and climate, an analysis based on NOAA advanced very high resolution radiometer data. NASA Technical Report, GSFC/CR-1998-206852.

Louise, J.F., 1979: A parametric model of vertical eddy fluxes in the atmosphere. Bound.-Layer Meteor., 17, 187-202.

Louis, J.F., M.Tiedtke, and J.F. Geleyn, 1982: A short history of the PBL parameterization at ECMWF. Proc. 1981 Workshop on PBL Parameterization, Shinfield Park, Reading, UK, ECMWF, 59-71.

Mahrer, Y., and R. A. Pielke, 1977: A numerical study of the airflow over irregular terrain., Beit. Phys. der Atmos., 50, 98-113.

McCumber, M.C., 1980: A numerical simulation of the influence of heat and moisture fluxes upon mesoscale circulations. Ph.D. Dissertation, University of Virginia, 255pp.

McCumber, M.C., and R.A. Pielke, 1981: Simulation of the effects of surface fluxes of heat and moisture in a mesoscale numerical model, Part I: Soil layer, J. Geophys. Res., 86, 9929-9938.

McNider, R.T., and R.A. Pielke, 1981: Diurnal boundary-layer development over sloping terrain, J.Atmos. Sci., 38, 2198-2212.

Mearns, L.O., C. Rosenzweig and R. Goldberg, 1996: The effect of changes in daily and interannual climatic variability on CERES-Wheat: A sensitivity study. Climatic Change, 32, 257-292.

Metherell, A.K., L.A. Harding, C.V. Cole, and W. J. Parton, 1993: CENTURY soil organic matter model environment. Technical Documentation, Agroecosystem Version 4.0, Great Plain System Research Unit, USDA-ARS.

Meyers, M. P., 1995: The impact of a two-moment cloud model on the microphysical structure of two precipitation events, Ph.D. dissertation, Atmospheric Science Paper No. 575, Department of Atmospheric Science, Colorado State University, Fort Collins, Colorado, 165 pp.

Meyers, M. P., P. J. DeMott, and W. R. Cotton, 1992: New primary ice nucleation parameterizations in an explicit cloud model, J. Appl. Meteor., 31, 708-721.

Mihailovic, T., 1996: Description of a land-air parameterization scheme (LAPS). Global and Planetary Change, Amsterdam, The Netherlands, 13(1-4): 207-215.

Miller, D.A., and R.A. White, 1998: A conterminous United States multi-layer soil

characteristics data set for regional climate and hydrology modeling. Earth Interactions, 2, (Available on line at http://EarthInteractions.org).

Monteith, J.L., and M.H. Unsworth, 1990: Principles of Envrionmental Physics. Edward Arnold, 291 pp.

Myneni, R.B., C.J. Tucker, G. Asrar, and C.D. Keeling, 1998: Interannual variations in satellite-sensed vegetation index data from 1981 to 1991. J. Geophys. Res., 103, D6, 6145-6160.

Neilson, R.P., 1995: A model for predicting continental-scale vegetation distribution and water balance. Ecological Applications, 5(2), 362-385.

Nemani, R. R., S.W. Running, R.A. Pielke, and T.N. Chase, 1996: Global vegetation cover changes from coarse resolution satellite data. J. Geophys. Res., 101, D3, 7157-7162.

Noilhan, J. and S. Planton, 1989: A simple parameterization of land surface processes for meteorological models. Mon. Wea. Rev., 117, 536-549.

Nicholls, M.E., R.A. Pielke, J.L. Eastman, C.A. Finley, W.A. Lyons, C.J. Tremback, R. L. Walko, and W.R. Cotton, 1995: Applications of the RAMS numerical model to dispersion over urban areas. In: Wind Climate in Cities, J.E. Cermak et al., Editors. Kluwer Academic Publishers, The Netherlands, 703-732.

Ojima, D.S., W.J. Paron, D.S. Schimel, J.M.O. Scurlock, and T.G.F. Kittel, 1993: Modeling the effect of climatic and CO2 changes on grassland storage of soil C. Water, Air, Soil Poll., 70, 643-657.

Ojima, D.S., D.S.Schimel, W.J. Parton, and C. Owensby, 1994: Short- and long-term

effects of fire on N cycling in tallgrass prairie. Biogeochemistry, 24, 67-84.

Parton, W.J., D.S. Schimel, C.V. Cole, and D.S. Ojima, 1987: Analysis of factors controlling soil organic matter in Great Plains Grassland. Soil Sci. Soc. Amer. J., 51, 1173-1179.

Parton, W.J., J.W.B. Steward, and C.V. Cole, 1988: Dynamics of C, N, P and S in grassland soils: A model. Biogeochemistry, 5, 109-131.

Parton, W.J., J.M.O. Scurlock, D.S. Ojima, T.G. Gilmanov, R.J. Scholes, D.S. Schimel, T. Kirchner, H.C. Menaut, T. Seastedt, E. Garcia Moya, A. Kamnalrut, and J.L. Kinayamario, 1993: Observations and modeling of biomass and soil organic matter dynamics for the grassland biome worldwide. Global Biogeochemical Cycles, 7, 785-809.

Parton, W.J., and P.E. Rasmussen, 1994: Long-term effects of crop management in wheat-fallow: II. CENTURY model simulations. Soil Sci. Soc. Amer. J., 58, 530-536.

Parton, W.J., D.S. Schimel, D.S. Ojima, and C.V.Cole, 1994a: A general model for soil organic matter dynamics: Sensitivity to litter chemistry, texture and management. In R.B. Bryant and R.W. Arnold (Eds) Quantitative Modeling of Soil Forming Processes. SSSA Spec. Publ. 39. ASA, CSSA and SSA, Madison, WI, 137-167.

Parton, W.J., J.M.O. Scurlock, D.S. Ojima, and K. Paustian, 1994b: Modelling soil biology and biochemical processes for sustainable africultural research. In: Soil Biota. Management in Sustainable Farming Systems (Eds: C.E.) Pankhurst, B.M. Doube, V.V.S.R. Gupta and R. Grace, CSIRO, Information Services, Melbourne, 182-193.

Parton, W.J., J.M.O. Scurlock, D.S. Ojima, D.S. Schimel, D.O. Hall, M.B. Coughenour, E. Garcia Moya, T.G. Gilmanov, Apinan Kamalrut, J.I. Kinyamario, T.

Kirchner, S.P. Long, J.C. Menaut, O.E. Sala, R.J. Scholes, and J.A. van Veen, 1995: Impact of climate change on grassland production and soil carbon worldwide. Global Change Biology, 1, 13-22.

Parton, W.J., 1996: The CENTURY model. NATO ASI Series, Vol. I38, Evaluation of Soil Organic Matter Models, D.S. Powlson, P. Smith, and J.U. Smith, Eds., Springer-Verlag, Berlin Heidelberg, 283-291.

Parton, W.J., D.S. Ojima, and D.S. Schimel, 1996: Models to evaluate soil organic matter storage and dynamics. In M.R. Carter (ED.) Structure and Organic Matter Storage in Agricultural Soils. CRC Press, Inc., 421-448.

Parton, W.J., M. Hartman, D. Ojima, and D. Schimel., 1998: DAYCENT and its land surface submodel: Description and testing. Global and Planetary Change, 19, 35-48.

Penman, H. L., 1948: Natural evaporation from open water, bare soil and grass. Proceedings of the Royal Society of London, Series A, Vol. 193, 120-145.

Pielke, R.A., 1974: A three-dimensional numerical model of the sea breezes over south Florida, Mon. Wea. Rev., 102, 115-139.

Pielke, R.A., 1984: Mesoscale meteorological modeling. Academic Press, New York, N.Y., 612 pp.

Pielke, R.A., and R. Avissar, 1990: Influence of landscape structure on local and regional climate. Landscape Ecol., 4, 133-155.

Pielke, R.A., W.R. Cotton, R.L. Walko, C.J. Tremback, M.E. Nicholls, M.D. Moran, D.A. Wesley, T.J. Lee, and J. H. Copeland, 1992: A comprehensive meteorological modeling system-RAMS. Meteor. Atmos. Phys., 49, 69-91.

Pielke, R.A., T.J. Lee, J. H. Copeland, J.L. Eastman, C.L. Ziegler, and C.A. Finley, 1997a: Use of USGS-provided data to improve weather and climate simulations. Ecological Applications, 7, 3-21.

Pielke, R.A., X. Zeng, T.J. Lee, and G.A. Dalu, 1997b: Mesoscale fluxes over heterogeneous flat landscapes for use in larger scale models, J. Hydrology, 190, 317-336.

Pielke, R.A., R.A. Avissar, M. Raupach, H. Dolman, X. Zeng, and S. Denning, 1998a: Interactions between the atmosphere and terrestrial ecosystems: Influence on weather and climate. Global Change Biology, 4, 101-115.

Pielke, R.A. Sr., 1998b: Climate prediction as an initial value problem. Bull. Amer. Meteor. Soc., 79, No. 12, 2743-2746.

Pitman, A.J., 1988: The development and implementation of a new land surface scheme for use in general circulation models, Ph.D. thesis, University of Liverpool, Liverpool, UK, 481 pp.

Pitman, A.J., 1991: A simple parameterization of sub-grid scale open water for climate models. Climate Dynamics, 6, 99-112.

Rabin, R.M., S. Stadler, P.J. Wetzel, D.J. Stensrud, and M. Gregory, 1990: Observed effects of landscape variability on convective clouds. Bull. Amer. Meteor. Soc., 71, 272-280.

Raupach, M.R. 1999: Radiative, physiological, aerodynamic and boundary-layer feedbacks in the terrestrial surface energy balance. Global Change Biology, in press.

Rhea, J.O., 1978: Orographic precipitation model for hydrometeorological use. Ph.D.

Dissertation, Atmospheric Science Paper No. 287, Department of Atmospheric Science, Colorado State University, Fort Collins, Colorado, 199 pp.

Rosenberg, N.J., B.L. Blad, and S.B. Verma, 1983: Microclimate, the biological environment. John Wiley and Sons, New York, 495 pp.

Segal, M. and Avissar, R., 1988: Evaluation of vegetation effects on the generation and modification of mesosale circulations. J. Atmos. Sci., 45: 2268-2292.

Sellers, P.J., Y. Mints, R.C. Sud, and A. Delcher, 1986: A simple biosphere model (SiB) for use within general circulation models. J. Atmos. Sci., 43, 505-531.

Sellers, P.J., S.O. Los, C.J. Tucker, C.O. Justice, D. A. Dazlich, G. J. Collatz, and D.A. Randall, 1996: A revised land surface parameterization (SiB2) for atmospheric GCMs. Part II: The generation of global fields of terrestrial biophysical parameters from satellite data. Journal of Climate.

Shukla, J. and Y. Mintz, 1982: Influence of land-surface evapotranspiration on the earth's climate. Science, 215, 1498-1501.

Stevens, W.R., 1998: Unix network programming. Volume 1. Prentice Hall.

Texier, D., and Coauthors, 1997: Quantifying the role of biosphere-atmosphere feedbacks in climate change: Coupled model simulations for 6000 years BP and comparison with paleodata for northern Eurasia and northern Africa. Climate Dynamics, 13, 865-882.

Tremback, C. J., 1990: Numerical simulation of a mesoscale convective complex: Model development and numerical results, Ph.D. dissertation, Atmospheric Science Paper No. 465, Department of Atmospheric Science, Colorado State University, Fort

Collins, CO, 247 pp.

Tremback, C. J., and R. Kessler, 1985: A surface temperature and moisture parameterization for use in mesoscale numerical models, Preprints, 7th Conference on Numerical Weather Prediction, Montreal, Canada, AMS, 17-20 June, 1985.

Tremback, C. J., G. J. Tripoli, and W. R. Cotton, 1985: A regional scale atmospheric numerical model including explicit moist physics and a hydrostatic time-split scheme, Preprints, 7th Conference on Numerical Weather Prediction, Montreal, Quebec, AMS, 17-20 June, 1985.

Tripoli, G. J., and W. R. Cotton, 1980: A numerical investigation of several factors contributing to the observed variable intensity of deep convection over south Florida, J. Appl. Meteor., 19, 1037-1063.

Tripoli, G. J., and W. R. Cotton, 1982: The Colorado State University three-dimensional cloud/mesoscale model - 1982, Part I: General theoretical framework and sensitivity experiments, J. de Rech. Atmos., 16, 185-220.

Tripoli, G. J., and W. R. Cotton, 1986: An intense, quasi-steady thunderstorm over mountainous terrain. Part IV: Three-dimensional numerical simulation. J. Atmos. Sci., 43, 896-914.

Tsvetsinskaya E., 1998: Investigating the effect of seasonal plant growth and development in 3-dimensional atmospheric simulations. Ph.D. Thesis, University of Nebraska, Lincoln, Nebraska, 147 pp.

VEMAP Members, 1995: Vegetation/Ecosystem Modeling and Analysis Project: Comparing biogeography and biogeochemistry models in a continental-scale study of terrestrial ecosystem responses to climate change and CO2 doubling. Global

Biogeochem. Cycles, 9, 407-437.

Xue, Y., P.J. Sellers, J.L. Kinter, and J. Shukla, 1991: A simplified biosphere model for global climate studies. J. Climate, 4. 345-364.

Xue, Y., M.J. Fennessy, and P.J. Sellers, 1996: Impact of vegetation properties on U.S. summer weather prediction. J. Geophys. Res., 101, 7419-7430.

Xue, Y., 1997: Biosphere feedback on regional climate in tropical north Africa. Quart J. Roy., Meteor. Soc., 123, 1483-1515.

Walko, R. L., W. R. Cotton, M. P. Meyers, and J. Y. Harrington, 1995a: New RAMS cloud microphysics parameterization Part I: the single-moment scheme, Atmos. Res., 38, 29-62.

Walko, R. L., C. J. Tremback, R. A. Pielke, and W. R. Cotton, 1995b: An interactive nesting algorithm for stretched grids and variable nesting ratios, J. Appl. Meteor., 34, 994-999.

Walko, R.L., L.E. Band, J. Baron, T.G.F. Kittel, R. Lammers, T.J. Lee, R.A. Pielke, C. Tague, C. Taylor, C.J. Tremback, and P.L. Vidale, 1999 Coupled atmosphere-biophysics-hydrology models for environmental modeling. J. of Appl. Meteor., accepted.